MELAMINE PHOSPHATE AS A COMPONENT OF INTUMESCENT COATINGS

Michael Kay

Presented for the Degree of

DOCTOR OF PHILOSOPHY

of

The University of Aston in Birmingham

September 1980

SUMMARY

Michael Kay

Presented for the Degree of Doctor of Philosophy

1980

Melamine orthophosphate has been shown to exhibit variations in its chemical constitution, and crystal shape and size, dependent upon the method of production. These crystal types have been incorporated with epoxy resin to produce intumescent coatings, which have been tested on a small scale fire testing device, designed and calibrated within this project. The factors influencing performance in three fire test regimes are the percentage loading of melamine phosphate, its chemical constitution, crystal size and shape, thermal degradation, and state of agglomeration and dispersion in the coating, determined by the method of incorporation into the coating. When melamine phosphate is heat treated at 210°C, a process designed to reduce its solubility, the performance of coatings produced with such material is profoundly affected, depending mainly on crystal size and shape alone. Consideration of heat transfer across the chars produced has allowed a quantitative evaluation of the thermal resistance of chars throughout a test. An optimum production route for melamine phosphate has been suggested, taking into account the requirements for weatherability of coatings as well as performance in a fire.

KEY WORDS

Fire Testing

Fire Protection

Intumescence

Melamine Phosphate

ACKNOWLEDGEMENTS

In recognition of their help and support offered during the course of this project, I would like to express my appreciation to the following:

Professor G.V. Jeffreys, for his financial and moral support;

Mr. A.F. Price, my project supervisor, for his advice, support, and friendship;

The technical staff of the workshop, photographic laboratory, and stores of the Department of Chemical Engineering for their prompt and efficient service;

The Department of Safety and Hygiene, particularly Dr. I. Lavery for his help in the early stages of the project, and the technical staff for the use of instruments in the department;

The Department of Construction and Environmental Health, for the use of their Differential Thermal Analyser;

The Department of Chemistry for sundry chemical analyses carried out on my behalf;

Dr. W.D. Woolley, of the Fire Research Station, Borehamwood, Herts., for the loan of a radiometer;

Mr. J. Schreeves, of British Industrial Plastics Ltd., Oldbury, West Midlands, for the use of a triple roll mill on several occasions, and for the supply of melamine for the project;

Kronos Titanium Pigments Ltd., of Wilmslow, Cheshire, for the supply of titanium dioxide, and for advice on rheological additives;

Miss Teresa Hill, for the diligent typing of this thesis.

CONTENTS

TABLES

FIGURES

PLATES

CHAPTER I

INTRODUCTION

CHAPTER 1

INTRODUCTION

1.1 Intumescent Coatings

Fire protection is a major industry today, and any means of reducing deaths and damage to property is of world wide concern. Active fire fighting includes such devices as sprinkler systems, but much can be done to reduce fire damage by protecting structures with fire retardant coatings, amongst which intumescent coatings are being commercially developed. Intumescent coatings act sacrificially, forming on exposure to fire, a foamed char which gives limited protection to the substrate, the philosophy being to allow time to extinguish the fire before the collapse of the structure. By virtue of their expansion they can also act to block gaps through which fire could spread and are thus used on fire doors on the surfaces between the frame and the door. The active ingredients of an intumescent coating are a polyhydric alcohol or resin containing sufficient hydroxyl groups, a source of phosphate or other dehydrating agent, a source of gas to foam the char, known as the spumific agent, and in most cases a catalyst, normally an amide, although this is less necessary when a condensed phosphate is included in the formulation. The techniques may also be applied to rendering articles of epoxy resin or polyurethane less flammable by adding a dehydrating fire retardant such as phosphate and a spumific agent.

Melamine phosphate is widely cited in patents for intumescent compositions, providing a source of gas from the melamine component, fire retardant dehydrating phosphate, and mass for the char. A detailed review of the role of intumescent coatings in structural fire protection and other areas has been published by Kay, et al (1). This paper, which is reproduced in Appendix A.6 of this thesis, includes sections on the

historical development of intumescent coatings, and reviews the literature on melamine phosphates in terms of manufacture and uses up to 1977. Many problems are however associated with the use of intumescent coatings, and it has not been possible to solve all the problems in any one situation. However it has been possible to solve those problems specific to certain situations by different formulation techniques, and consequently intumescent coatings fall essentially into two categories: paints for use internally, and resinous coatings, sprayed on as mastics, for external use.

a. Intumescent paints are normally applied as coatings of typical paint thickness, and can thus only protect the substrate for a short time. They usually exhibit a high degree of expansion, being used especially in fire doors or ventilation ducts (2), where there is a specific requirement to close a gap and prevent fire spreading around a building. The active ingredients of intumescent paints do not behave well with respect to good paint characteristics, so much research has been carried out in developing multifunctional chemicals which can be used at low loadings, for example, a melamine-formaldehyde phosphate ester polyol (3). Uniform cover must be achieved, such that the actual thickness is in no part significantly less than the stated nominal thickness. In addition in the protection of personnel it is important that emissions of noxious fumes from the reaction of the intumescent paint are minimised. To achieve these objectives, good weatherability is usually sacrificed in internal applications.

b. Intumescent mastics are normally sprayed onto structural steelwork, and are suitable for the protection of flammable stores, petroleum tankers, and chemical process equipment. The prime requirements are weatherability and resistance to damage by mechanical means. In such

cases it has been found that formulations which enable these requirements to be met normally emit noxious fumes on burning, and such coatings are not therefore suitable for the protection of personnel. Formulations based upon epoxy resin and phosphates of melamine are of this type, and many examples of formulations containing melamine phosphate and pyrophosphate are given in the patent literature (1).

The search for improved weatherability in intumescent coatings has been a long and continuing one. Recent patents suggest the premixing of a water resistent resin with the other components (4,5,6), and many other patents mention leach resistance and weatherability specifically amongst the properties of their products (7,8).

The use of intumescent coatings on structural steelwork has been discussed recently by several researchers (9-12).

1.2 Phosphates of Melamine

1.2.1 Production of Melamine Orthophosphate

Melamine orthophosphate has traditionally been produced from a suspension of melamine mixed with phosphoric acid, which results in a gelatinous product. Lack of uniformity in composition, due to the intractable nature of the suspension produced and the encapsulation of unreacted solid melamine by newly formed crystals of melamine phosphate, has been a major problem with this production route.

Yeadon, et al. (13) recommended treatment of melamine phosphate at 205°C for five hours to reduce its solubility, and thus increase the resistance to weathering of coatings in which it is incorporated.

1.2.2 Production of Melamine Pyrophosphate

Melamine pyrophosphate has traditionally been produced by mixing a suspension of melamine with hydrochloric acid in equimolar proportions, followed by the addition of tetrasodium pyrophosphate, and a further

quantity of hydrochloric acid similar to that already added. This results in a gelatinous product also. An alternative process was propounded by Fessler and Tredinnick (14) in 1970, in which all the acid is reacted with the melamine prior to the introduction of the tetrasodium pyrophosphate. This was claimed to result in a product which did not gel in suspension, and could consequently be used in aqueous intumescent formulations. This new product was also claimed to have differences in its X-ray diffraction pattern, infra red spectrum, and thermal breakdown characteristics from the traditional material.

The overall stoichiometry of the production processes is

$$2\ C_3H_6N_6 + 4\ HCl + Na_4P_2O_7 = (C_3H_6N_6)_2.H_4P_2O_7 + 4NaCl \qquad (1.1)$$

To examine this claim, several experiments were carried out in the course of the current research. Melamine pyrophosphate was produced by four routes:

a. the traditional route, at 90°C) following the instructions

b. the route suggested by Fessler) given in U.K. Patent
and Tredinnick, at 85°C) 1,270,624

c. by the addition initially of all the tetrasodium pyrophosphate in solution, followed by all the acid.

d. by the route suggested by Fessler and Tredinnick, but using a 50% excess of hydrochloric acid.

Tetramelamine pyrophosphate was also produced by the addition of acid followed by tetrasodium pyrophosphate at 85°C in the proportions indicated by the equation:

$$4\ C_3H_6N_6 + 4HCl + Na_4P_2O_7 = (C_3H_6N_6)_4.H_4P_2O_7 + 4NaCl \qquad (1.2)$$

The materials were chemically analysed, infra-red spectra obtained, their crystal structure examined under an optical microscope, and their

thermal degradation investigated using differential thermal analysis.

During the manufacture of these materials it was noted that in those cases where the new procedure was followed, i.e. (b) and (d), a product that settled very well was produced, whereas procedures (a) and (c) led to somewhat gelatinous suspensions. The tetramelamine pyrophosphate production procedure resulted initially in a very highly gelatinous suspension which however, on shaking, changed to a precipitate which settled very well. Under microscopic examination, these crystals of tetramelamine pyrophosphate were shown to be well formed block-like plates. The products of routes (b), (c) and (d) were also block-like plates, only the traditional procedure (a) leading to thinner plates (which appeared similar to the thin plates of the orthophosphate on microscopic examination, as produced as explained in Chapter 2, but did not have the reflective qualities of these crystals).

On chemical analysis, using the technique for melamine described in Appendix A.1.1, the values of n in the formula $(C_3H_6N_6)_{2n}.H_4P_2O_7$ were found for the four routes described above to be respectively 1.00, 0.93, 0.99, 0.98. The value of n for tetramelamine pyrophosphate was found to be 1.85. (The error in all determinations was around 0.05).

Differential thermal analysis on materials produced by methods (a) to (c) (see Appendix A.1.4) revealed no obvious differences in the positions of peaks. In all these cases, a peak occured at around 335°C, spanning a range of around 35°C, and a further peak at around 402°C. In the products of the traditional route, and that formed by adding successively all the tetrasodium pyrophosphate and then the acid, a further peak at an intermediate temperature of 395°C was encountered. These findings do not concur with the observations of Fessler and

Tredinnick using thermogravimetry, in which they state that the traditional form loses weight in the region 285°C up to 315°C, and then again above 350°C, whereas their novel form loses weight substantially continuously from 300°C to above 350°C.

However differences were encountered in the infra-red spectra of the compounds which agreed with the observations of Fessler and Tredinnick. The form produced by the successive addition of all the tetrasodium pyrophosphate followed by all the acid, of similar crystal shape to the novel form, also yielded a substantially similar infra-red spectrum to the new form, except for minor differences in the region 1300 cm^{-1} - 1450 cm^{-1}, where it differed also from the spectrum of the traditional form (these two forms having similar spectra in this region).

It thus appears that there exist at least two forms of melamine pyrophosphate, with the traditional form differing from products of other origin.

1.2.3 Uses of Salts of Melamine

The production and uses of melamine phosphates in the literature up to 1977 have been extensively reviewed (1). Since that time further patents have been applied for worldwide. The use of melamine orthophosphate together with epoxy resin is recorded in two patents, claiming a coating for structural steelwork incorporating inorganic fibres (15), and the production of intumescent capsules which may be added to suitable paints (16) respectively. Another coating for steel claims an aqueous mixture given resistance to weathering by the addition of a urea-formaldehyde polymer resin (10). The majority of patents claim coatings and adhesives for the treatment of wood products (such as particle chipboard) (17-20). It is also mentioned as an additive to

nylon (21) (melamine itself is more often mentioned in this context), and in intumescent putty compositions (22). Melamine pyrophosphate is also occasionally utilised in intumescent formulations (23,24), but it is noteworthy that the orthophosphate occurs in the literature with a frequency greater by a factor of five. However, even with this high level of interest in melamine orthophosphate it became apparent that little was actually known about the material compared to the work undertaken on the pyrophosphate.

Other melamine salts are also mentioned in the recent patent literature, most commonly melamine molybdate (25), which acts as a smoke suppressant. Melamine sulphate (26) and hydrochloride (27) also occur in isolated references.

1.3 Tests of Fire Resistance

The assessment of a coating for fire resistance obviously requires that it be tested in a reproducible fire simulation situation. The question arises, however, what is a true simulation? The development and behaviour of fires varies widely, being dependent upon the nature of the fuel, the geometry of the site and meteorological conditions; furthermore, different materials react in different ways on exposure to fire. This has led to a large number of tests specifically designed for certain situations.

Petroleum fuelled fires develop with greater rapidity, and may reach 1100°C in less than three minutes, engendering very high radiant heat fluxes. Mobil have developed a test of resistance to such fires, using a propane burner (28). A series of spectacular tests was carried out by the U.S. Department of Transportation to test the ability of petroleum filled railroad cars to withstand a petroleum fuelled fire,

noting the effectiveness of a fire retardant coating in terms of the increase in time with respect to an uncoated car before explosion occured, and by the decrease in the violence of the explosion (29-33). Similar tests have also been carried out in the U.K. on road tankers (34).

In contrast, a wood fuelled fire develops considerably more slowly, reaching a temperature of around 500°C after five minutes, and a temperature of around 900°C after around 45 minutes. It is upon such a scale of development that the standard time-temperature curve to which structural elements are to be exposed in the British Standard test of fire resistance BS 476 : 1972 Part 8, is based.

Two parameters are of especial importance in determining the effect of a fire in a particular situation. Flame spread is an indication of the rate at which a fire propagates itself. Fire resistance of a structural element is a measure of the destructive effects of a fire to that element, and according to BS 476 : 1972 Part 8, is a complex parameter incorporating measures of the insulation (i.e. rise in temperature of unexposed areas), integrity (propagation of cracks allowing penetration of flames), and stability (resistance to collapse due to fatigue, or strains arising from differential expansion of various parts) of the element. Fire resistance is a property of a structure or structural element, to which a coating may contribute; but it is not a property of the coating itself. The fire resistance of a whole building may be calculated by heat transfer models from the fire resistance of its component structural elements (35).

Due to the many variables in the conditions of a fire and of a multitude of fire tests, the meaning of any fire test result will require careful interpretation. Much has been written on the philosophy

of fire tests (36-39). Different national standard tests pose further problems (40); in the U.S. for instance, the ASTM test E-119 is used; this is a tunnel test, measuring a complex quantity including both flame spread and fire resistance.

The more artificial the conditions of a fire test, the less correlation with a real fire may be expected. A large scale test is a better simulation of a real situation than a small scale laboratory test (41). Many laboratory pyrolysis techniques may indeed give results at variance with those in a real fire, due to the higher surface temperatures and higher temperature gradients in a real fire.(42). In fact, the problems arising from the lack of correlation between different fire tests for coatings are so severe that insurers are often considerably more willing to give clients premium reductions for the installation of sprinkler systems in buildings than for the use of fire retardant coatings (43). However coatings do have the major advantage of being easily applied to an existing building, whereas a sprinkler system is preferably installed during construction.

Despite the disadvantages of laboratory fire tests, it was however considered necessary to devise a small scale test to evaluate coatings, enabling a high throughput of samples at low cost, with good reproducibility of conditions, to be achieved. The fire testing facility described in Chapter 4, was designed for the investigation of the behaviour of a large number of coatings under several reproducible sets of conditions, in terms of the heat transfer across the coatings, and of their physical development. No work on structural fire resistance is however possible on this device. By this means, the effects of variations in the chemical formula, particle shape and size

distribution of melamine phosphate in an intumescent formulation, as well as the means of incorporating the melamine phosphate component into such a coating, have been evaluated in terms of their impact upon the performance of the product during the course of this project. Nevertheless the conditions of these fire tests are in many ways unlike those of any real fire, especially in the continuing highly oxidative environment throughout a test. In a real fire, the concentration of oxygen declines rapidly in the heart of the fire. From this point of view, these tests are severe. However the intumescent formulation used was also unlike a commercially available type, but consisted only of those components necessary for intumescence to occur, without additives, to enable a fundamental study of the effects of the above variations in the nature of melamine phosphate upon coating performance in a fire to be undertaken. Further studies may attempt to apply these findings to commercially acceptable coatings, containing, for example, fibres, titanium dioxide, and solvents, and large scale tests will be required to prove their efficacy after initial studies on the Aston fire testing device.

CHAPTER 2

CRYSTALLISATION PROCESSES OF MELAMINE ORTHOPHOSPHATE

CHAPTER 2

CRYSTALLISATION PROCESSES OF MELAMINE ORTHOPHOSPHATE

Nomenclature

n	molar ratio of melamine to phosphate in crystalline melamine orthophosphate
k_p	equilibrium constant for dissociation of dihydrogen phosphate ion
T	temperature, Kelvin
[ ]	concentration in solution.

2.1 Introduction

Since melamine pyrophosphate appears to form two crystallographically distinct crystal forms with different thermal behaviour (14), it seemed possible that the orthophosphate might also behave in a similar manner. The commercial orthophosphate product obtained by mixing a stirred suspension of melamine with phosphoric acid at ambient temperature consists of small (around 10 μm) needles of fairly low aspect ratio, which form a gel in suspension and are consequently difficult to filter and not suitable for use in aqueous based intumescent formulations.

By analogy with the techniques used for the production of melamine pyrophosphate, three methods of producing the orthophosphate were conceived, as follows:

a. the traditional, commercial procedure, a reaction, at ambient

temperature, between a stirred aqueous suspension of melamine and phosphoric acid, viz.

$$C_3H_6N_6 + H_3PO_4 = C_3H_6N_6.H_3PO_4 \qquad (2.1)$$

b. a reaction at elevated temperature with hydrochloric acid in equimolar proportions, to form the hydrochloride, followed by the addition of monosodium orthophosphate to the suspension or solution of the hydrochloride, viz.

$$C_3H_6N_6 + HCl + NaH_2PO_4 = C_3H_6N_6.H_3PO_4 + NaCl \qquad (2.2)$$

c. a reaction at elevated temperature with twice the quantity of hydrochloric acid specified above, followed by addition of disodium orthophosphate to the solution or suspension formed, viz.

$$C_3H_6N_6 + 2HCl + Na_2HPO_4 = C_3H_6N_6.H_3PO_4 + 2NaCl \qquad (2.3)$$

As melamine hydrochloride is considerably more soluble than either melamine itself or any of its phosphates, a solution of the hydrochloride may readily be formed at elevated temperatures. This may be desirable from a practical point of view, as a suspension of the hydrochloride is highly gelatinous, and difficult to stir.

These three procedures were undertaken on a small scale, and crystals of a different shape were produced in each case. The traditional procedure produced a gelatinous suspension of needles as expected. A product which was considerably less gelatinous was produced using the second method, at ambient and elevated temperatures. This proved to consist of small block plates, reasonably well formed. The third procedure, undertaken at elevated temperature, did not precipitate immediately on addition of disodium phosphate to the solution of the hydrochloride, but after an induction period of around two minutes formed very thin highly reflective plates of indeterminate

size. A more detailed analysis of the possible production routes to various crystal sizes and shapes was then undertaken in order to provide a variety of types for incorporation into samples for fire testing. A detailed quantitative study of the kinetics of the different crystallisation processes was not however carried out, due to the complexity of the processes involved.

In the following discussion, the terms indicating size are defined as follows with respect to the longest dimension of the mean crystal size:

small	:	< 20 μm
medium	:	20 μm - 70 μm
large	:	70 μm - 150 μm
very large	:	>150 μm

2.2 Parameters Determining Crystal Size and Shape of Melamine Phosphate

In the course of investigating various processes for the production of melamine orthophosphate, the effects of several parameters were noted.

a. Temperature : the aspect ratio of crystals initially formed when immediate precipitation occurs on mixing of the reactants increases with an increase in temperature. The needle crystals formed at elevated temperatures may cause a system to become highly gelatinous. The phenomenon is however usually temporary; stirring causes mass transfer to take place after initial precipitation to change the crystal shape to a form determined by other parameters as well as temperature. In reasonably dilute systems produced from equimolar quantities of melamine and phosphate, increase in temperature does appear to reduce the thickness of plate crystals ultimately formed, causing them to become highly

reflective. Those precipitated at ambient temperature tend to be more blocky in type.

b. Concentration : In general an increase in concentration favours an increase in the aspect ratio of the crystals formed. Thin reflective plates are only formed from dilute systems. This is true in terms of the concentration of systems where precipitation occurs on cooling of a solution of melamine phosphate, or with respect to the overall concentrations of the reactants in solid and solution phases where precipitation occurs on mixing.

c. Relative quantities of reactants : a molar excess of phosphoric acid tends to increase the aspect ratio very significantly.

d. Degree of agitation of suspensions during the mixing process : as this increases, the aspect ratio of the product likewise increases. However agitation on completion of the mixing process has little or no effect on crystal shape.

e. Cooling rate from solutions of melamine phosphate at elevated temperature : increase in the cooling rate tends to promote plate formation at the expense of needles. This is only really marked when excess phosphoric acid is used; a sufficiently fast cooling rate can then overcome the tendency to form needles of high aspect ratio, and some thin reflective plates are formed also. These two distinct crystalline types only are formed under these conditions, without block plates or needles of low aspect ratio.

These parameters have been found to be generally applicable, and are illustrated in the recommendations for the production of various crystal types.

2.3 Stoichiometry of the Product

The use of reactants in equimolar proportions does not produce a product in which melamine and phosphate are present in equimolar proportions, by any production route. Table 2.1 shows the results of analyses of several batches of a variety of crystal types, from which it may be seen that on the whole the molar ratio of melamine to phosphate is around 1.2, irrespective of the production route. The ratio appears to be somewhat higher for thin reflective plates which are normally produced from dilute systems.

The analyses were carried out by dissolving weighed quantities of solid in dilute hydrochloric acid at elevated temperature, and adding water to a known volume in a graduated flask. Normally around 0.2g would be dissolved in a total volume of 100 cm^3. Spectroscopic analyses, as detailed in Appendix A.1.1 for melamine and phosphate were then carried out, and the quantites obtained by these results summed to check against the original weight of solid.

The excess melamine with respect to phosphate is not due to unreacted melamine, since samples crystallised from solutions, which are uniform in appearance exhibit this stochiometry. The explanation is believed to lie in the fact that at the pH of the reaction, phosphate is present as a mixture of $H_2PO_4^-$ and HPO_4^{2-}, both of which are precipitated with melamine. The equilibria may be represented thus:

$$H_2PO_4^- (aq) \overset{K_P}{\rightleftharpoons} HPO_4^{2-}(aq) + H^+ (aq) \qquad (2.4)$$

$$n\ C_3H_7N_6^+ (aq) + (2-n)H_2PO_4^- (aq) + (n-1)\ HPO_4^{2-} (aq) = (C_3H_6N_6)_n.H_3PO_4 (s) \qquad (2.5)$$

From this it follows that the molar ratio, n, of melamine to phosphate in the product depends upon the pH of the solution from which crystall-

isation is taking place. It may be assumed that $H_2PO_4^-$ and HPO_4^{2-} are incorporated into the precipitate in a ratio equal to their relative concentrations in the solution at any time during the crystallisation process. Then if K_p is the equilibrium constant for the dissociation of $H_2PO_4^-$, it follows that

$$K_p = \frac{[HPO_4^{2-}][H^+]}{[H_2PO_4^-]} = \frac{(n-1).[H^+]}{(2-n)} \qquad (2.6)$$

$$\text{therefore } n = \frac{2K_p + [H^+]}{K_p + [H^+]}$$

Thus when a solution of melamine phosphate is cooled, as crystallisation takes place, HPO_4^{2-} is lost from the aqueous phase, but H^+ formed with it from dissociation of $H_2PO_4^-$ is not. The solution thus decreases in pH as cooling progresses, and consequently the ratio n decreases. As the solution becomes more acidic the tendency to form needles rather than thin reflective plates increases, resulting in some cases in a mixture of crystal forms (slower cooling also probably contributes in the later stages of the cooling process). The value of n obtained by chemical analysis is therefore a mean macroscopic value for the product, and will depend upon concentrations of the reactants, and the temperature difference between that at which crystals first appeared and the filtration temperature. The lower concentration of solutions from which thin reflective plates are produced will cause the solution to have a higher pH and therefore a higher value of n = 1.3 than is normal for the other crystal types.

TABLE 2.1 Ratios of melamine to phosphate in several batches of crystal types produced from equimolar proportions of melamine and phosphate.

Crystal Type	Ratio of Melamine to Phosphate in Product, n
Thin reflective plates	1.30, 1.35, 1.31, 1.26, 1.29, 1.33, 1.30
Small block plates	1.20, 1.22, 1.21
Large needles	1.22, 1.22
Small needles	1.25, 1.16

It has been shown by Kler (44) that if crystals of melamine phosphate are left in their liquor after reaction the pH of the liquor rises abruptly after around two weeks from, for example, 4.8 to 5.2, at which pH it is then stable. This must indicate a reduction of n on storage.

If the reactants contain excess acid, the consequent reduction in pH leads to a reduction in the value of n in the crystals formed. This is true for phosphoric acid, where the use of 1.25 moles acid per mole melamine results in a product which normally has a value of n in the range 0.95 to 1.05, depending upon concentration and filtration temperature. Other acids, such as hydrochloric or acetic acids, have a similar effect, but the danger of coprecipitation of the other melamine salt exists if the other acid is present in sufficient concentration.

The addition of monosodium phosphate to the system does not change the pH and nor, consequently, the value of n. It simply serves to reduce the solubility of the melamine phosphate by the common ion effect, a process known as "salting out".

2.4 Production Considerations for the Crystal Forms of Melamine Phosphate

2.4.1 General Considerations

Reaction between melamine and phosphate has been shown by visual observation to take place in the solution phase. When phosphate is added to a suspension of melamine or its salt, crystals of melamine phosphate appear in the bulk solution as much as near the surfaces of existing reactant particles. The major difference therefore between a reaction carried out when melamine or its salt is in suspension compared to a system in which all the reactants are in solution, is that in the former case the dissolution of the reactant may become the rate determining step.

The solubilities of melamine, melamine hydrochloride, and melamine acetate are 0.023 mole litre^{-1}, 0.108 mole litre^{-1}, and 0.165 mole litre^{-1} respectively at 18°C and 0.049 mole litre $^{-1}$, 0.155 mole litre^{-1}, and 0.285 mole litre^{-1} respectively at 36°C (the results for the salts being obtained by the technique of Appendix A.1.2, and that for melamine from the formula (45)

$$\log_{10} (\text{solubility}) = {}^{-1642}/_{T} + 5.101 \qquad (2.8)$$

where solubility is given in grammes per 100 cm^3 water, and temperature T in Kelvin). In the reaction between one of these melamine salts and sodium phosphate therefore a much higher concentration of melamine is available in solution at any given temperature than in the reaction between melamine and phosphoric acid, assuming the use of saturated solutions with excess solid. Alternatively a reaction between solutions in the absence of solid can be carried out at a lower temperature using the melamine salt intermediates.

The solubility of the intermediate in the route utilising two moles of acid per mole melamine, then to be reacted with disodium phosphate, is slightly lower than that of the salt formed using one mole of acid. The second mole of acid does not react with melamine cation, but serves to lower the solubility of the intermediate by the common ion effect.

The differences in crystal type obtained by these three routes are presumed to be a function of the different kinetics of the reactions. At elevated temperatures, immediate precipitation occurs from the monosodium phosphate route, whereas there is a delay in precipitation in the disodium phosphate route.

The effects upon the yield of product of the presence of sodium and chloride ions in the filtrate were determined by using the solubility apparatus described in Appendix A.1.2 The overall ion composition prior to filtration will contain, depending upon the production route, zero, one or two moles of sodium and chloride (or acetate) ions per mole of melamine and phsophate ions. For each determination around 5g melamine in a total volume of 150 cm^3 were used, and the reactions carried out at 80°C in Clearfit (R) conical flasks, which were then incorporated in an apparatus for solubility determination, at a variety of temperatures from 10°C to 76°C. The concentrations of melamine and phosphate, which are lost in the filtrate, are shown in Figure 2.1. Sodium and chloride ions were also determined where present to indicate any retention in the precipitate, and to check the results by a charge balance, viz.

$$[C_3H_7N_6^+] + [Na^+] = [H_2PO_4^-] + [Cl^-] \qquad (2.9)$$

(dissociation of phosphate being neglected).

(R) Clearfit is a registered trade mark.

FIGURE 2.1 : Concentrations in solution of melamine and phosphate in a system containing equimolar total quantities of melamine and phosphate, and variable amounts of sodium and chloride.

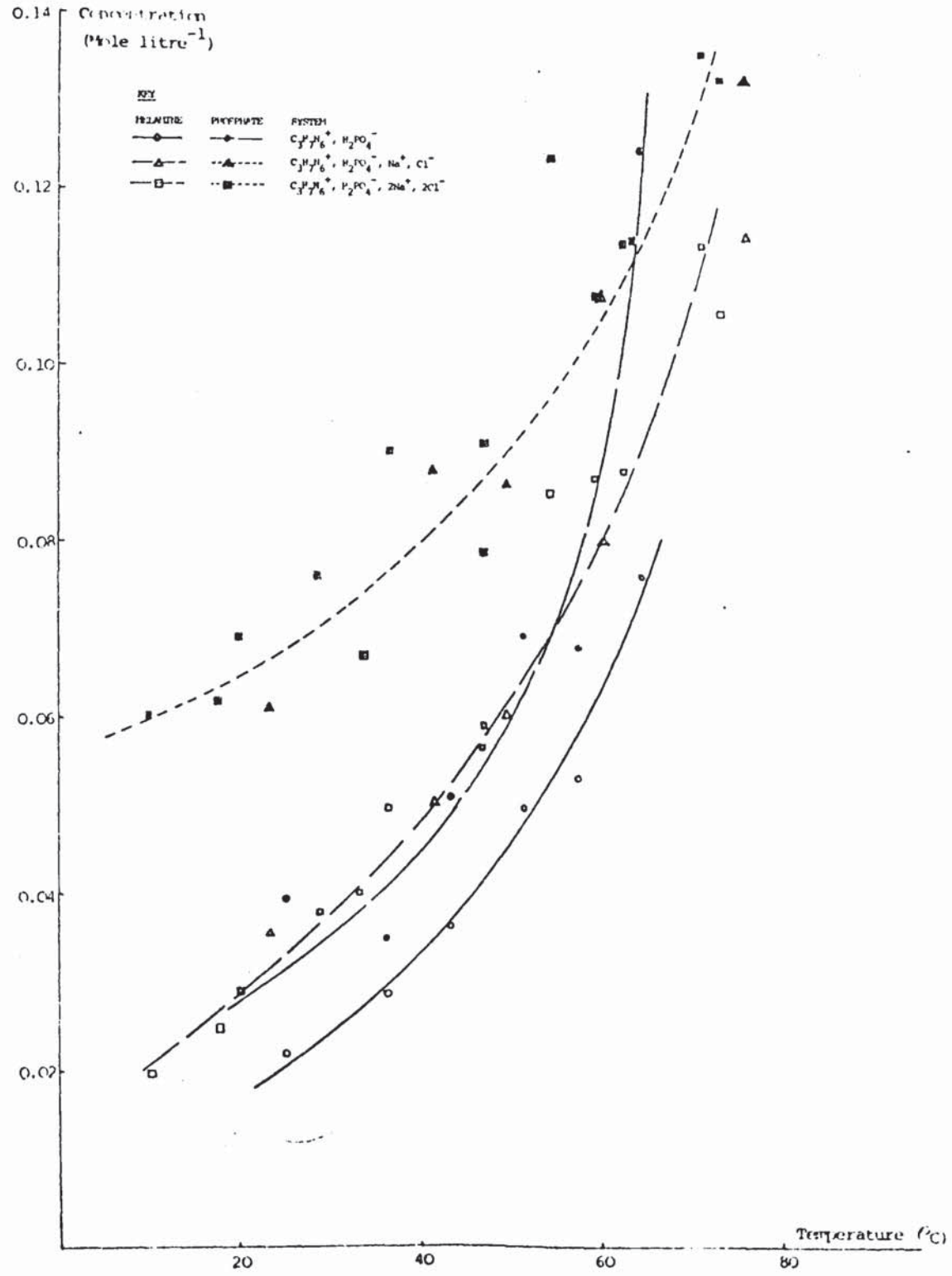

At temperatures below around 65°C a considerably higher yield of crystals will be obtained from a system containing only melamine and phosphate than in the presence of sodium and chloride. On increasing the levels of sodium and chloride from one mole to two moles per mole melamine and phosphate, little further variation in yield may then be expected. The lower yields in these systems are due to the greater solubilities of sodium phosphate and melamine hydrochloride with respect to melamine phosphate.

For the systems

$C_3H_7N_6^+$, Na^+, $H_2PO_4^-$, Cl^- (I)

and

$C_3H_7N_6^+$, $2Na^+$, $H_2PO_4^-$, $2Cl^-$ (II)

the compositions of the "synthetic complex", i.e. the overall composition, and a "wet residue", containing solid drained of most of the filtrate (46) were also determined, to obtain tie-lines at a variety of temperatures for the phase diagram for this reciprocal salt pair. These two points, together with the filtrate composition, exist in a linear relationship; they were plotted using Jänecke's projection (47) of the base from the peak of the pyramid, to show the ion composition; and on an elevation of moles water per mole salts vs. one ion pair. From the latter the dry composition at the intersection at zero water was obtained, and plotted onto the base projection to obtain the composition of the solid. However problems in obtaining an accurate assessment of the quantity of water present reduced the accuracy of this approach to such an extent that in many cases the elevations could not be plotted with satisfactory results. Normally such inaccuracies are cancelled when a full phase diagram is obtained, but this requires

up to one thousand points! Nevertheless the angles of the base projections yielded valuable information on the relative inclusions of sodium and chloride in the crystals. For an angle of 45°, as obtained in the system

$C_3H_7N_6^+$, Na^+, $H_2PO_4^-$, Cl^-

at all temperatures considered, sodium and chloride are present in equal quantities in both solid and filtrate, and can therefore be washed out of the solid to give a pure product. In the system

$C_3H_7N_6^+$, $2Na^+$, $H_2PO_4^-$, $2Cl^-$

however a deviation of this angle from 45° indicated excess chloride with respect to sodium in the solid. Some melamine hydrochloride is thus precipitated. Sodium levels in the solid were low in both systems, but up to 40% of the total anion in the precipitate from the latter system consisted of chloride at 20°C. The angle of the base projection in this system, 65° at 20°C, approaches 45° as the temperature of the system is increased. Schematic projections for both systems are shown in Figure 2.2.

2.4.2 Production of Specific Crystal Types

2.4.2.1 Small Needles, of Stoichiometry Around $(C_3H_6N_6)_{1.2}.H_3PO_4$

This type of crystal is produced by the traditional route of adding a solution of phosphoric acid to a vigorously stirred suspension of melamine, using equimolar quantities, at ambient temperature. The material becomes highly gelatinous; therefore vigorous stirring is required to prevent the viscosity rising. The stirring however itself leads to a needle-like crystal of aspect ratio around five. Raising the temperature of a concentrated system increases the aspect ratio of

FIGURE 2.2 : Schematic diagram showing typical tie-lines for the reciprocal salt pair

$C_3H_7N_6^+$, Na^+, $H_2PO_4^-$, Cl^- at 28°C

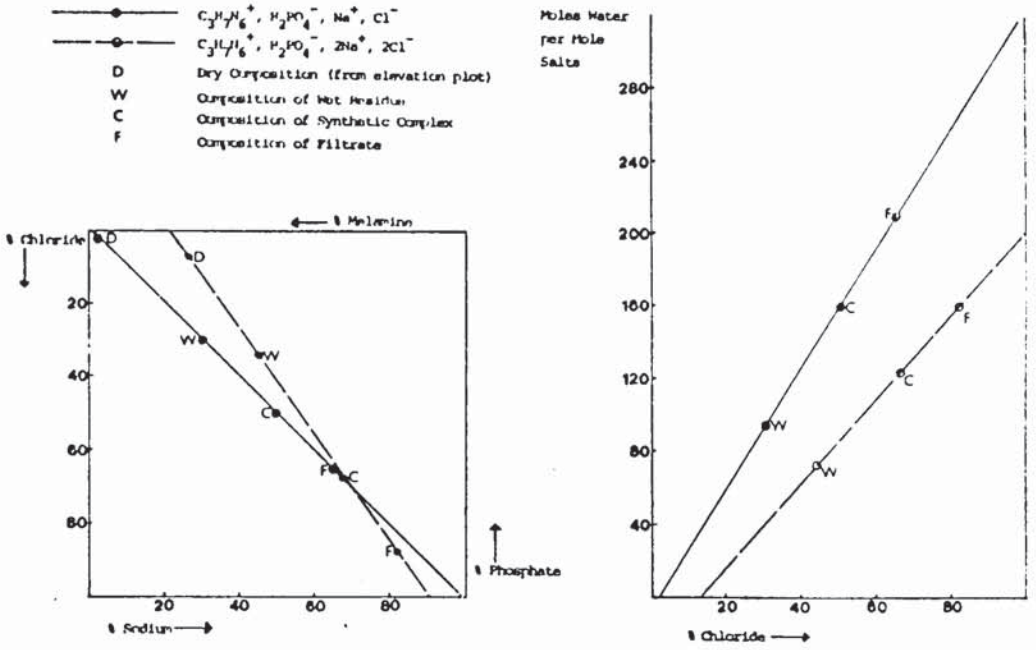

FIGURE 2.3 : Viscosities obtained by Ferranti Viscometer for small needles of melamine phosphate in aqueous and aqueous acetone media.

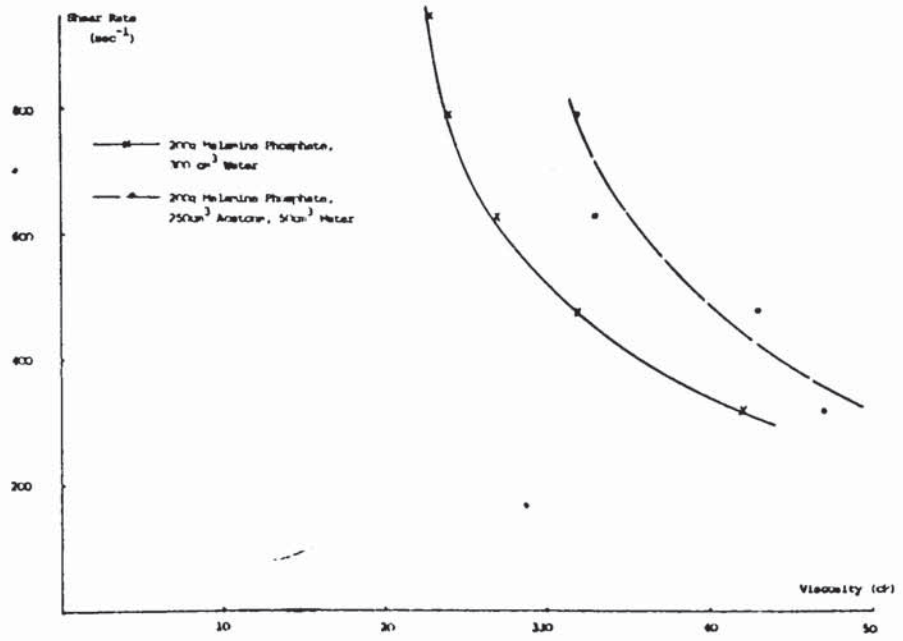

the crystals and the viscosity of the system.

In an attempt to alleviate the handling problem of such a gelatinous suspension, a trial production run was conducted using as solvent a mixture of five parts acetone and one part water. Dry melamine phosphate settles well in pure acetone. However it was found that the viscosity in the acetone-water mixture was higher than in pure water. The viscosities at a variety of shear rates, as determined with a Ferranti viscometer, are compared for the two media in Figure 2.3.. It is presumed that melamine phosphate, being more strongly attracted to water than to acetone, forms islets of solid with the available water, which because of the limited quantity of water, are highly gelatinous. It therefore appears that the only feasible production route to small needles is the traditional one using pure water as the suspending medium.

In a pilot scale batch production run, 76.61g melamine were mixed with an equimolar proportion of phosphoric acid in a total volume of 3.0 litre, to yield 97.3gproduct after filtration and drying. Based upon a formula $(C_3H_6N_6)_{1.2}.H_3PO_4$, this represents a percentage yield of 77%. This yield may be increased by the addition of monosodium phosphate.

2.4.2.2 Small Block Plates, of Stoichiometry Around $(C_3H_6N_6)_{1.2}.H_3PO_4$

Small block plates are produced when melamine and phosphoric acid are mixed at ambient temperature with minimal or no stirring. They are considerably less gelatinous than small needles, but do not settle as well as crystals of melamine pyrophosphate produced by the method of Fessler and Tredinnick. This is not a feasible production route on a large scale, where thorough agitation is required to mix effectively large quantities of reactants.

Small needles, left in contact with their liquor after production, will by a process of mass transfer be transformed to small block plates over a period of a few days.

At ambient temperatures both of the routes

$C_3H_6N_6$ + HCl + NaH_2PO_4 = product

and $C_3H_6N_6$ + 2HCl + Na_2HPO_4 = product

yield small block plates. However the former is obviously to be preferred since contamination of the product by melamine hydrochloride does not then occur. Acetic acid may be used, and is to be preferred for two reasons, namely the greater solubility of melamine acetate compared to melamine hydrochloride, and the plate-like crystal shape of the acetate in suspension leading to a lower viscosity for this system than for the hydrochloride. A danger exists with the gelatinous hydrochloride that unreacted melamine may be encapsulated by needles of the hydrochloride and prevented from taking part in the reaction. The hydrochloride should be warmed to near dissolution to prevent this occuring; warming is not however necessary for the acetate, even at a reactant concentration of 100g melamine per litre water, the highest concentration which may be used in this system. The major disadvantage of using the acetate intermediate is the foaming produced in this route. To the stirred suspension of the intermediate a solution of monosodium phosphate is then added, to produce melamine phosphate. A notable reduction in viscosity occurs when the hydrochloride intermediate in suspension is used. If the addition of phosphate takes place at elevated temperature, the product is initially gelatinous, but on stirring mass transfer takes plate to produce somewhat reflective plates. To avoid this gelatinous phase it is recommended that this

stage be carried out at ambient temperature. The product may then be filtered and washed.

In a pilot scale batch production run, 118.2g melamine and an equimolar quantity of hydrochloric acid were mixed in a volume made up to 1.5 litre. A solution containing 147g $NaH_2PO_4.2H_2O$ was slowly added and the volume made up to 3 litre. After filtration and drying, the yield was 165.2g, 85% based upon a formula $(C_3H_6N_6)_{1.2}.H_3PO_4$. The reaction was carried out at ambient temperature. The addition of excess monosodium phosphate will serve to increase the yield.

2.4.2.3 Large Needles, Average Length 80 μm, of Stoichiometry $(C_3H_6N_6)_{1.2}.H_3PO_4$

These may be produced by cooling from saturation at 90°C a solution containing equimolar quantities of melamine and phosphoric acid with minimal stirring. The product is of variable aspect ratio, and includes some block plates and equant crystals, but the majority of the crystals are needles of aspect ratio around five.

2.4.2.4 Thin Reflective Plates

These are formed from dilute systems. If a highly under-saturated solution at 90°C of melamine and phosphoric acid, containing around 20 grammes per litre melamine is cooled, thin plates will be formed. From equimolar reactants these will be highly reflective and of stoichiometry $(C_3H_6N_6)_{1.3}.H_3PO_4$; but if a 25% molar excess of phosphoric acid is used plates of stoichiometry $(C_3H_6N_6)_{1.1}.H_3PO_4$ are formed, which are considerably less reflective. The higher ratio of melamine to phosphate compared to the aforementioned products is due to the lower concentrations of reactants. When using excess phosphoric acid it is only possible to obtain plates rather than needles by large

dilutions or fast cooling rates. The cooling rate does appear to influence the reflectivity of the product, which is maximised by fast cooling and intermittent agitation. It is believed to be a function of the plate thickness, which when around 500 nm, of the same order as the wavelength of visible light, results in high reflectivity.

Several production routes involving the addition to melamine of phosphate at elevated temperature result in thin reflective plates. They are the product when a solution of melamine with hydrochloric acid in the ratio $C_3H_6N_6$ + 2HCl is mixed with a solution of disodium phosphate. Precipitation is delayed, and the product forms directly as thin reflective plates. Likewise the mixing of solutions of a melamine salt and monosodium phosphate will result in thin reflective plates if the phosphate solution is added dropwise, avoiding the gelatinousphase which occurs on fast mixing, which produces somewhat blockier plates. If phosphoric acid is added dropwise to a dilute suspension of melamine at elevated temperature, thin reflective plates are similarly obtained after passing through a gelatinous phase. Methods avoiding the addition of sodium and chloride or acetate ions are obviously to be preferred to obtain higher yields (since filtration at ambient temperature is then possible) and avoid contamination of the product.

2.4.2.5 Needles, of Stoichiometry $(C_3H_6N_6)_{1.0}.H_3PO_4$

A stochiometry of this type requires a reduced pH, produced by the addition of excess phosphoric acid. Whilst other acids also serve to reduce pH, the solubility of the product is increased, the common ion effect countering this tendency when phosphoric acid is used, and contamination by the other anion is likely. Hydrochloric acid does also produce needles when used to reduce pH, but acetic acid

does not have this effect.

The needles produced have large aspect ratios, often in excess of one hundred. Most production routes utilising a 25% excess of phosphoric acid in reasonably concentrated systems lead to the formation of similar crystals. If the reactants are mixed at ambient temperature, the product will initially be in the form of small block plates or small needles of low aspect ratio, but will change to medium needles of length around 50 μm after a few hours. This transformation will be hastened by warming the system to 50°C, a process which also increases the product aspect ratio. If a solution of melamine and phosphoric acid, the latter present likewise in 25% molar excess, is cooled from saturation at 100°C, medium needles are also formed on stirring. If unstirred, very large needles, up to 30 mm in length, are formed.

2.5 Dimelamine Phosphate

If melamine and phosphoric acid are mixed in a ratio of two moles to one the product is of exact stoichiometry $(C_3H_6N_6)_2.H_3PO_4$. When these reactants are mixed at ambient temperature the initial reaction appears to be between phosphoric acid and a little more than half the melamine to form a mixture of ordinary melamine phosphate (small plates) and melamine, but further stirring gives crystals of dimelamine phosphate. These are large blocky plates, rarely less than 50 μm side, which settle well. An entirely similar product may be formed from the reaction

$$2C_3H_6N_6 + 2HCl + Na_2HPO_4 \xrightarrow{60°C} (C_3H_6N_6)_2.H_3PO_4 + 2NaCl \qquad (2.14)$$

It has been noted that the rate of cooling of a solution of dimelamine phosphate affects the aspect ratio of the plates formed, fast cooling

favouring a larger aspect ratio. If a suspension of the product is left standing for 24 hours, Ostwald ripening occurs, and very large rhomboid block plates, and even a few equant crystals, are produced, of average size 200 μm side.

2.6 Other Melamine Salts

It appears that many salts of melamine vary in crystal shape according to the conditions of their manufacture. This is well known in the case of melamine pyrophosphate. For example, the hydrochloride, which normally forms needles in a gelatinous suspension when produced at ambient temperature from the mixing of melamine and hydrochloric acid, can be produced in the form of plates by the fast cooling in ice of a solution at 60°C.

CHAPTER 3

PROPERTIES OF MELAMINE PHOSPHATE AND THE EFFECT OF HEAT TREATMENT

CHAPTER 3

PROPERTIES OF MELAMINE PHOSPHATE AND THE EFFECT OF HEAT TREATMENT

3.1 Introduction

Three parameters have been measured for the different crystalline types of melamine orthophosphate to gain insight into the nature of the materials and the probable weathering properties of coatings incorporating them. The solubility and water uptake from an atmosphere of 100% relative humidity, both at 28°C, will give an indication of the latter; together with a knowledge of the thermal breakdown of the materials, obtained by differential thermal analysis, the former objective may be advanced. Details of the experimental techniques for these three types of measurement may be found in Appendix A.1.

Attempts to use infra-red spectra and X-ray diffraction powder traces were inconclusive in determining possible cell structure differences between the crystalline types. This may be due to the variable stoichiometry of the products. However examples of infra-red spectra are shown in Section 3.5.

The materials were heat treated, as recommended by Yeadon, et al. (13), to reduce their solubility. The effect on water uptake was carefully monitored; too high a temperature of treatment had been found by Yeadon, et al. to increase water uptake of melamine phosphate considerably.

Initially a detailed investigation of the effects of temperature and duration of heat treatment on the solubility and water uptake of three crystal types of melamine phosphate was carried out. Small needles, small block plates, and thin reflective plates, the last produced by the disodium phosphate route at 85°C, and filtered at 70°C, were manufactured, and dried for sixty hours at 110°C. The products were then subdivided for treatment at 170°C, 195°C, 220°C, and 252°C

respectively (except that the thin reflective plates were treated only at 170°C and 220°C), and samples withdrawn after five hours, twenty hours, and forty eight hours.

The results of the above investigation being in broad agreement with Yeadon, et al., several crystalline types were produced and treated at 210°C for forty eight hours for use in the fire testing programme. The solubility, water uptake, and thermal breakdown of these materials were also investigated. Some discolouration of materials treated at 210°C and higher temperatures was noted, this being most pronounced in the case of thin reflective plates. This problem is acknowledged in the patent literature and a remedy suggested (48).

3.2 Solubility of Melamine Phosphate

All solubilities were determined at 28.0° $\pm$ 0.5°C, using both spectroscopic and gravimetric methods of analysis. Within the limits of experimental error there was total agreement in trends using these two techniques. Mean measured values for solubilities after drying at 110°C and treatment at 210°C respectively are shown in Table 3.1. It is noteworthy that the solutions produced from suspensions of small needles and small block plates are richer in phosphate than in melamine, whereas the reverse is always true for solutions produced from thin reflective plates (all materials being dried at 110°C), although the mole ratios of melamine to phosphate in the solids are 1.2 and 1.3 respectively, differing by only 0.1. The overall solubility of thin reflective plates, dried at 110°C, is also lower than that of the aforementioned materials.

The investigation into the effects of temperature and duration of treatment revealed no significant effects at 170°C. At 195°C, a slight reduction in solubilities occured after treatment for twenty four hours. A temperature of 210°C was however sufficient to reduce to

TABLE 3.1 Mean measured values for solubility of melamine phosphate, (a) dried at 110°C; (b) treated for 48 hours at 210°C (values for phosphate not available, since condensation of orthophosphate invalidates the analytical technique used).

	(a) Dried at 110°C			(b) Treated at 210°C	
Crystal Type	Melamine (mole litre^{-1})	Phosphate (mole litre^{-1})	% (w/w)	Melamine (mole litre^{-1})	% * (w/w)
Needles $(C_3H_6N_6)_{1.0}.H_3PO_4$	0.022	0.026	0.55 0.75*	0.0025	0.07
Small needles $(C_3H_6N_6)_{1.2}.H_3PO_4$	0.023	0.036	0.65	-	0.06
Small block plates $(C_3H_6N_6)_{1.2}.H_3PO_4$	0.023	0.036	0.65	0.0025	0.05
Thin reflective plates $(C_3H_6N_6)_{1.3}.H_3PO_4$	0.015	0.014	0.35	0.0114	0.2 (0.05% at 220°C)
Block plates $(C_3H_6N_6)_{2.0}.H_3PO_4$	0.014	0.008	0.25	0.0036	0.05

*obtained gravimetrically

around 0.05% the solubilities of all types except thin reflective plates, although at 220°C this material was likewise reduced in solubility.

A full listing of all experimental solubility data appears in Appendix A.2.1.

3.3 Water Uptake by Melamine Phosphate

Although the errors in the technique for the measurement of water uptake are high, and repetition of experiments always necessary, general trends are apparent. Needles of $(C_3H_6N_6)_{1.0}.H_3PO_4$ gave the lowest water uptakes whether dried or treated at 210°C, being below the limit of detection in the former case, and around one per cent in the latter.

The other materials, when dried at 110°C, all had water uptakes of around 5%, although there appeared to be a slight increase in water uptake as the mole ratio of melamine to phosphate increased from 1.2 to 2.0. Treatment at temperatures between 170°C and 195°C appeared to reduce water uptake to around 2%, but above this temperature, water uptake increased (the first signs of this increase being apparent for samples treated for forty eight hours at 195°C). At 210°C, small needles and small block plates of $(C_3H_6N_6)_{1.2}.H_3PO_4$ took up around 9% water; increase in the molar ratio of melamine to phosphate leads to an increase in water uptake, around 10% for thin reflective plates of $(C_3H_6N_6)_{1.3}.H_3PO_4$, and 15% for dimelamine phosphate.

A full listing of results appears in Appendix A.2.2.

3.4 Thermal Degradation of Melamine Phosphate

Differential thermal analyses at temperatures up to 800°C were carried out on five crystal types of melamine orthophosphate, using long stemmed quartz crucibles, a sample size of 0.060 g to 0.095 g, and a heating rate of 20°C per minute. Such a fast heating rate tends to

increase the temperatures at which peaks occur with respect to their true position (49), but is satisfactory for comparative purposes, and all the quoted results are as obtained experimentally. Details of the experimental techniques appear in Appendix A.1.4. Differential thermal analysis is a useful technique for determining differences between materials, and has been used for matching components of intumescent formulations (50). However, the technique is not an absolute guide to performance, since the mixture of chemicals in a coating may behave in a manner different from that of the individual components.

The peaks in the temperature range 190° - 500°C obtained for these samples are shown in Table 3.2. In addition all the samples showed a peak at 740°C, probably representing loss of phosphorus from the sample. Traces for the materials are shown in Figure 3.1. All the samples displayed have at least two peaks, the maxima of which occurred within the temperature ranges 325° - 360°C and 390° - 420° respectively. Most showed evidence of a further less strong peak at between 15° and 40°C above the latter peak, occuring as a shoulder of this peak. The two major peaks in needles of $(C_3H_6N_6)_{1.0}.H_3PO_4$ occurred at the low end of the quoted ranges whether dried at 110°C or treated at 210°C. The other crystal types, dried at 110°C, tended to exhibit these peaks at around 350°C and within the range 410° - 420°C, although thin reflective plates exhibited its lower peak at 360°C. This material alone had no maxima within the range 300°C - 350°C. Treatment at 210°C tended to lower the positions of these peaks by 10° - 20°C in small needles and small block plates of $(C_3H_6N_6)_{1.2}.H_3PO_4$. The lower peak in the case of thin reflective plates was likewise lowered to 345°C. Materials dried at 110°C also displayed peaks in the range 190° - 320°C, which were

TABLE 3.2 Differential Thermal Analysis peaks occurring in samples of melamine phosphate, dried at 110°C and heat-treated at 210°C, in the range 190° - 500°C.

Dried at 110°C	Low Temperature Peaks	Intermediate Peak	High Temperature Peaks
Medium Needles: $(C_3H_6N_6)_{1.0}\cdot H_3PO_4$	269	325	392
Small Needles: $(C_3H_6N_6)_{1.2}\cdot H_3PO_4$	290, 320	350	411, 443
Small Block Plates: $(C_3H_6N_6)_{1.2}H_3PO_4$	290, 315	350	410, 439
Thin Reflective Plates: $(C_3H_6N_6)_{1.3}\cdot H_3PO_4$	190, 295	360	419
Plates: $(C_3H_6N_6)_{2.0}\cdot H_3PO_4$	279	349	419, 460
Treated at 210°C			
Medium Needles: $(C_3H_6N_6)_{1.0}\cdot H_3PO_4$		336	400
Small Needles: $(C_3H_6N_6)_{1.2}\cdot H_3PO_4$		336	403, 435
Small Block Plates: $(C_3H_6N_6)_{1.2}\cdot H_3PO_4$		333	403, 419
Thin Reflective Plates: $(C_3H_6N_6)_{1.3}\cdot H_3PO_4$	295	345	419
Plates: $(C_3H_6N_6)_{2.0}\cdot H_3PO_4$	320	350	419, 460

absent from materials treated at 210°C, except in the case of thin reflective plates, where solubility studies have shown that conversion is incomplete at temperatures below 220°C. The exact pattern of these peaks was very variable, one or two peaks occurring at different temperatures within the quoted range. The low temperature peak at 270°C of needles of $(C_3H_6N_6)_{1.0}.H_3PO_4$ was particularly strong with respect to the other peaks in its trace, compared to materials of a higher melamine to phosphate ratio. The traces of materials dried at 210°C were very similar to those of the respective pyrophosphates (small needles or small block plates to $(C_3H_6N_6)_2.H_4P_2O_7$, and dimelamine phosphate to tetramelamine pyrophosphate). The low temperature peaks in materials dried at 110°C therefore probably represent condensation of orthophosphate, and are not directly relevant to intumescence.

Thus differences in the materials resulting from their production and subsequent heat treatment have been detected, and may explain some of the differences in the performances of coatings in fire tests, probably arising mainly from variations in the exact position of the peak occurring within the temperature range 325° - 360°C, within the range where epoxy resin, cured as for fire tests for nine days at 55°C, shows activity in its DTA trace (see Figure 3.2).

3.5 Infra-red Spectra of Melamine Phosphate

Infra-red spectra over the region 2000 cm^{-1} to 300 cm^{-1} were obtained for needles of $(C_3H_6N_6)_{1.0}.H_3PO_4$, small needles of $(C_3H_6N_6)_{1.2}.H_3PO_4$ and thin reflective plates of $(C_3H_6N_6)_{1.3}.H_3PO_4$, all dried at 110°C, using potassium bromide discs.

Needles of $(C_3H_6N_6)_{1.0}.H_3PO_4$ gave a good spectrum with well

defined peaks and bands, as shown in Figure 3.3(a). The other materials however yielded poor spectra, despite exactly similar sample preparation techniques. In as much as any deductions were possible these latter spectra appeared similar to each other, but differed in some respects from the former, especially in lacking peaks at 1245 cm^{-1}, and 600 cm^{-1}.

The non-integral stoichiometry of the latter materials has led to difficulties in determining whether differences in the crystal unit cell exist; further work is required to investigate the crystalline structures of the various types of melamine phosphate.

FIGURE 3.1 : Differential Thermal Analysis Traces for five crystalline types of Melamine Phosphate, dried at 110°C, and heat-treated at 210°C for 48 hours.

Dried at 110°C

Treated at 210°C

Medium Needles of $(C_3H_6N_6)_{1.0}\cdot H_3PO_4$

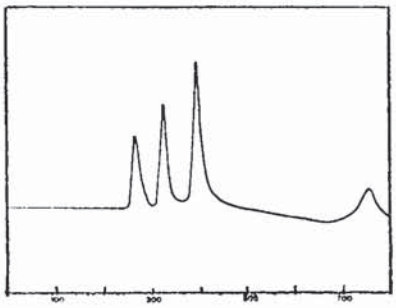

Temperature (°C)

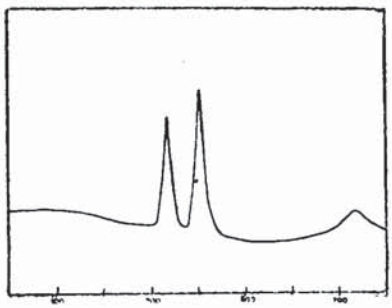

Temperature (°C)

Small Needles of $(C_3H_6N_6)_{1.2}\cdot H_3PO_4$

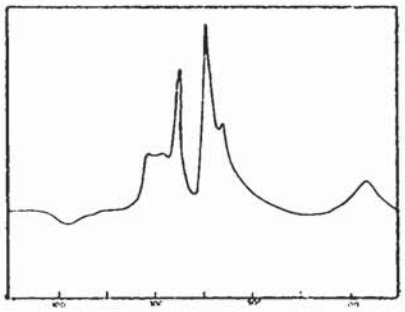

Temperature (°C)

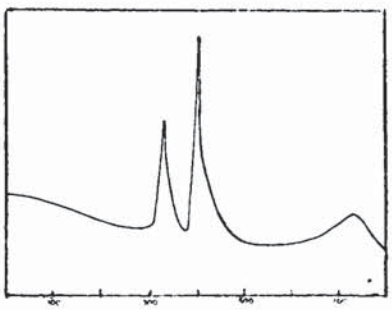

Temperature (°C)

Small Block Plates of $(C_3H_6N_6)_{1.2}\cdot H_3PO_4$

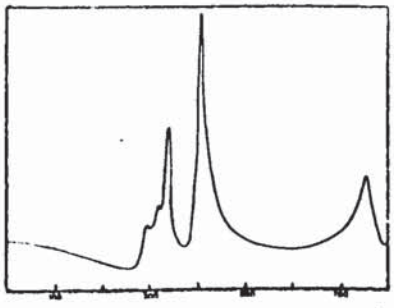

Temperature (°C)

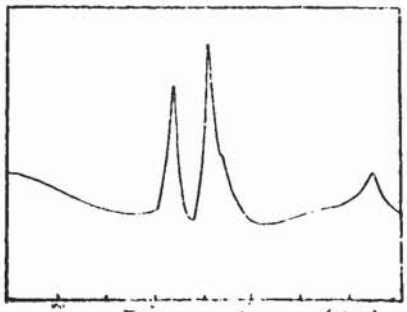

Temperature (°C)

FIGURE 3.1 (cont.)

Dried at 110°C

Thin reflective plates of $(C_3H_6N_6)_{1.3}\cdot H_3PO_4$

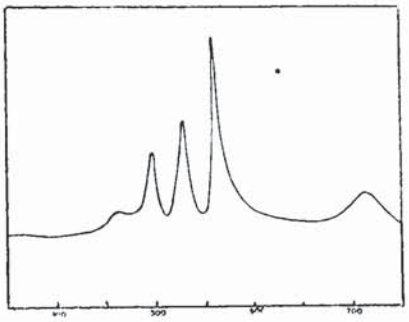

Temperature (°C)

Treated at 210°C

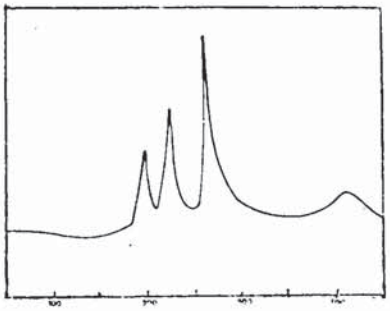

Temperature (°C)

Plates of $(C_3H_6N_6)_{2.0}\cdot H_3PO_4$

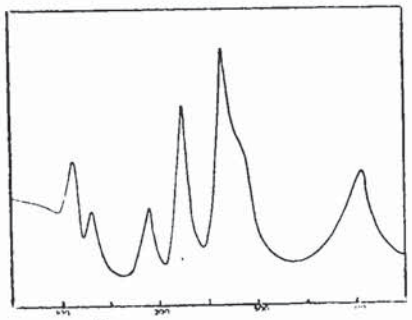

Temperature (°C)

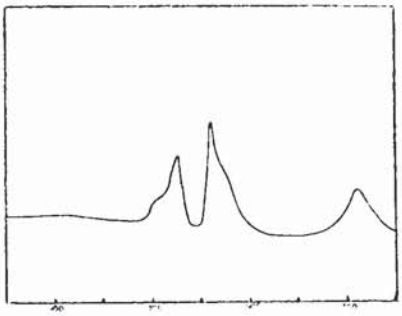

Temperature (°C)

FIGURE 3.2 : Differential Thermal Analysis trace for epoxy resin and hardener cured for twenty four hours at ambient temperature followed by nine days at 55°C.

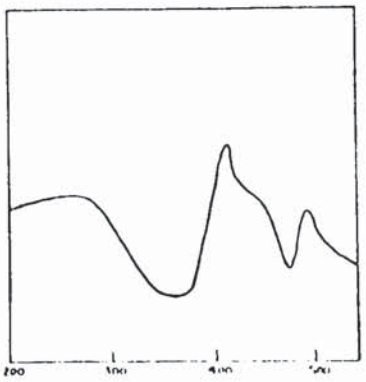

Temperature (°C)

FIGURE 3.3 : Infra-red spectra in the range 2000 - 300 cm^{-1} of needles of $(C_3H_6N_6)_{1.0}.H_3PO_4$ and thin reflective plates of $(C_3H_6N_6)_{1.3}.H_3PO_4$

(a) Needles of $(C_3H_6N_6)_{1.0}.H_3PO_4$

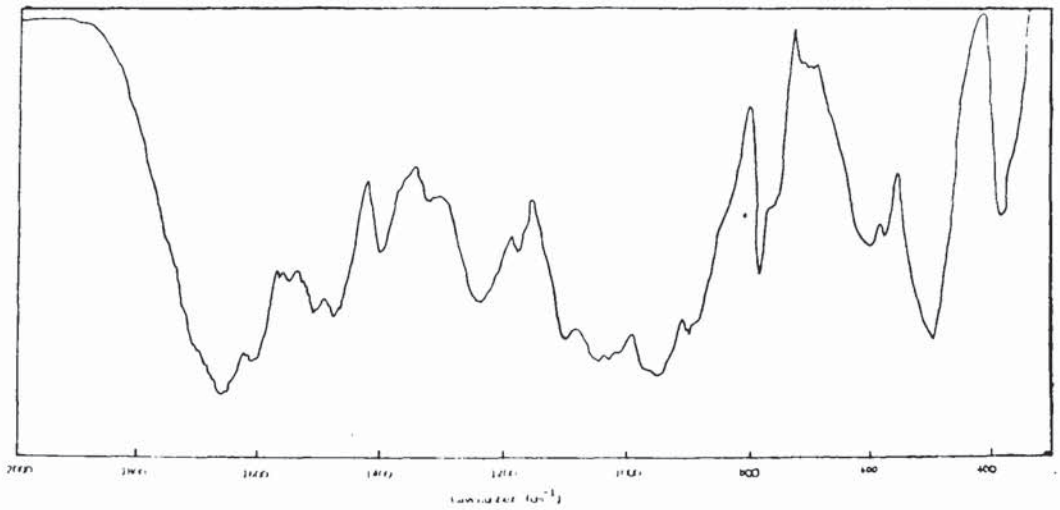

(b) Thin reflective plates of $(C_3H_6N_6)_{1.3}.H_3PO_4$

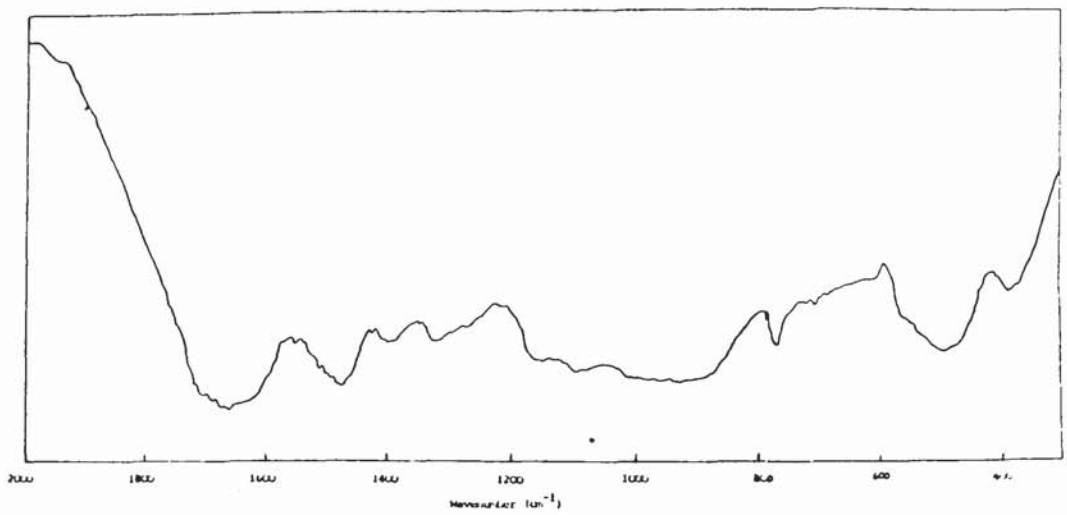

CHAPTER 4

THE FIRE TESTING DEVICE

CHAPTER 4

THE FIRE TESTING DEVICE

Nomenclature

a, b : parameters of the exponential decay model

a',b' : parameters of the exponential decay model at low ranges

a", b" : parameters of the exponential decay model at high ranges

p, q : parameters of the power law decay model

p', q' : parameters of the power law decay model at low ranges

p", q" : parameters of the power law decay model at high ranges

u, v : parameters of the linear decay model

R : range

S : range of the boundary

W : incident heat flux

4.1 The Construction of the Fire Testing Device

The Fire Testing Device, shown in Plate 4.1 and schematically outlined in Figure 4.1, consists essentially of a tunnel burner of face measuring 152 mm x 102 mm, burning a mixture of air and natural gas. The sample to be tested, which takes the form of a coating of thickness 6 mm on a mild steel substrate plate measuring 95 mm square, is positioned facing the burner, at a distance which may be varied to achieve a range of temperatures to which the sample is exposed. The whole device is mounted on a bench top, protected by means of a 6 mm thickness of Sindanyo,(R) on top of which have been placed a row of 38 mm high fire bricks laterally in the fire testing zone itself. The test sample is placed in a well in a frame of Sindanyo, such that it is positioned in the same horizontal plane as the burner. This is indicated in Figure 4.2. The frame is constructed of four 6 mm layers of Sindanyo bolted

(R) Sindanyo is a registered trade mark of T.A.C. Construction Materials Ltd.

together; the cut-out for the well in the outer layers is smaller by 6 mm along the sides and base than that in the inner layers, thus providing a secure groove for seating a sample. The outer layers are also 6 mm higher than the inner layers; into the groove thus formed along the top of the frame fits a block of Sindanyo of height 150 mm consisting of two 6 mm sections bolted together, which encloses and isolates the back of a sample from the burner. A sheet of 1.5 mm mild steel is loosely bolted onto the front of the frame around the sample well at two points to give extra protection to the Sindanyo frame by reducing thermal stresses. The frame may be moved manually on steel bearers, lubricated by means of a spray containing aluminium and graphite in a non-drying medium. Rods of Tufnol (R) are attached to the back of the frame to enable it to be moved. The burner to sample distance, hereinafter known as its range, may be varied from 60 mm to 600 mm.

The working area is surrounded by an extraction hood, from which a duct leads via a bifurcated fan to the atmosphere. Sliding doors, of heat resistant glass, are provided in front of the working area; the other three sides and the ceiling of the hood are of 1.15 mm mild steel sheet covered with aluminium paint for protection.

The pipework for the air and gas supplies, shown in Plate 4.2 and Figure 4.3, incorporates several measuring and safety devices. Flow rates may be measured by means of rotameters, Type 18 with a Duralumin float for gas, and Type 24 with a Koranite float for air. Manometers are provided to read air pressure (by mercury), gas pressures prior to pressure reduction and after passing a "zero" governor, and mixture pressure (all by water). Manufacturers instructions recommend an air pressure of 53 mm Hg, which is achieved by a two stage reduction from the available compressed air supply. Typical values for gas pressures

(R) Tufnol is a registered trade mark.

Plate 4.1 : The Fire Testing Device

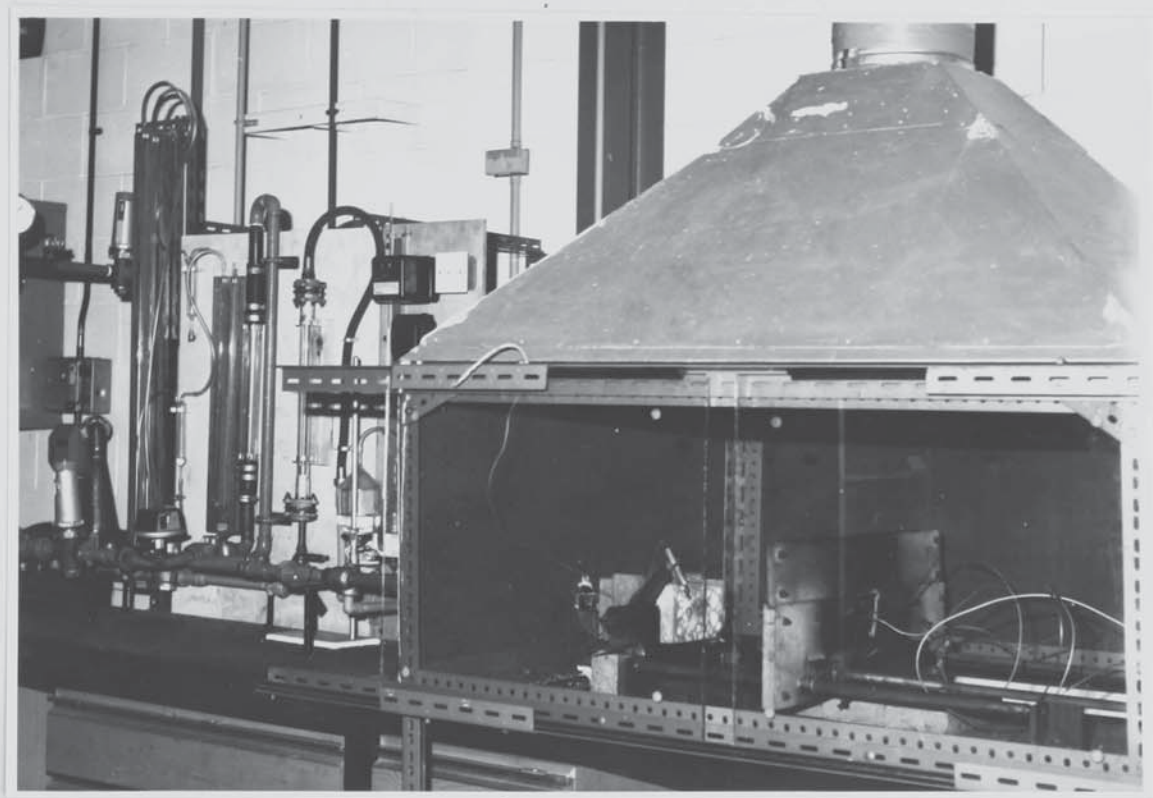

Plate 4.2 : Air and Gas Supply Pipelines and Controls for the Fire Testing Device

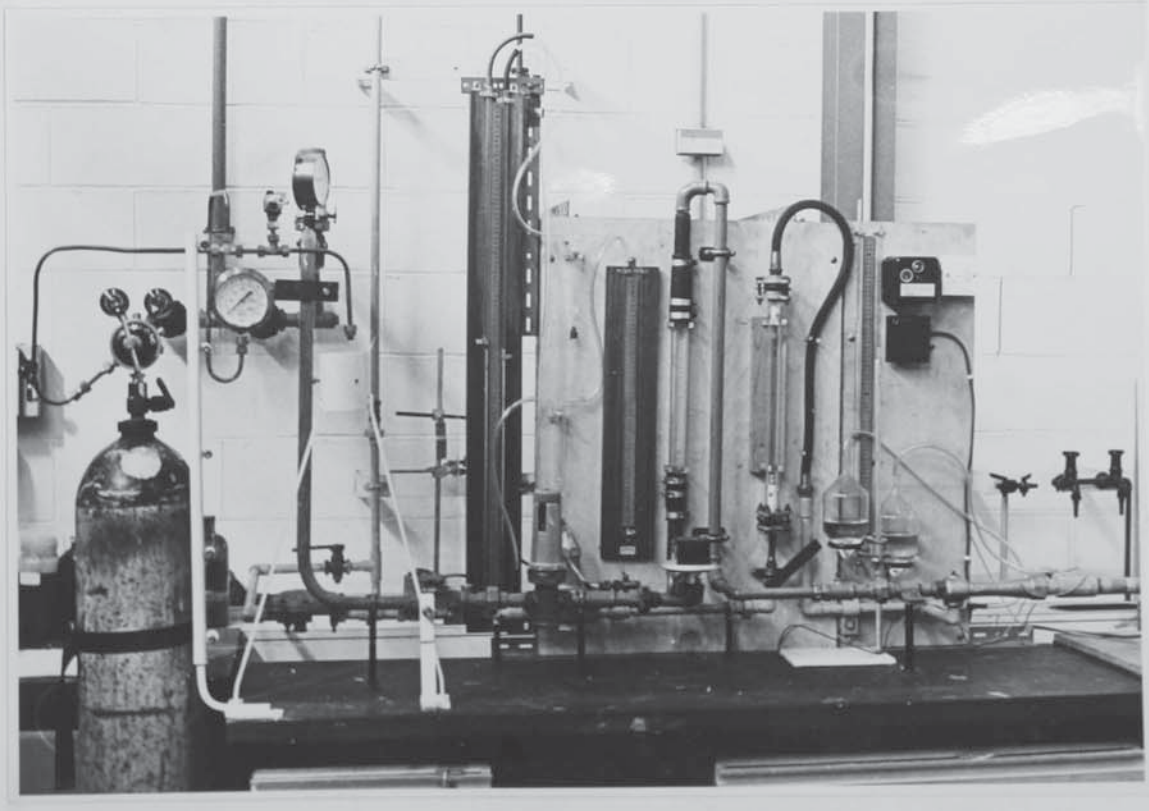

FIGURE 4.1 : Schematic Diagram of the Fire Testing Device (all measurements in mm)

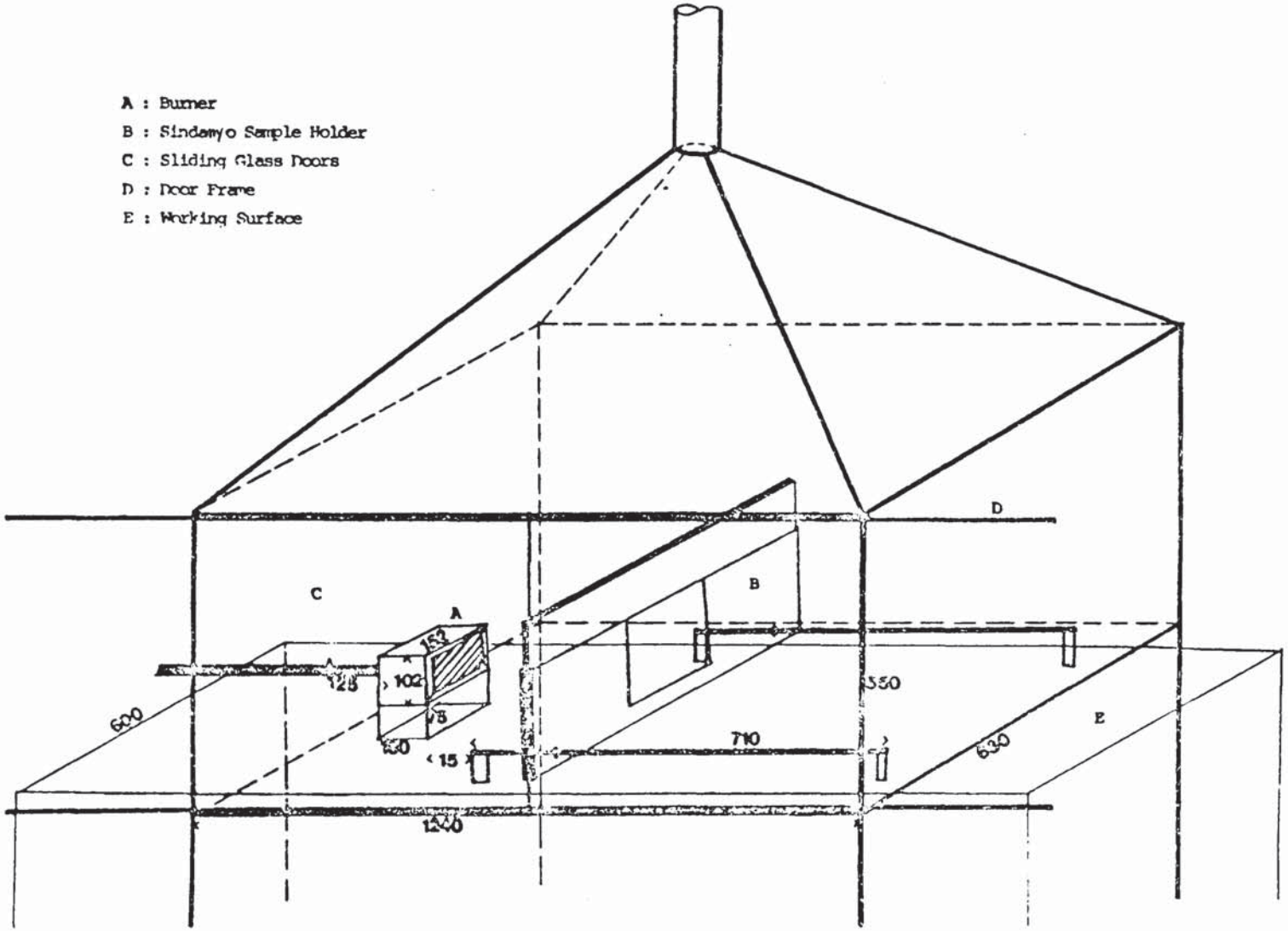

FIGURE 4.2 : Schematic Diagram of the Sindanyo Sample Holder, viewed from the Burner. (all measurements in mm).

A : Sample Well

B : Holes for thermocouples measuring face temperature

C : Mild Steel Plate

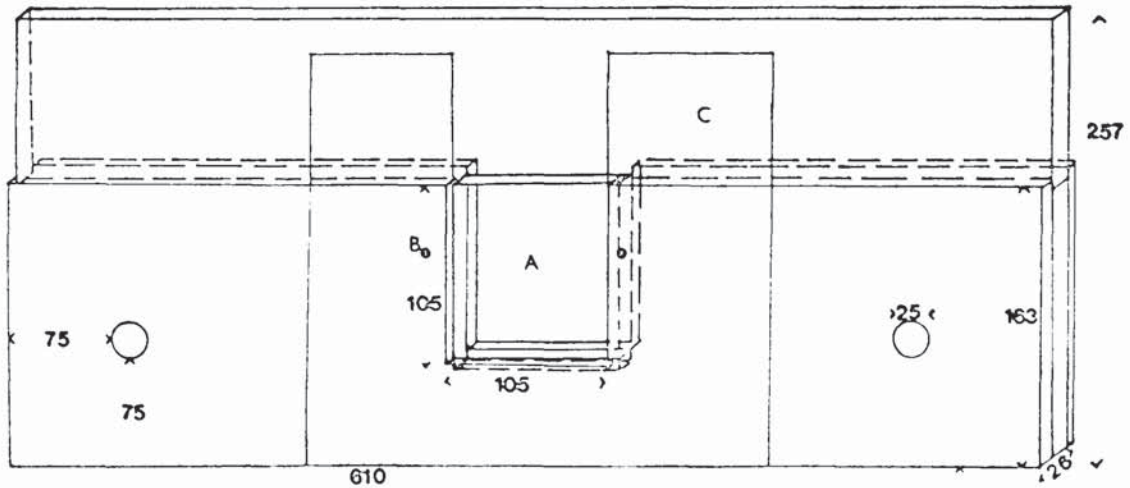

FIGURE 4.3 : Schematic Diagram of the Air and.Gas Supply Pipelines and Controls for the Fire Testing Device.

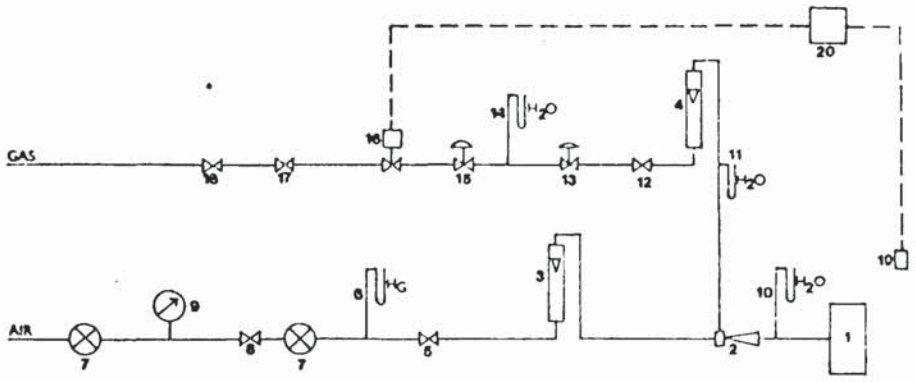

1 : Burner

2 : Air blast injector

3 : Air flow measurement; Rotameter, size 24

4 : Gas flow measurement; Rotameter, size 18

5 : Value with Butterfly Positioning

6 : Air pressure measurement, Mercury manometer

7 : Pressure Reduction Valves (Spirax)

8 : Shut-off valve

9 : Pressure gauge (0 - 100 p.s.i.)

10 : Mixture pressure measurement, Water manometer

11 : Gas pressure (reduced) measurement, Water manometer

12 : Shut - off valve

13 : Zero governor

14 : Gas pressure measurement, Water manometer

15 : Pressure control governor

16 : Solenoid operated shut-off valve

17 : Non-return Valve (otan)

18 : Shut - off valve

19 : Photo-cell

20 : Electrical control

before and after reduction are 80 mm water gauge and -10 mm water gauge respectively (i.e. being entrained by the air stream); 140 mm water gauge is typical for the mixture. The gas to air flow rate ratio may be varied at the point of admixture.

Ignition is controlled automatically being brought about by an electric spark after a delay of approximately one minute from initiation. The sparking device is hinged, enabling its removal from the flame after ignition by means of a wire attached to it leading to the front of the working area. An ultra-violet sensitive photocell monitors the burner continuously and causes an immediate cessation of gas flow by means of a solenoid valve in the gas supply pipeline, should the flame fail at any time. The gas supply is also automatically shut off if the air supply is cut off or the electronic system switched off.

4.2 Temperature Measurement of Test Conditions

Two chromel-alumel thermocouples, mineral insulated to 3 mm diameter and sheathed in Inconel (R), pass through the Sindanyo frame at a height of 160 mm above the Sindanyo working surface on either side of the sample. The projecting sections of the thermocouples are turned down to a depth of 15 mm to minimise conduction losses. The thermocouple tips became blackened during the initial test, and remained thus.

It is very difficult to measure accurately the temperature of a hot gas by means of a thermocouple, the main causes of inaccuracy being

a. Radiation from the thermocouple to cooler surroundings,

b. Conduction down the thermocouple wires,

c. The gas velocity,

d. Inaccuracies in calibration.

(R) Inconel (76/16/7 Nickel Chromium Iron) is a registered trade mark of Henry Wiggin & Co. Ltd.

For this purpose, the use of a suction pyrometer is recommended (51).

The thermocouples incorporated in the Fire Testing Device are therefore mainly to ensure the reproducibility of conditions, ie. that for a given sample range and burner conditions the temperature readings are similar on any occasion of use, and to detect any differences. Variation in the readings from the two thermocouples indicates an air flow across the face of the sample. The thermocouples are especially required in ensuring reproducibility when the sample range is varied during a test.

In a calibration experiment, two chromel-alumel mineral insulated thermocouples of diameter 1 mm, coiled in a semi-circle near their tips to reduce conduction losses, were mounted along the central axis of the test area, one in the plane of the sample frame, in front of a mild steel plate placed in the sample well, and the other 45 mm in front of the former thermocouple. During a fire test, char expansion causes the char front to approach the burner, and its face temperature is thus further increased. From the calibrations obtained from these two thermocouples it is possible to relate thermocouple temperature readings from either side of the sample, together with an observation of the char thickness, to the temperature on the front face of a char. This procedure was utilised in the analysis of char thermal resistance (Section 6.4). Reradiated heat is a major influence on thermocouple readings; the frame is the main source of such reradiated heat, and the influence of the frame is considerably reduced in the latter calibration. According to char thickness, either of these calibration curves, or a mean curve was used, in modelling the front face temperature of a char. It should be stated that gas temperatures are not being modelled; but the blackened

tip of a thermocouple was considered to be a reasonable model for the face of a black char. The calibration curves obtained are shown in Figure 4.4. Noteworthy is the dip in temperature beyond a range of around 250 mm, a phenomenon observed also in calibrating the fire testing device with respect to incident heat. The side-mounted thermocouples appear to give an approximately linear decay response pattern for ranges from 100 mm to 400 mm.

The meter used for all thermocouples was a manually compensated voltmeter, calibrated in degrees Celsius, and accurate to within $\pm$ 2°C in the range 0° - 1100°C.

4.3 Fire Testing Procedure

The process of fire testing was designed to give information about the nature of the chars produced from a variety of formulations of coating. This was obtained by means of a thermocouple attached to the sample substrate, and by visual and photographic observation, as follows:

(1) By reading substrate temperatures at regular intervals and thus compiling a time-temperature response curve for the substrate which might be compared to the temperature to which the char face was exposed (this is modelled as explained in Section 4.2).

(2) By noting the thickness of char present throughout a test. A wooden one metre rule has been mounted on the side of the working surface. The conditions of a fire test make it impracticable to mount a rule of either wood or metal closer to the sample; however by careful alignment of the eye perpendicular to the burner to sample axis, a measurement accurate to within around 3 mm may be obtained. All measurements took as zero position the original surface plane of the sample. During the course of a fire test the boundary between burned and unburned material retreats towards the substrate, but within the limits of

FIGURE 4.4 : Relationships between readings of several thermocouples on the fire testing device and their range.

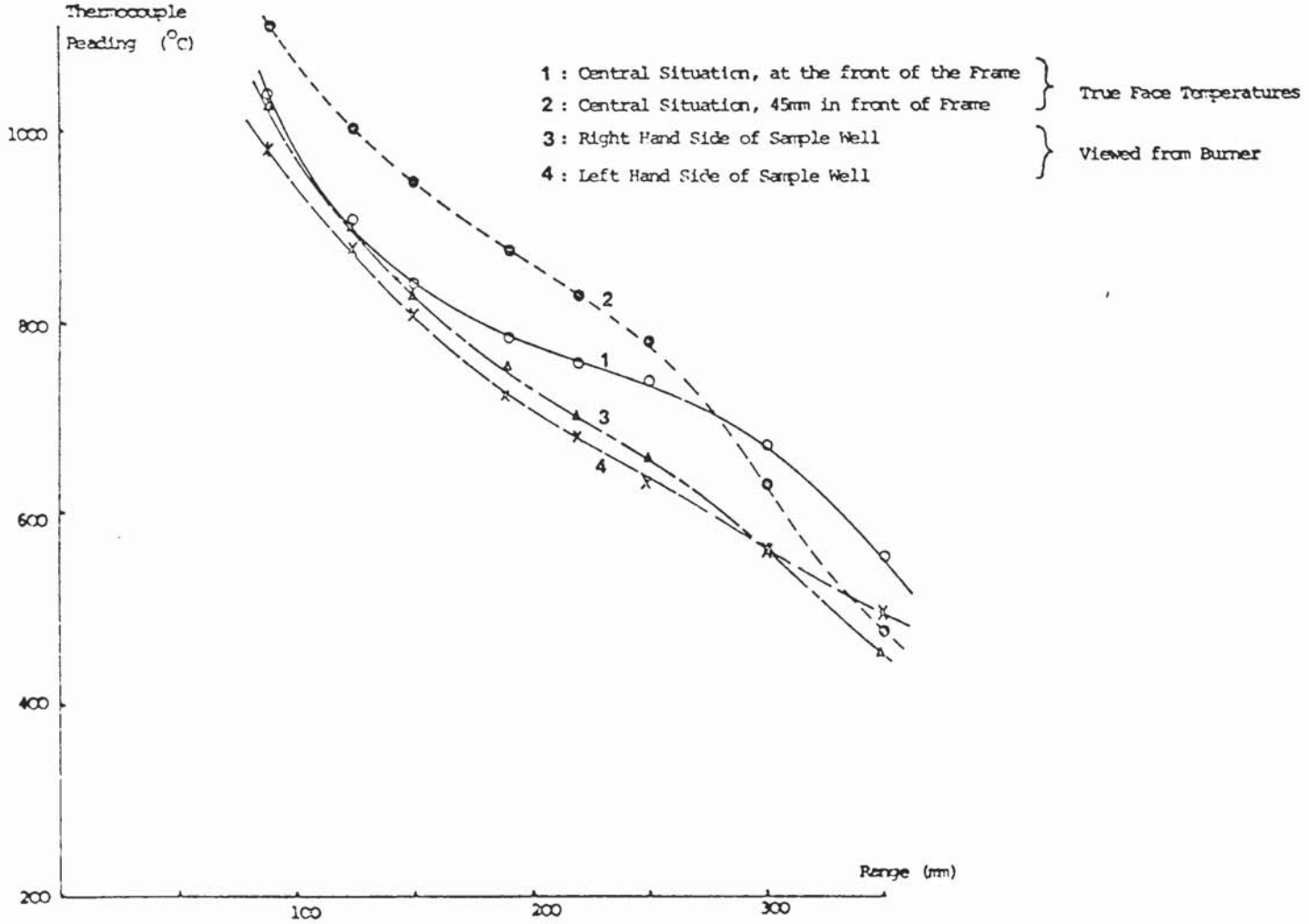

accuracy of the technique of measurement, the above is a reasonable approximation (the maximum error due to this being 6 mm).

(3) By recording the progress of a test photographically. It was found that "fast" film, of rating ASA 400 was most suitable. A variety of cameras and lenses were used. In general best results were obtained by an exposure slightly in excess of that suggested by the electronic exposure meter. The camera was mounted slightly above the plane of the sample outside the test area, with the glass door of the test area drawn back to give a clear field of view. No special filters were used.

The record of char performance during a test is an integral part of the test result together with the face and substrate time-temperature curves. The dissimilar behaviour in terms of substrate time-temperature response pattern of two similar samples tested under apparently similar conditions is usually mirrored in a difference in the expansion and structure of their respective chars. It has frequently been found that a sample exhibiting a large degree of expansion in the early stages of a test deteriorates more rapidly thereafter than an apparently similar sample which expands to a lesser extent in the early stages. Whilst not explaining such differences, a link is thereby established between substrate time-temperature response and char performance.

The normal operating procedure common to all fire tests is described in this section; individual fire testing regimes are described in Section 6.1. The sample was placed in the frame at a specified range and its thermocouple reading the substrate temperature connected. One or more thermocouples were, in some tests, placed at

increasing distances of 2 mm, 4.5 mm, 9 mm behind the substrate to indicate the heat transfer taking place to the environment from the substrate. It was found that complete insulation of the substrate to avoid heat losses was impossible. Therefore rather than using any form of partially effective insulation, the heat losses were measured in a series of specially designed experiments described in Section 6.4, and after compensating for these losses an assessment of the thermal resistance of a variety of chars was made possible. It was assumed that at any given range the heat transfer characteristics to the environment would be similar; this assumes that the air flow patterns and velocities are similar for any particular configuration on any occasion of use. This was substantially verified.

After ensuring that the hinged ignition sparker was in place in front of the burner, and that the gas valves were open, the air supply was turned on, its pressure being checked as 52 ± 3 mm Hg. The automatic ignition sequence was then activated; after around one minute gas is allowed into the burner and ignition occurs. This was taken as the start of the test. The ignition sparker was then removed from the flame by means of a wire reaching over the glass doors from the sparker. Throughout the test the fume extraction was active, even when no coating was being burned. This prevents excessive heating of the surrounds, such as the upper runners for the glass doors.

At the end of a fire test, either turning off the air or switching off the automatic ignition control causes an automatic cut of the gas supply to the burner, and thus extinguishes the flame.

During the fire tests a constant check on air and gas flow rates was maintained, these being set at 370 litre min^{-1} and 26 litre min^{-1}

respectively. Immediately after ignition the gas flow rate tended to rise to 29 litre min^{-1}, but returned within around thirty seconds to its preset level of 26 litre min^{-1}. Under normal circumstances air and gas flow rates remained constant to within 10 litre min^{-1} and 0.5 litre min^{-1} respectively, slight fluctuations in either however resulting in variations of up to 20°C in the temperatures monitored by the side mounted thermocouples on the frame.

Fire tests were carried out under a single set of air and gas flow conditions as described above. The fire testing device has however been calibrated for use at other air and gas flow rates. At any given air flow rate, there exists a limited range of gas flow rates at which the burner is capable of operating. Thus at an air flow rate of 370 litre min^{-1}, the range of permissible gas flow rates is 24 litre min^{-1} up to 31 litre min^{-1}.

4.4 Air Flow Patterns Within the Test Area

Smoke tests were carried out using MSA smoke tubes to establish air flow patterns within the test area with the fan operational. As expected, there was a considerable updraught centred above the frame, irrespective of its range. This updraught crossed the face of the sample and the rear of the substrate with the burner operational, and in this case was largely thermal in nature. Without the burner being operational, the sample frame itself was below the level of the main updraught in an area of relative quietitude. There were under both circumstances a few eddies and cross-currents near the base of the frame. These air flow patterns are shown schematically in Figure 4.5.

It is apparent that a considerable contribution to the heat transfer to the samples is convectional; the thermal updraught therefore causes a vertical gradient on the sample with respect to incident

FIGURE 4.5 : Air Flow Patterns within the Fire Test Area, with burner turned off and operational respectively.

Figure 4.5.a : Air flow patterns with burner not operational (fan working)

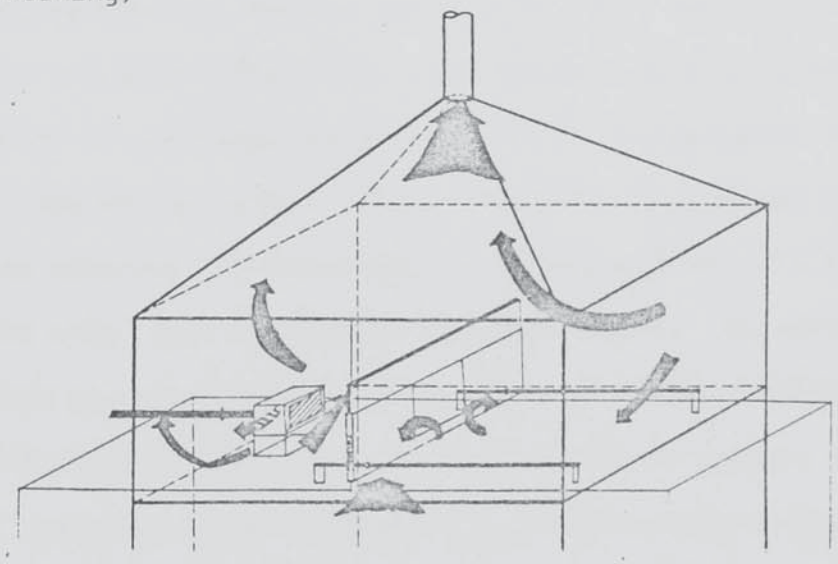

Figure 4.5.b : Air flow patterns with burner (and fan) operational.

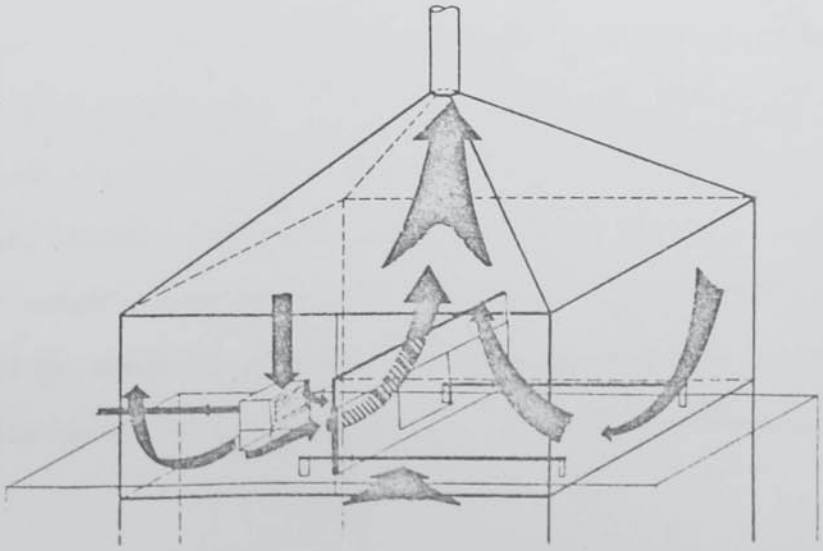

heat, the upper parts of the sample receiving the most heat. In most cases this led to the coating failing first on the upper regions of the substrates.

4.5 Radiometry

4.5.1 The gold-disk radiometer

A gold-disk radiometer was supplied by the Fire Research Station, Borehamwood, to calibrate the fire testing device. This instrument is of the type described by McGuire and Wraight (52). It consists basically of two gold disks 100 μm thick which give a rapid response time, to which 40 swg gauge chromel-constantan thermocouples are silver soldered in opposition to each other. The front face of one disk is blackened to increase its absorptivity, and mounted behind a thin mica window; the other disk is shielded from the window. The working parts are supported on ceramic posts and contained in a water cooled, chromium-plated brass enclosure. The voltage may be read on a suitable instrument connected to the radiometer by ordinary copper wires. The output was also recorded on a chart recorder. A calibration curve to convert voltage to radiation in Watts cm^{-2} was provided by the Fire Research Station, and is reproduced in Figure 4.6.

The radiometer was clamped onto the handles at the back of the frame, in such a way that the mica window was placed in the same plane as the front of a sample prior to a fire test. Its height within the sample area was varied to give results at heights of 175 mm, 160 mm, 143 mm and 125 mm above the working surface, thus giving a representative set of results from the sample area which reaches from between 90 mm and 185 mm above the surface. Computational analyses were carried out on results obtained at all except 125 mm for which insufficient data

FIGURE 4.6 : Calibration curve for the radiometer used for calibration of the Fire Testing Device (supplied by the Fire Research Station)

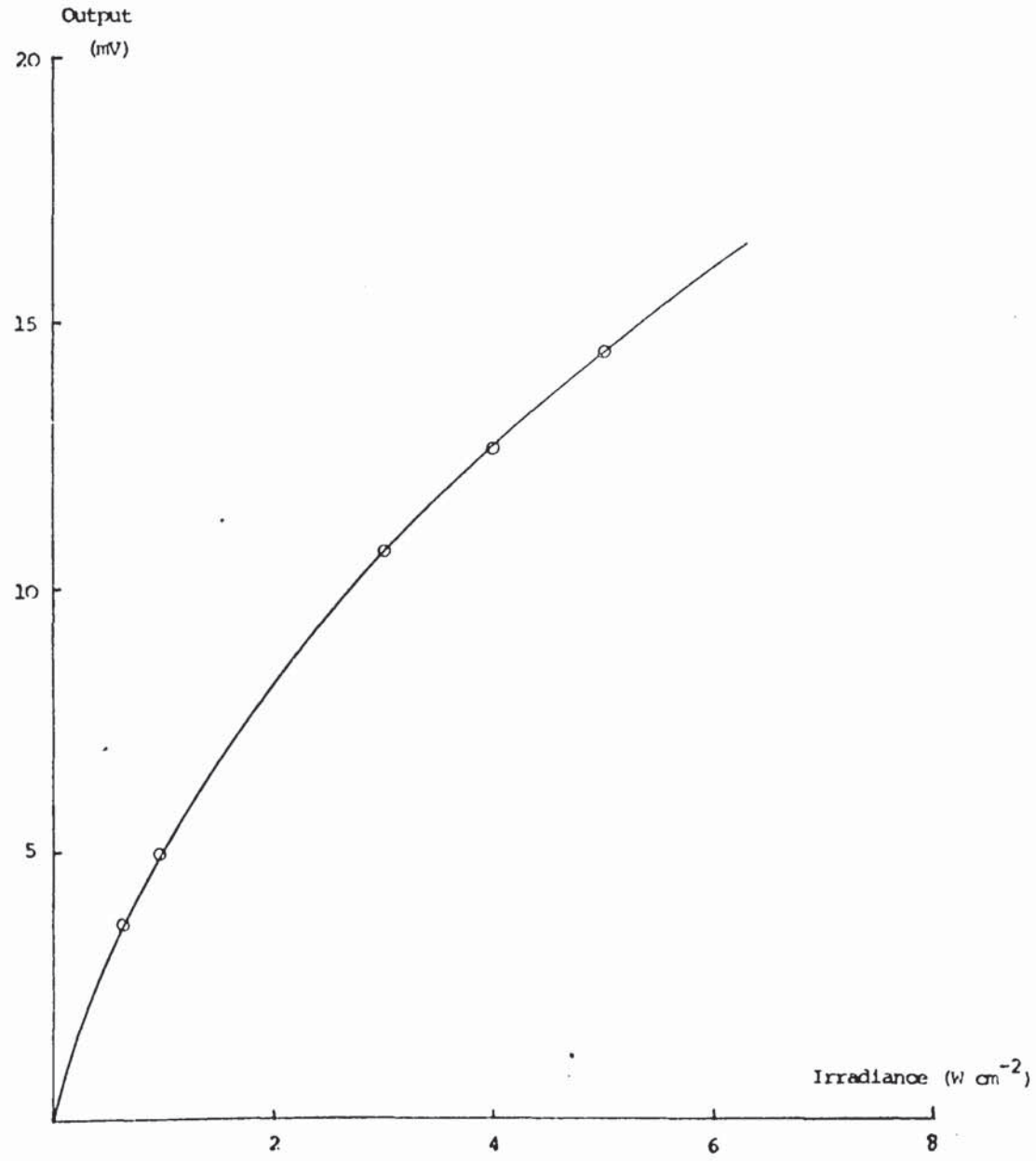

were available. Three air/gas flow regimes were used:

(a) normal : 370 litre min^{-1} air, 26 litre min^{-1} gas

(b) high : 370 litre min^{-1} air, 29 litre min^{-1} gas

(c) low : 280 litre min^{-1} air, 23 litre min^{-1} gas

The largest quantity of experimental data was obtained at normal flow rates and heights of 175 mm and 143 mm.

4.5.2 Results of Radiometry

The results obtained from radiometry were initially plotted on linear axes. Illustrative of the type of behaviour encountered, Figure 4.7 shows the variation of incident heat flux with range at a height of 175 mm above the working surface at normal air and gas flow rates. Noticeable is the dip beyond a range of around 250 - 300 mm; this is similar behaviour to that of temperature with respect to range and shows an increase in the rate of decline of incident heat flux. A summary of results appears in Table 4.1, which gives values obtained from graphs at regular intervals of range.

It may be seen that in general the incident heat flux is greater with increasing height above the working surface, which gives rise to the earlier failure of the top of a sample coating in a fire test. However at very low ranges where the updraught is not so significant, the centre of the sample well receives most heat, as it faces the centre of the burner. At the low flow rate the decrease in incident heat flux with increasing range is more marked than at higher flow rates, especially beyond a range of around 250 mm.

During the process of obtaining data, the radiometer was held in each position for a minimum of five minutes. During this time rapid fluctuations in incident heat flux were noted; the values in Table 4.1

TABLE 4.1 :Mean Typical Values of Incident Heat Flux at Various Heights Above the Working Surface Within the Sample Well Using Three Flow Regimes; Values are given in Watts cm^{-2}.

Range	Normal Flow Rates				High Flow Rates			Low Flow Rates	
(mm)	175mm	160mm	143mm	125mm	175mm	160mm	143mm	175mm	143mm
150	3.4	3.5	3.4			3.8	4.6	4.0	3.7
200	2.7	2.7	2.4		3.08	3.0	3.1	2.7	2.65
250	2.20	2.10	1.95		2.52	2.40	2.40	2.1	1.95
300	1.78	1.70	1.58	1.15	2.16	1.95	2.00	1.8	1.20
350	1.45	1.23	1.20	0.95	1.70	1.40	1.36	0.80	0.75
400	1.06	0.90	0.90	0.65	1.12	1.00	0.92	0.45	0.40
450	0.64	0.56	0.55	0.40	0.80	0.70	0.60	0.20	0.20
500	0.40	0.40	0.40		0.50	0.40	0.40	0.20	0.20

FIGURE 4.7 : Results of radiometry showing limits of variability for each reading, at a height of 175 mm above the surface with normal air and gas flows (370 litre min^{-1} & 26 litre min^{-1} respectively)

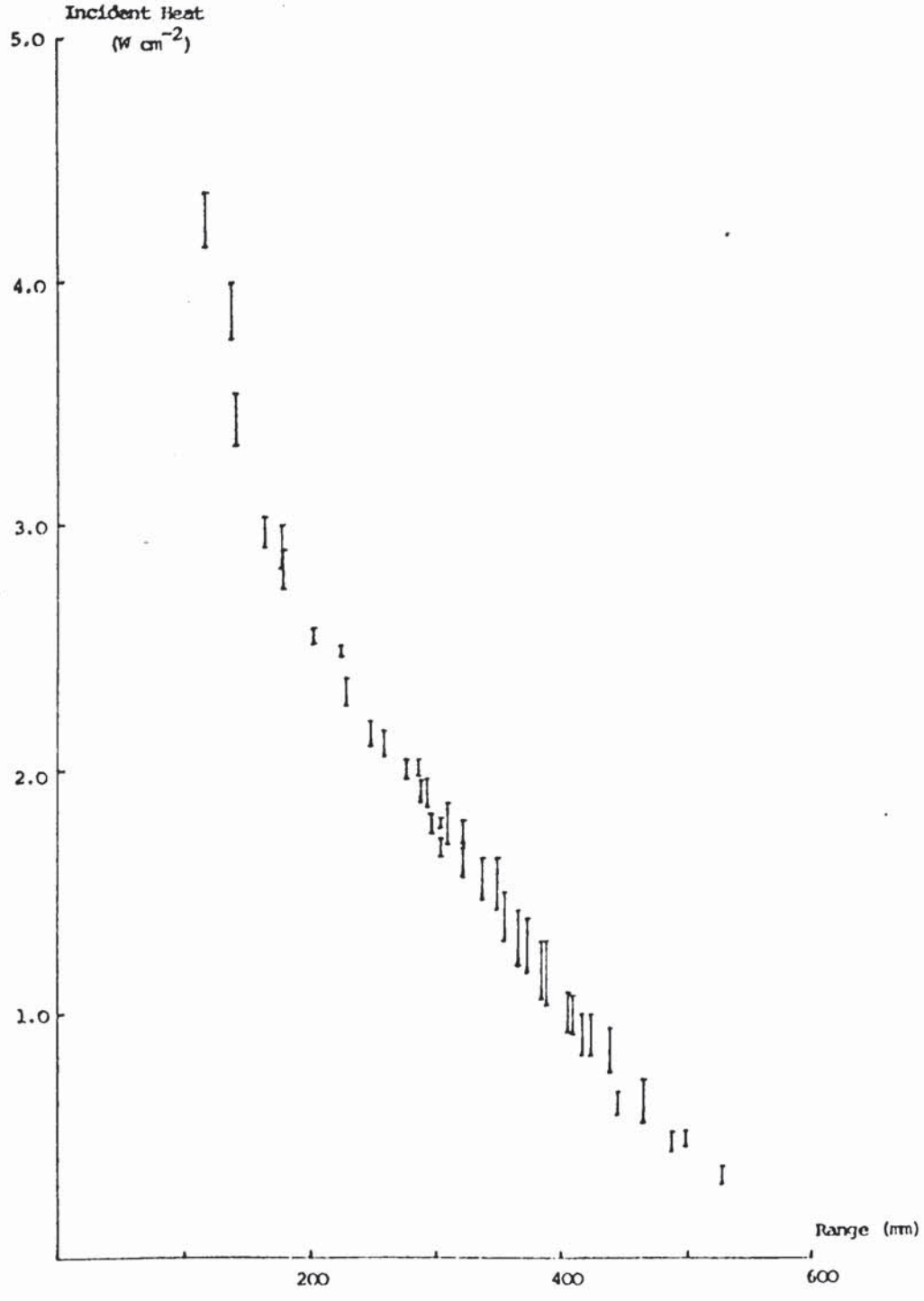

are mean values. These fluctuations were greatest at low range (this is however a small percentage deviation), and at ranges beyond the upcurve, generally between 300 mm and 400 mm, where a typical fluctuation would be around 0.25 W cm^{-2}. At a range of around 250 mm, the typical fluctuation was around 0.10 W cm^{-2}. This is illustrated in Figure 4.7.

4.5.3 Models for incident heat flux variation with range

Three mathematical regressive model types have been used to account for the above behaviour. Linear regression analysis was used, converting to logarithmic forms to accommodate non-linear behaviour. A NAG library routine (53) was used for computational purposes. The basic models are as follows:-

(a) Linear decline in incident heat flux. This is applicable to the greatest extent over the range 100 mm $<$ R $<$ 450 mm, as it underestimates severely the heat flux at low and high ranges, and may underestimate slightly where the rate of decline changes.

$W = u - vR$: 100 mm $<$ R $<$ 450 mm

(b) Exponential decay in incident heat flux. This tends to overestimate the incident heat at low ranges, except perhaps at extreme low ranges, and at high ranges; within the zone where the rate of decline changes, the model tends to underestimate the incident heat flux.

$W = a.\exp(bR)$

$\ln W = \ln a + bR$

(c) Power law model for the decay in incident heat flux. This was found to be totally inapplicable for use as a single equation over the full range of the fire testing device.

$W = p.R^q$

$\ln W = \ln p + q \ln R$

Figures 4.8 and 4.9 show plots of ln W vs. R and ln W vs. ln R respectively at normal air and gas flow rates and a height of 175 mm. In both cases there appears to be evidence of a change of gradient between a range of 280 mm and 400 mm. Inspection of the plots shows that a power law model, ln W vs. ln R gives a very good fit when two lines are used except in the area where the gradient is changing, whereas in the exponential model, ln W vs. R, there is also a suggestion that such a bizonal consideration would give a better model. In this case however the single zone model is not entirely unreasonable, although less accurate than a bizonal model for analysis by exponential decay. Both bizonal models give a boundary between the two zones at a range of 360 mm. Figure 4.10 shows on a linear plot the single zone linear and exponential models and the bizonal exponential and power law decay models for the calibration under consideration. These may be compared with the actual results shown in Figure 4.7. The change in the rate of decay of incident heat flux occurs within the zone over which the gradients of the logarithmic plots change.

A technique was developed to obtain the position of the boundary computationally, using for computational trials the above calibration at a height of 175 mm at normal air and gas flow rates. Using regression analysis on the models

$\ln W = \ln a' + b'R, \quad R < S$

and

$\ln W = \ln p' + q' \ln R, \quad R < S$

successively for the boundary S increasing in steps of 50 mm, it was noted that the values of a', b' and p', q' were minimised at around S= 300 mm. As this value of S is approached the values of the coefficients

FIGURE 4.8 : Plot of log (Incident Heat) vs. Range, to show applicability of a bizonal exponential model for the relationship between incident heat and range at a height of 175 mm with normal air and gas flows.

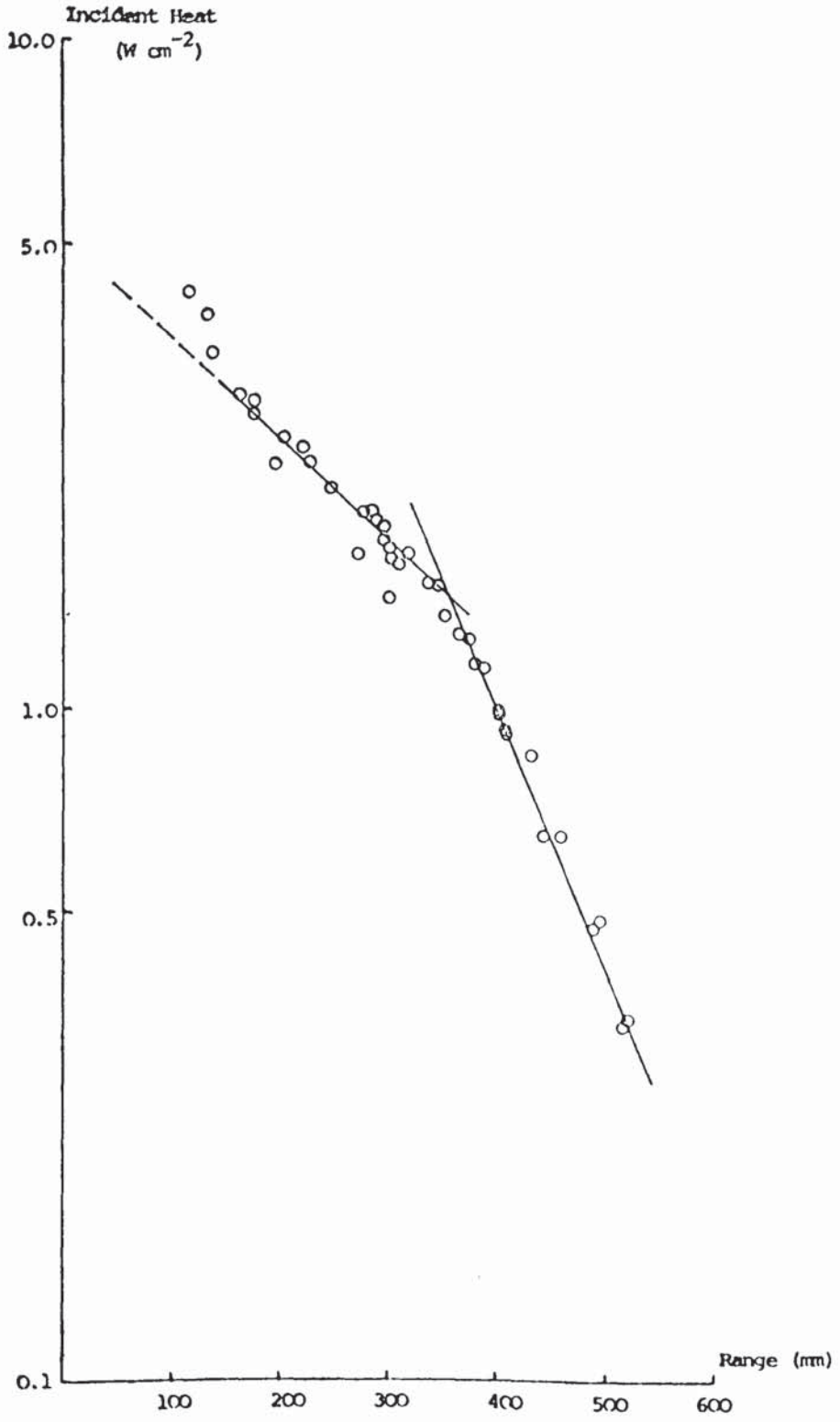

FIGURE 4.9 : Plot of log (Incident Heat) vs. log (Range), to show applicability of a bizonal power law model for the relationship between incident heat and range at a height of 175 mm with normal air and gas flows.

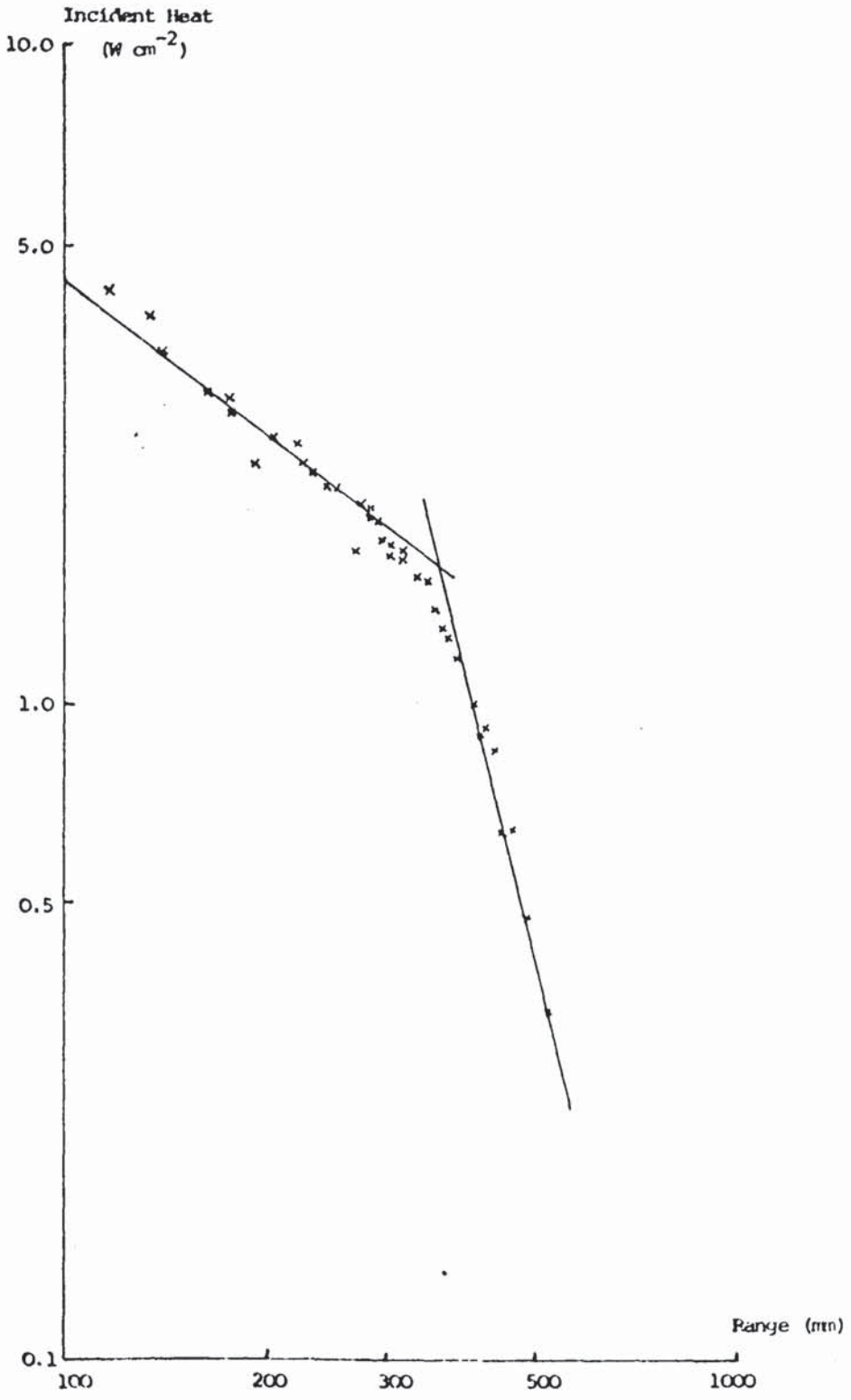

FIGURE 4.10 : Four models for the relationship between Incident Heat and Range (Linear Plots) at a height of 175 mm above the surface with normal air and gas flows.

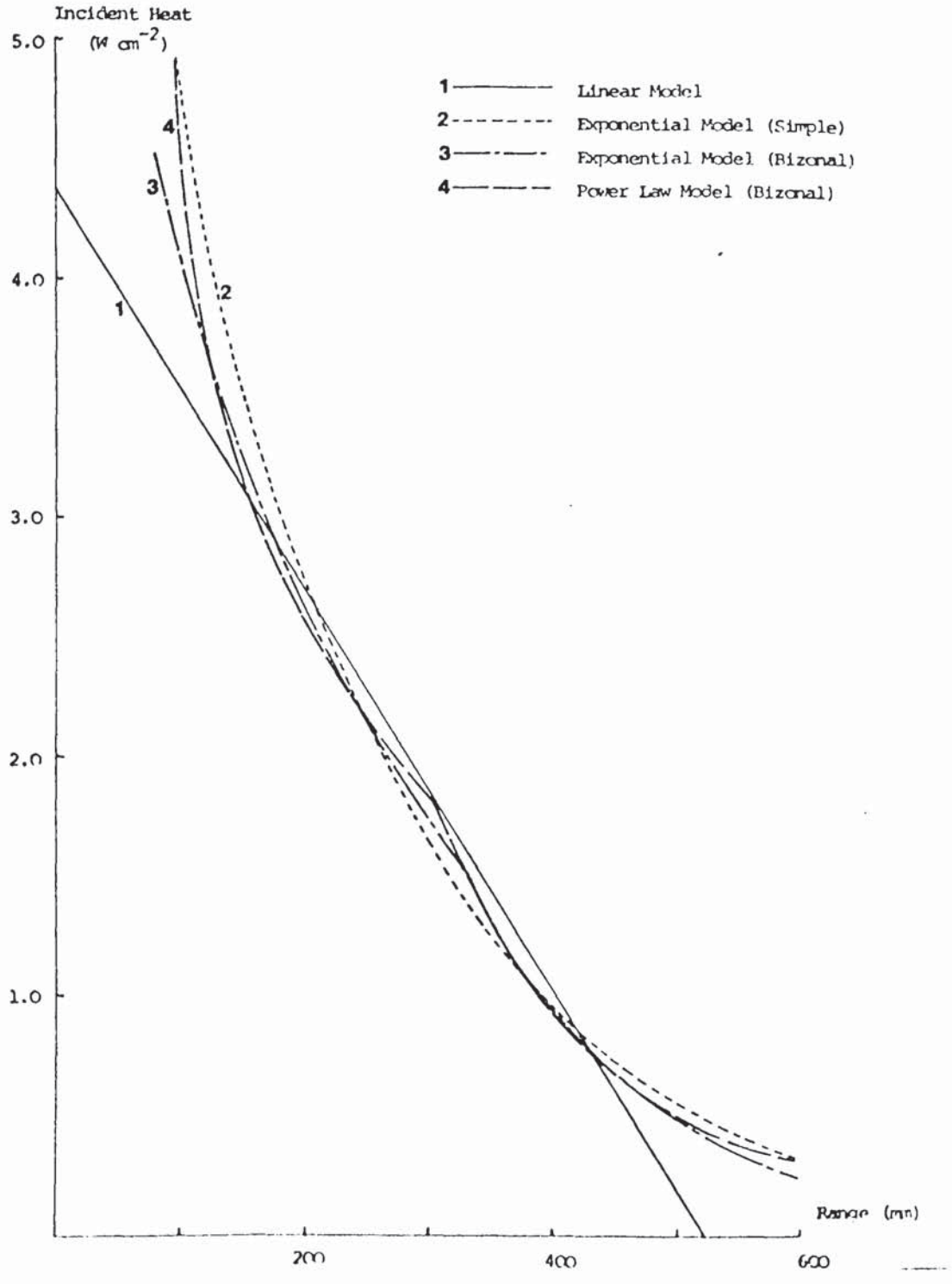

and constants should not, in a perfect model, change. The tendency to decrease as further points were included in the regression is evidence of inaccuracy in the models, and this tendency was marked in the exponential model. The power law decay model appeared more accurate and in many cases it was found that no systematic decrease occurred However beyond the range where the gradients of these models begin to change significantly, the decline in incident heat becomes faster, and the inclusion of such points in the regression leads to an increase in the absolute values of the coefficients and constants. In the exponential model therefore the minimum values occur at the range where these changes begin to occur, and this range may be used as the computational boundary. In the power law model, it is necessary to obtain the boundary by inspection of the coefficients and constants at all values of S; below the boundary these fluctuate (with a decreasing trend, but often giving false minima), beyond it they increase fast. The computational boundary thus obtained is therefore not identical with the graphical boundary which is in the centre of the changeover zone but around 50 mm closer to the burner. This is due to the gradual nature of the changeover. The equations obtained for the low ranges are the best that these models afford.

The equations given for behaviour at high ranges were computed assuming the same boundaries calculated by the aforementioned techniques. They represent averaged models for the changeover zone and the high range zone, and are thus not identical with the graphically deduced equations. However they probably represent a fair description of behaviour at medium to high ranges. Separate consideration of the changeover zone using a third more complex model appears not to be warranted.

Table 4.2 lists the equations obtained by the two single zone models and the two bizonal models discussed, including the computational boundaries. It should be noted that some of the equations are based on very few points. In Table 4.3 is shown an anlysis for the computational trial on the exponential model used to obtain the computational boundary for the case of normal flow rates at a height of 175 mm.

In causal terms, the entrainment of air from beyond the confines of the burner is probably the reason for an accelerating decay in the incident heat flux beyond the boundary. The effects of range on the incident heat flux from the burner in a state where no such convectional heat transfer took place would probably give a simple power law or exponential decay curve. Entrainment of air becomes a particularly major factor from beyond 250 mm or 300 mm at the near edge of the chimney, where there is a major updraught, and continues to increase slightly thereafter. At very low ranges the exponential model tends, for normal and high flow rates, to underestimate slightly the incident heat flux; but for low flow rates, this model overestimates considerably. The source heat flux output is given in this model for R = 0 (The power law model gives an infinite value at R = 0).

A copy of the exponential decay computer program for a typical calibration is given in Appendix A3. Both this program and the similar power law decay program obtain equations by linear regression analysis at low ranges for a boundary S successively increased in intervals of 50 mm. The data to accomplish this is abstracted from the original data by producing new arrays containing only data points for which the range is less than the stipulated value of S. From these equations, the minimum value of the constant a' is then calculated in a

subroutine which compares all the values of this constant obtained. This gives the position of the optimum boundary; equations are then also obtained using this boundary for the high range points, from arrays produced only from those points where the range is greater than S. Using the bizonal model thus generated, values of incident heat flux over all ranges at 50 mm intervals are then calculated. In using the power law model, should inspection reveal a false minimum, an equation for the high ranges would be computed by inserting the boundary value obtained by inspection.

TABLE 4.2 : Equations Obtained By Regression Analysis For Four Models Of The Decay Of Incident Heat Flux As Measured By A Radiometer With Respect To Range In The Aston Fire Testing Device. Standard Errors For The Linear Regressions Given Are Not Directly Comparable Between Models, Since They Are Dependent Upon The Value Of The Constants And Coefficients And Refer To Different Equation Types, viz. $W = u - vR$ (linear), $\ln W = \ln a + bR$ (exponential), $\ln W = \ln p + q \ln R$ (Power Law Decay).

Table 4.2a : Equations For A Linear Model : $W = u - vR$

	Flow Rate	Height of Radiometer (mm)	No. of Points Used in Regression	Model	Standard Errors	
					Constant u	Coefficient v ($\times 10^{-4}$)
(1)	Normal	175	42	W = 4.37 - 0.00835R	0.122	3.7
(2)	Normal	160	14	W = 4.55 - 0.00871R	0.247	7.1
(3)	Normal	143	12	W = 4.31 - 0.00845R	0.260	7.6
(4)	High	175	12	W = 4.63 - 0.00850R	0.140	4.1
(5)	High	160	8	W = 5.16 - 0.01034R	0.205	6.1
(6)	High	143	10	W = 5.30 - 0.01081R	0.468	14.3
(7)	Low	175	12	W = 5.13 - 0.01126R	0.279	8.7
(8)	Low	143	7	W = 5.05 - 0.01172R	0.447	14.6

Table 4.2b : Equations For A Monozonal Exponential Model : $W = a.\exp(bR)$

	Flow Rate	Height of Radiometer (mm)	No. of Points Used in Regression	Model	Standard Errors	
					Constant ln a	Coefficient $b(\times 10^{-4})$
(1)	Normal	175	42	$W = 8.16 \exp(-0.00537R)$	0.069	2.1
(2)	Normal	160	14	$W = 11.33 \exp(-0.00668R)$	0.100	2.9
(3)	Normal	143	12	$W = 8.31 \exp(-0.00577R)$	0.071	2.1
(4)	High	175	12	$W = 10.24 \exp(-0.00556R)$	0.137	4.1
(5)	High	160	8	$W = 11.13 \exp(-0.00605R)$	0.123	3.7
(6)	High	143	10	$W = 11.24 \exp(-0.00631R)$	0.060	1.8
(7)	Low	175	12	$W = 17.65 \exp(-0.00886R)$	0.144	4.5
(8)	Low	143	7	$W = 16.30 \exp(-0.00899R)$	0.112	3.7

Table 4.2.c : Equations For A Bizonal Exponential Model $W = a'.\exp(b'R)$, $R < S$; $W = a''.\exp(b''R)$ $R > S$

The equations for high ranges are given also for a range co-ordinate zero-ed at the boundary.

Flow Rate	Height of Radiometer	No. of Points Used in Regression	Model	Standard Errors Constant ln a', ln a"	Coefficient b', b" ($\times 10^{-4}$)
1 Normal	175		Boundary 300 mm		
Low ranges		19	$W = 6.27 \exp(-0.00428R)$	0.070	3.1
High ranges		23	$W = 14.76 \exp(-0.00685R)$	0.180	4.6
			$= 1.89 \exp(0.00685 [R-300])$		
2 Normal	160		Boundary 350 mm		
Low ranges		9	$W = 7.75 \exp(-0.00506R)$	0.069	2.7
High ranges		5	$W = 24.41 \exp(-0.00840R)$	0.284	6.1
			$= 1.29 \exp(-0.00840 [R-350])$		
3 Normal	143		Boundary 350 mm		
Low ranges		8	$W = 7.02 \exp(-0.00506R)$	0.058	2.2
High ranges		4	$W = 16.15 \exp(-0.00731R)$	0.361	7.9
			$= 1.25 \exp(-0.00731 [R-350])$		

Flow Rate		Height of Radiometer (mm)	No. of Points Used in	Model	Standard Errors Constant ln a', ln a"	Coefficient b', b" (x $10'^{-4}$)
4 High		175		Boundary 350 mm		
	Low ranges		7	W = 6.24 exp (-0.00370R)	0.148	5.5
	High ranges		5	W = 27.67 exp (-0.00794R)	0.253	6.0
				= 1.72 exp (-0.00794 [R-350])		
5 High		160		Boundary 300 mm		
	Low ranges		3	W = 8.32 exp (-0.00487R)	0.042	1.8
	High ranges		5	W = 22.17 exp (-0.00780R)	1.80	4.6
				= 2.14 exp (-0.00780 [R-300])		
6 High		143		Boundary 350 mm		
	Low ranges		7	W = 10.32 exp (-0.00596R)	0.086	3.3
	High ranges		3	W = 16.44 exp (-0.00720R)	0.173	4.0
				= 1.32 exp (-0.00720 [R-350])		

Flow Rate	Height of Radiometer (mm)	No. of Points Used In Regression	Model	Standard Errors Constant ln a', ln a"	Standard Errors Coefficient b', b" ($\times 10'^{-4}$)
7 Low	175		Boundary 300 mm		
Low ranges		6	W = 8.51 exp (-0.00541R)	0.099	4.6
High ranges		6	W = 39.73 exp (-0.01092R)	0.225	5.7
			= 1.50 exp (-0.01092 [R-300])		
8 Low	143		Boundary 250 mm		
Low ranges		3	W = 10.56 exp (-0.00681R)	0.011	0.5
High ranges		4	W = 20.83 exp (-0.00967R)	0.286	7.8
			= 1.86 exp (-0.00967 [R-250])		

Table 4.2.d : Equations For A Bizonal Power Law Decay Model.

$W = p'.R^{q'}$, $R < S$; $W = p''.R^{q''}$, $R > S$ * boundary by inspection

Flow Rate	Height of Radiometer (mm)	No. of Points Used in Regression	Model	Standard Errors Constants ln p', ln p"	Coefficient q' , q" ($\times 10^{-2}$)
1 Normal	175		Boundary 300 mm		
Low ranges		19	$W = 268\ R^{-0.877}$	0.269	5.01
High ranges		23	$W = 7.85 \times 10^{6}\ R^{-2.66}$	1.242	20.87
2 Normal	160		Boundary 300 mm		
Low ranges		6	$W = 751\ R^{-1.060}$	0.408	7.70
High ranges		8	$W = 5.11 \times 10^{8}\ R^{-3.38}$	1.106	18.41
3 Normal	143		Boundary 300 mm*		
Low ranges		5	$W = 688\ R^{-1.066}$	0.123	2.32
High ranges		7	$W = 1.15 \times 10^{7}\ R^{-2.75}$	0.988	16.51
4 High	175		Boundary 350 mm*		
Low ranges		7	$W = 492\ R^{-0.961}$	0.763	13.70
High ranges		5	$W = 4.59 \times 10^{8}\ R^{-3.31}$	1.875	31.10

Table 4.2d (cont.)

Flow Rate		Height of Radiometer (mm)	No. of Points Used In Regression	Model	Standard Errors Constants ln p', ln p"	Coefficients q', q" ($\times 10^{-2}$)
5 High		160		Boundary 300 mm		
	Low ranges		3	$W = 908\ R^{-1.073}$	1.777	3.29
	High ranges		5	$W = 7.49 \times 10^{7}\ R^{-3.03}$	1.407	23.66
6 High		143		Boundary 300 mm		
	Low ranges		5	$W = 2238\ R^{-1.247}$	0.327	6.08
	High ranges		5	$W = 1.90 \times 10^{7}\ R^{-2.82}$	1.592	26.66
7 Low		175		Boundary 300 mm*		
	Low ranges		6	$W = 820\ R^{-1.072}$	0.508	9.52
	High ranges		6	$W = 9.81 \times 10^{10}\ R^{-4.35}$	0.749	12.56
8 Low		143		Boundary 250 mm		
	Low ranges		3	$W = 3089\ R^{-1.333}$	0.398	7.54
	High ranges		4	$W = 4.98 \times 10^{8}\ R^{-3.49}$	1.261	21.46

TABLE 4.3 : A Full Analysis For All Possible Positions Of The Boundary For Exponential Decay Analysis Of The Calibration At Normal Flow Rates, At Height 175 mm (42 Points) From Which The Optimum Computational Boundary Was Determined As That At Which a' And b' Are At A Minimum (S = 300mm)

	Low Ranges					High Ranges				
Boundary S	No. of Points	a'	b'	Standard Errors SE(lna')	SE(b') $\times 10^{-4}$	No. of Points	a"	b"	Standard Errors SE(lna")	SE(b") -10^{-4}
100	-	-	-	-	-	42	8.16	-0.00537	0.069	2.1
150	3	11.31	-0.00826	0.0468	35.7	39	8.43	-0.00546	0.084	2.5
200	7	10.27	-0.00747	0.1198	7.5	35	9.95	-0.00589	0.098	2.8
250	12	7.08	-0.00498	0.0989	5.2	30	12.10	-0.00638	0.125	3.4
300	19	6.27	-0.00428	0.0702	3.1	23	14.76	-0.00685	0.180	4.6
350	27	6.63	-0.00455	0.0873	3.4	15	28.04	-0.00828	0.144	3.4
400	32	6.51	-0.00446	0.0704	2.5	10	38.27	-0.00894	0.253	5.6
450	38	7.05	-0.00480	0.0624	2.0	4	57.4	-0.00975	0.781	15.8
500	41	7.76	-0.00518	0.0655	2.0	1	-	-	-	-
550	42	8.16	-0.00537	0.0692	2.1	-	-	-	-	-

CHAPTER 5

SAMPLE PREPARATION FOR FIRE TESTING

CHAPTER 5

SAMPLE PREPARATION FOR FIRE TESTING

Nomenclature

m	:	mass flow rate
n	:	power law exponent, given actual shear rate
n'	:	power law exponent, given apparent shear rate
$\dot{u}$	:	shear rate
$\dot{u}_w$	:	shear rate at wall of extrusion tube
v_z	:	velocity of fluid along extrusion tube
x	:	molar ratio of melamine to phosphate
L	:	length of extrusion tube
N_f	:	Bagley correction factor
ΔP	:	pressure differential between entrance and exit of extrusion tube
Q	:	volumetric flow rate
R	:	radius of extrusion tube
β	:	coefficient of effective slip
κ	:	actual viscosity
κ'	:	apparent viscosity
ρ	:	density
τ_{rz}	:	shear stress at radius r in extrusion tube for fluid velocity z
τ_R	:	shear stress at wall of extrusion tube

5.1 Crystal Types Used in the Fire Tests

The variety of crystal sizes and shapes of melamine orthophosphate has been described in Section 2.4 with suitable production routes. All of these have been used in fire tests. Filtration and

drying of the product, and subsequent mechanical breaking up of any cakes formed by needle-like crystals of aspect ratio around five leads to damage to the crystals. A brief description of the dried crystal types as used in the fire tests follows, with sizing information related to the state of the dried product. The ratio of melamine to phosphate, ^{x} , for the product $(C_3H_6N_6)_x.H_3PO_4$ is given. Most of the crystal types are illustrated in plates 5.1 - 5.8.

(a) Very large needles, $x \doteq 1.0$

Mean length 200 μm, range from 80 μm to 10 mm, of large aspect ratio, in excess of ten. Plate 5.1.

(b) Medium needles, $x \doteq 1.0$

Mean length 25 μm, range from 15 μm to 80 μm in length, aspect ratio in excess of ten. Plate 5.2.

(c) Small needles, $x \doteq 1.2 - 1.25$

Mean length 5 μm, maximum 20 μm, aspect ratio low, from 3 to 5. Tends to agglomerate in clusters which, even when roll-milled under close-set rolls with epoxy resin, still range up to 40 μm. Plate 5.3.

(d) Small block plates, $x \doteq 1.2 - 1.25$

Generally of side 5 to 10 μm, with the range being 2 μm to 30 μm side. Plate 5.4.

(e) Large needles, $x \doteq 1.2 - 1.25$

These are very variable in size and aspect ratio. Mostly needles typically 80 μm long x 15 μm wide, but ranging up to 300 μm x 50 μm. Some plates also, typically 60 μm x 60 μm. The smallest crystals are around 20 μm side (plates). Plate 5.5.

(f) Thin reflective plates, x ≐ 1.3

The size of these varies considerably due to their extreme frangibility. The superposition of layers of crystals also makes it difficult to identify individual crystals under miscroscopic examination. However typically there are chips ranging from 1 μm to 20 μm, but some crystals up to 300 μm x 100 μm have been identified. Thickness is around 500 nm. Plate 5.6.

(g) Plates, x ≐ 1.1

As thin plates (f), but of lower reflectivity.

(h) Medium block plates, x = 2.0

Mean size 45 μm; range 20 μm x 20 μm up to 180 μm x 60 μm. Plate 5.7.

(i) Large block plates, x = 2.0

Major population typically 300 μm x 200 μm. There are also a few much smaller crystals in this material of around 50 μm side, with a more reflective surface. Plate 5.8.

The only practicable method of particle size analysis proved to be by microscopic examination. Methods based on electronic techniques tend to give optimum results for spherical, unagglomerated particles, a description which is not true for any of the crystal forms of melamine phosphate! Microscopic examination allows observation of agglomerates and gives the ability to distinguish particle size and shape. The major problem is that of sampling, since only a very small sample is required. As a result of this, agglomerate sizes suggested may be smaller than actually are typical, but it is believed that the dimensions of individual crystals are accurate. The dry particles adhere reasonably well to glass slides used in microscopy, and excess

Plate 5.1 : Very Large Needles of $(C_3H_6N_6)_{1.0}\cdot H_3PO_4$

magnification x 100

Plate 5.2 : Medium Needles of $(C_3H_6N_6)_{1.0}\cdot H_3PO_4$

magnification x 180

Plate 5.3 : Small Needles of $(C_3H_6N_6)_{1.2}.H_3PO_4$, magnification x 200

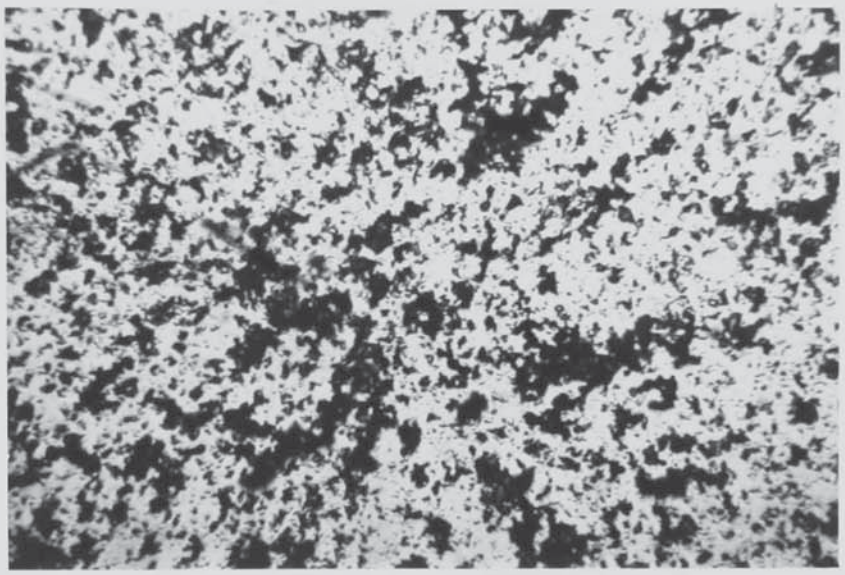

Plate 5.4 : Small Block Plates of $(C_3H_6N_6)_{1.2}.H_3PO_4$, magnification x 200

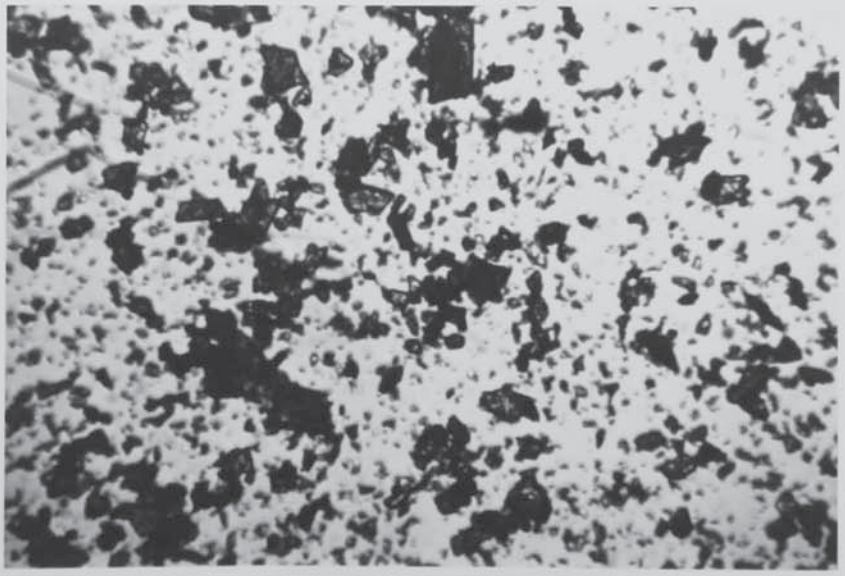

Plate 5.5 : Large Needles of $(C_3H_6N_6)_{1.2}\cdot H_3PO_4$, magnification x 200

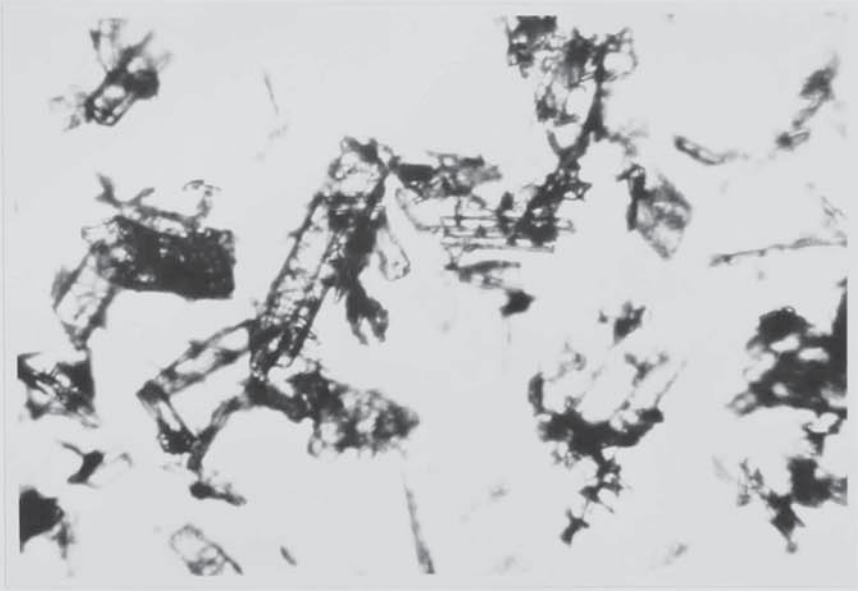

Plate 5.6 : Thin Reflective Plates of $(C_3H_6N_6)_{1.3}\cdot H_3PO_4$, magnification x 180

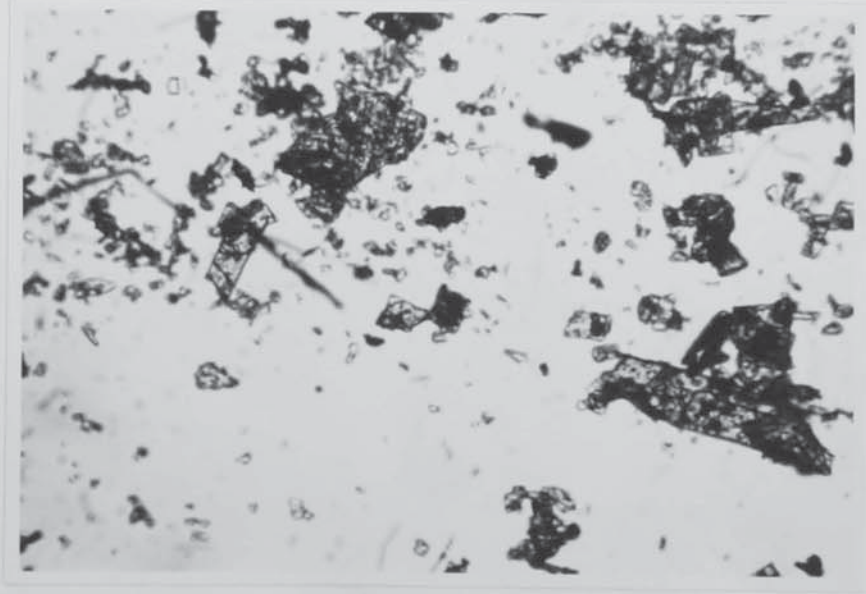

Plate 5.7 : Medium Block Plates of $(C_3H_6N_6)_{2.0}\cdot H_3PO_4$, magnification x 180

Plate 5.8 : Large Block Plates of $(C_3H_6N_6)_{2.0}\cdot H_3PO_4$, magnification x 100

material is not blown off, so that the larger particles are as far as possible not removed. No suspending liquid was used; melamine phosphate is slightly soluble in many suitable liquids, such as glycerol, and this would lead to changes in the particle shape.

Microscopic examination was also used to analyse the size distribution in samples dispersed with epoxy resin and hardener. These are the mixtures used in the fire tests themselves, and the particle characteristics of these dispersions are those of the fire test samples themselves. In addition, the sampling method is likely after dispersion in such a viscous medium to give a more representative size distribution than can be obtained from the dry powder. A drop of mixture, dispersed either using an orbital mixer or by roll milling, was placed on a glass slide and a cover slip pressed over it. This sets to form a permanent sample. Tests were also carried out on the dispersions using a Hegmann fineness-of-dispersion gauge, consisting of angled channels of depth ranging from zero to 100 μm. A drop of sample is placed at the deep end and dispersed up the channel by a doctor blade. This technique was especially useful in determining the effectiveness of roll-milling in breaking down agglomerates.

It was not considered necessary to obtain accurate statistical particle size distributions, since the differences between the various types of crystal used were reasonably large. For this purpose the above techniques of analysis were considered adequate.

Some sieve analysis was also carried out in the case of small needles with fine grade sieves. It was found that the size distribution obtained by sieve analysis was time dependent, no unchanging distribution being obtained even after prolonged shaking. This is an indication of

the state of agglomeration of the particles presented to the sieves, and the strength of the bonds within the agglomerates. Around 20 g of small needles of melamine phosphate were sieved using an Endrock shaker, and as a control, a similar quantity of ballotini were then also sieved. The variations in size distribution for these materials are shown in Table 5.1, from which it is apparent that an original majority of agglomerates in the size range 75 μm to 120 μm was successively broken down by mechanical attrition, although it is doubtful, even so, that many primary particles (of mean size around 15 μm) were obtained. Sieve analysis is not therefore a suitable means of particle size analysis for melamine phosphate.

5.2 Sample Preparation

5.2.1 The Substrate

The substrate used for all the tests was a container of $^1/_{16}$ inch (1.5 mm) mild steel shaped to a square base of side 95 mm and sides of height 6 mm (internal dimensions). The corner joints were welded. Two holes of diameter 3 mm were drilled at the base of one side to enable passage of thermocouples, affixed to the inner surface of the substrate, to a meter. Normally only one thermocouple was used, situated centrally on the substrate surface and peened in, although on early fire tests two thermocouples were placed in the upper left and lower right hand quarters of the substrate (as viewed from the front of the sample). Thermocouples were of Ni-Cr/Ni-Al 0.376 mm gauge wires of length at least 1.2 metre, sheathed in PVC sleeving. The hole in the base of the substrate allows one of the wires to pass through sheathed, thus maintaining electrical insulation of the wires. During the later stages of tests when thermal breakdown of the sheathing normally occurs,

TABLE 5.1 : Frangibility Analysis by Sieving : Percentages by Weight at Various Times Within The Size Ranges of Standard Sieves For Small Needles of Melamine Phosphate and Ballotini.

Size Range	Melamine Phosphate			Ballotini		
(μm)	5 min	19 min	64 min	5 min	25 min	56 min
45	9.1	34.6	63.2	7.6	8.6	8.6
45 - 53	2.7	7.0	6.2	3.7	3.7	3.6
53 - 63	8.7	16.0	8.2	6.3	6.2	6.3
63 - 75	11.0	22.1	5.6	4.0	4.5	4.5
75 - 90	23.0	9.9	7.9	16.3	17.8	18.6
90 - 105	24.0	0.6	0.6	0.4	0.2	0.2
105 - 120	19.3	8.0	6.5	55.2	52.7	52.1
120	2.2	1.8	[1.8]*	6.3	6.3	6.1

* 120 μm aperture sieve removed after 19 min.

char formed in the holes maintains electrical insulation by preventing contact of the wires - in only two cases in around 200 tests has this failed. By placing the thermocouple on the inner surface of the substrate, around 50 mm of each wire behind the junction is maintained at a temperature similar to that of the junction, thus reducing conduction down the wires and avoiding a significant conduction error in the determination of substrate temperatures.

The container fits into the well in the substrate frame, and is smaller in cross-section than the burner. Nevertheless convection effects cause a greater intensity of heat flux.in the upper regions of the sample, and cross-currents cause smaller variations in the horizontal plane. This leads to earlier failure in the upper regions of a sample during a fire test compared with the lower regions. The time-temperature response pattern and the time to failure of a sample are referred to the centre of each sample.

5.2.2 The Coating

A suitable coating material for assessing the effects of various characteristics of melamine phosphate upon performance in a fire test, based on work carried out by the Atomic Weapons Research Establishment (54) consisted of melamine phosphate in a matrix of Araldite (R) MY753 epoxy resin and Versamid (R) 125 hardener. For a few tests other ingredients were included as specified in the following sections. Araldite MY753 is a low molecular weight resin of the di-glycidyl ether of bis-phenol A type, including also 10% dibutyl phthalate as a plasticiser (55), which lowers the melting point of the cured resin and increases its flexibility and toughness. Versamid 125 is an amino-

(R) Araldite is a registered trademark of Ciba-Geigy (UK) Ltd.
(R) Versamid is a registered trademark of General Mills Chemical, Inc. (USA), and marketed in the UK by Cray Valley Products Ltd.

polyamide hardener of amine value 290 - 320 mg KOH g^{-1} (56). These two ingredients were always used in the weight ratio of five parts resin to two parts hardener, a mixture which, with melamine phosphate present, is tack free in around 180 minutes at 25°C.

Two methods of blending melamine phosphate crystals with epoxy resin and hardener were used. The standard method involved mixing the three ingredients in a Kenwood Major orbital mixer using an anchor stirrer until uniform on visual inspection. The main source of shear is within the components of the mixture itself; a smaller contribution arises between the mixture and the walls. Aeration of the mixture is inevitable, the degree of aeration depending not only upon the vigour and time of mixing, but also upon the loading of melamine phosphate and even the crystal size and shape. Aeration is reduced for a 30% loading of melamine phosphate compared to a 12½% loading, and for samples incorporating large crystals. The degree of aeration is reflected in the weight of the coating which is of a standard thickness of 6 mm. For samples prepared in this manner, the mean coating weight at a 12½% level of incorporation was 45.1 g, standard deviation 3.83 g; and at a 30% level of incorporation 57.0 g, standard deviation 5.04 g. Some early fire tests used samples mixed manually and were of average weight 80 g.

To achieve a finer degree of dispersion, small crystals could be roll-milled into Araldite epoxy resin on a triple roll mill and subsequently mixed with hardener in the orbital mixer. Melamine phosphate needles and plates are frangible and large crystals have been found not to survive the process of roll milling without severe size reduction.

Consequently this method was used only for the incorporation of small needles, small block plates and thin reflective plates. Even with final mixing with hardener in the orbital mixer, aeration of the sample was less than that occuring with comparable samples entirely mixed on the orbital mixer. The coating weight did not vary significantly with melamine phosphate loading; the mean coating weight for all roll-milled samples was 57.3 g, standard deviation 5.34 g, for a 6 mm thickness of coating. To achieve an appreciable reduction in the size of agglomerates the melamine phosphate and epoxy resin were milled at minimum roller separation; it is expected that the agglomerative tendencies of small needles and thin plates are greater than those of small block plates, and therefore the difference in the effective particle sizes obtained with the former by roll-milling is expected to be greater. By analogy with the separation of plates of bentone (R) thixotropic agent (57) prior to milling, a mixture of 95% methanol - 5% water was added at a 2% level of incorporation to the thin plates and epoxy resin mill base, and this achieved considerable success in reducing the agglomerate size of thin plates to around 30 μm in diameter (Plate 5.9). This may be compared with thin plates incorporated under low shear in which an almost continuous matrix of plates is apparent (Plate 5.10). The effects of roll-milling on small needles, in which 90% of the agglomerates were below 45 μm, may be seen in comparing Plates 5.11 and 5.12. All roll milling was carried out using three parts by weight of melamine phosphate and five parts epoxy resin; further dilution with excess epoxy resin was carried out where required when mixing with hardener. Three passes over the rolls were normally required to

(R) Bentone is a registered trademark of NL Industries, Inc.

Plate 5.9 : Thin Reflective Plates of $(C_3H_6N_6)_{1.3}\cdot H_3PO_4$ incorporated into epoxy resin/hardener mixture by roll milling, magnification x 180

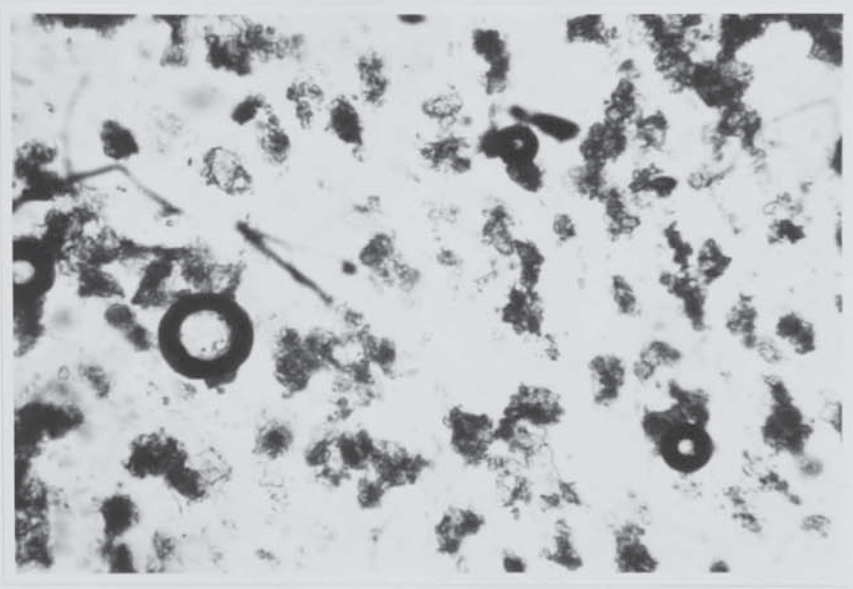

Plate 5.10 : Thin Reflective Plates of $(C_3H_6N_6)_{1.3}\cdot H_3PO_4$ incorporated into epoxy resin/hardener mixture under low shear in an orbital mixer, magnification x 180

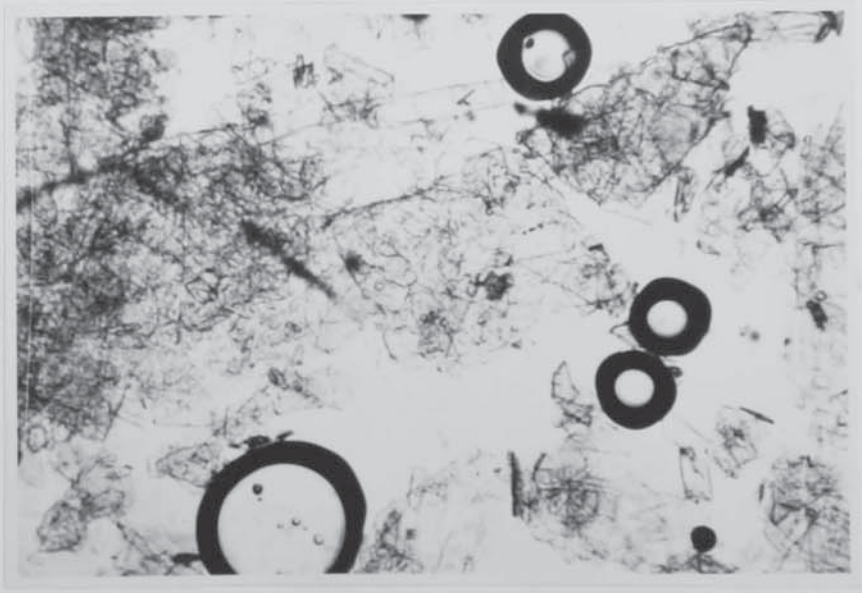

Plate 5.11 : Small Needles of $(C_3H_6N_6)_{1.2}.H_3PO_4$ incorporated into epoxy resin/hardener mixture by roll milling, magnification x 200

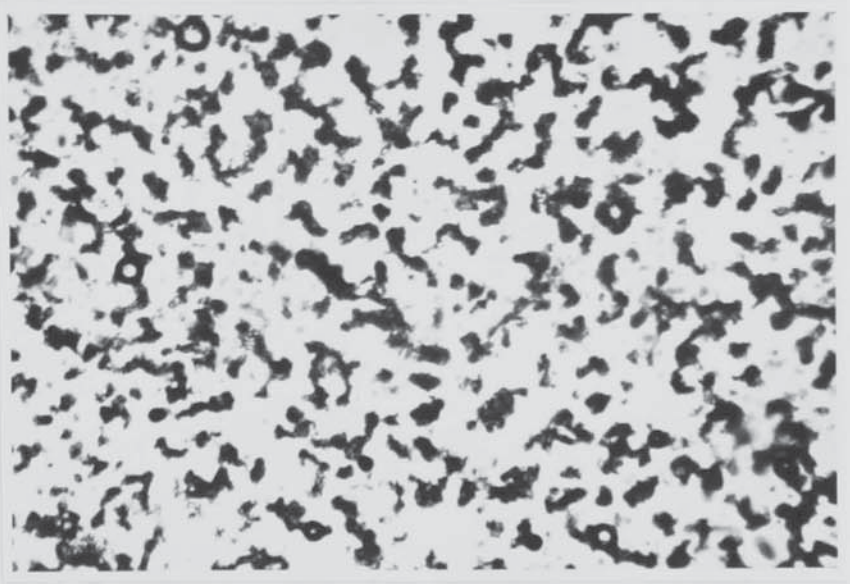

Plate 5.12 : Small needles of $(C_3H_6N_6)_{1.2}.H_3PO_4$ incorporated into epoxy resin/hardener mixture under low shear in an orbital mixer, magnification x 200

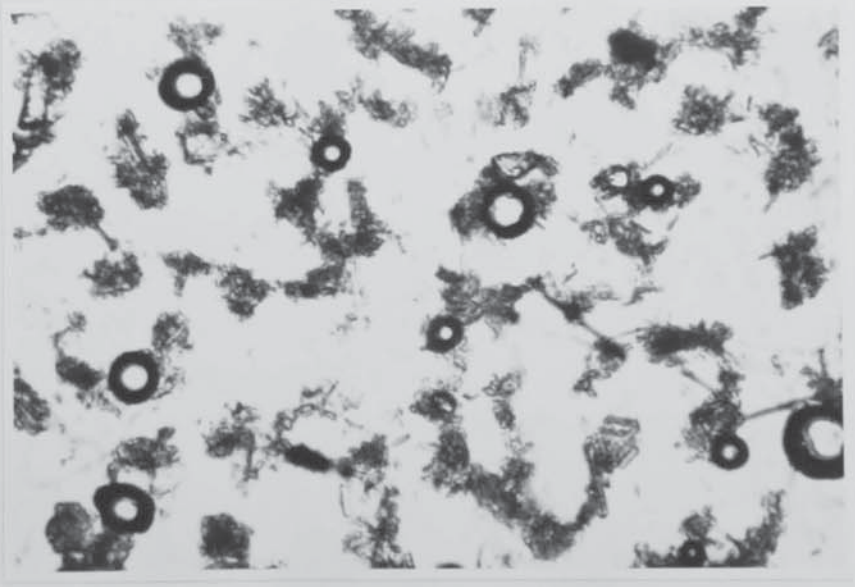

Plate 5.13 : Large Needles of $(C_3H_6N_6)_{1.2}.H_3PO_4$ incorporated into epoxy resin/hardener mixture under low shear in an orbital mixer, magnification x 180

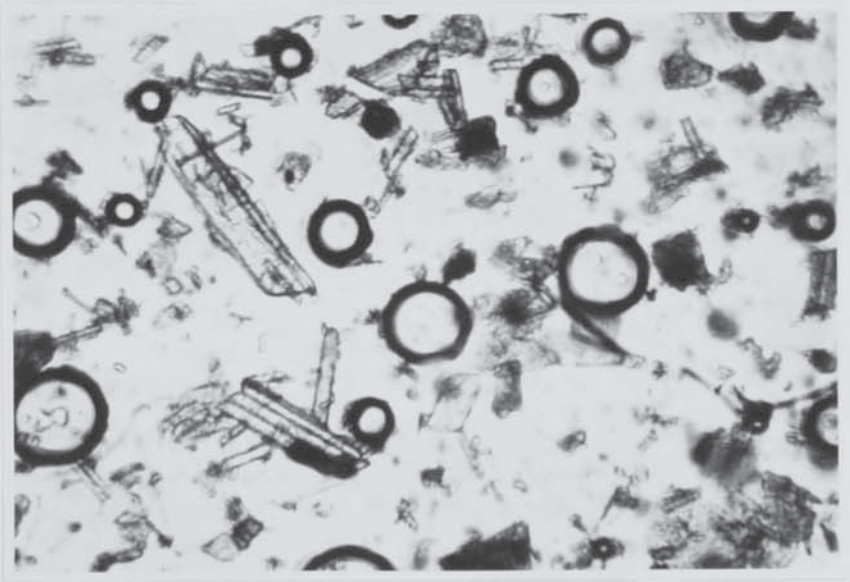

Plate 5.14 : Very Large Needles of $(C_3H_6N_6)_{1.0}.H_3PO_4$ incorporated into epoxy resin/hardener mixture under low shear in an orbital mixer, magnification x 100

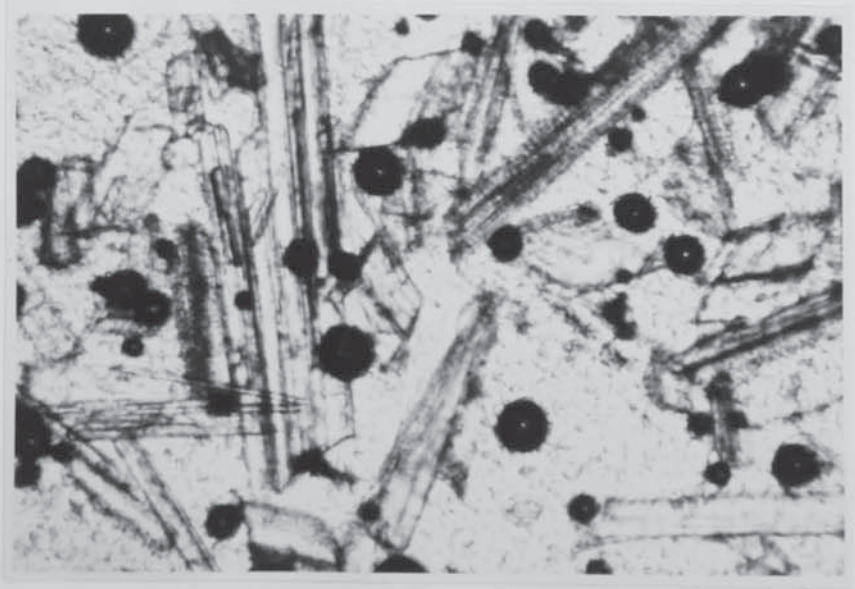

Plate 5.15 : Large Block Plates of $(C_3H_6N_6)_{2.0}\cdot H_3PO_4$ incorporated into epoxy resin/hardener mixture under low shear in an orbital mixer , magnification x 200

achieve the above particle size reduction.

Even under low shear conditions of mixing, the large crystals, due to their frangibility, suffer some size reduction. Typical crystal sizes after mixing are as follows:

Large Needles $(C_3H_6N_6)_{1.2}.H_3PO_4$: 45 μm x 6 μm

Very Large Needles $(C_3H_6N_6)_{1.0}.H_3PO_4$: < 200 μm

Large Block Plates $(C_3H_6N_6)_{2.0}.H_3PO_4$: 100 μm x 150 μm

These are illustrated in Plates 5.13 to 5.15

5.2.3. The Cure Regime

The standard cure regime used for samples was 24 hours at ambient temperature, followed by nine days at 55°C. Several fire tests were however carried out on samples cured for different lengths of time and at different temperatures. It is only as cure takes place that large numbers of hydroxyl groups, required for esterification by phosphate, are formed. This esterification is the first stage in the reactions leading to intumescence.

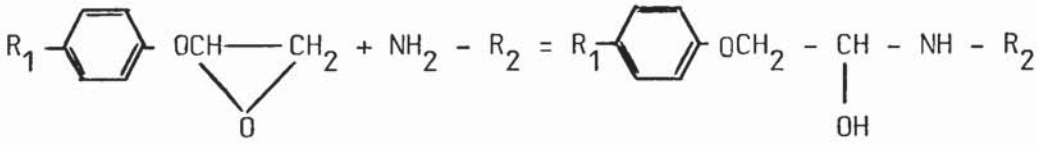

(5.1)

A few hydroxyl groups are of course already present in oligomers of the diglycidyl ether of bis-phenol A, viz.

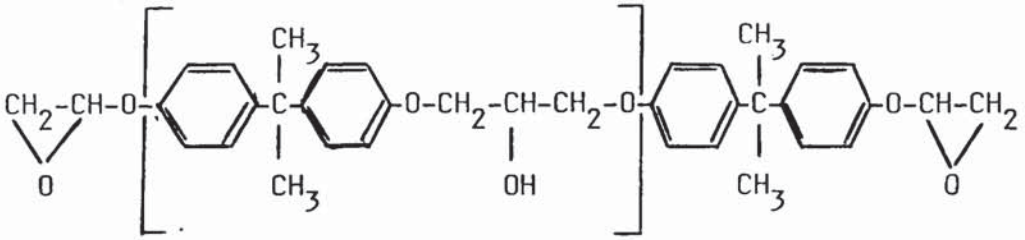

n=0,1,2

Three sets of tests investigating the effects of cure regime were carried out. The earliest set used a 12½% loading of small

needles of $(C_3H_6N_6)_{1.2}.H_3PO_4$, incorporated by roll-milling and cured for two days, one week, and two weeks respectively at ambient temperature. They were tested at 850° - 900°C at a range of 125 mm. All intumesced voluminously, and gave similar substrate time-temperature response patterns. However the sample cured for only two days appeared to give a slightly superior performance to the other two. When samples containing 12½% small block plates of $(C_3H_6N_6)_{1.2}.H_3PO_4$ cured for 24 hours, one week and three weeks respectively at ambient temperature and for three weeks at 55°C were tested at 750° - 800°C (a sample distance of 190 mm) the latter three behaved in a similar manner, but the sample cured for only 24 hours intumesced to a considerably lesser extent, managing nevertheless to give protection as good as the other samples to the substrate. The lower level of intumescence is probably due to the lower level of hydroxyl groups available in the partially cured material. However during the course of a test, further cure probably takes place as the temperature rises, thus causing intumescence to be slower and more controlled. However there is still considerably more surface flaming of partially cured samples than of more highly cured samples. When a set containing 12½% thin plates $(C_3H_6N_6)_{1.3}H_3PO_4$ was tested at 750° - 800°C the results were surprising. This crystal type has generally been found to give more restricted intumescence and inferior performance to other crystal types of similar stoichiometry. A sample cured for one day and two cured for three weeks at ambient temperature and at 55°C respectively all gave similar substrate time-temperature response patterns, but the extent of the intumescence decreased

as the degree of cure increased! Full details of these tests are in Table 5.2.

It thus appears that a cure time of one week at ambient temperature gives a degree of cure close to the level normally found; the standard regime including nine days at 55°C is certainly satisfactory.

5.3 Rheology

5.3.1 Introduction

The rheological properties of mixtures of epoxy resin and various crystal types of melamine phosphate, used as models for the uncured mastics, were measured using an extrusion rheometer. These mixtures do not cure; therefore there exists no time dependence due to the progression of a cure reaction, and problems in cleaning the instrument are avoided.

The extrusion rheometer was designed and built as part of the project, according to the method of Severs and Austin (58,59).

The reservoir was of 12 mm wall thickness brass measuring 150 mm x 75 mm externally, and of capacity around 230 cm^3. It had a flanged opening, sealed by a rubber O-ring, at its base, to enable filling up and cleaning of the reservoir. A selection of four stainless steel extrusion tubes of length 300 mm and respective diameters 3.100 mm, 2.160 mm, 1.475 mm, 1.145 mm was provided. These screwed onto the base of the reservoir by means of a compatible thread. Pressure was provided by means of a nitrogen gas cylinder, linked by piping to the top of the reservoir. Pressures of up to 150 pounds per square inch (1.034×10^6 Pa) were available. Plate 5.16 illustrates the instrument in use, whilst the disassembled components are shown in Plate 5.17. The measurements required are the volumetric flow rate

TABLE 5.2 : Typical Results for Samples Fire Tested to Assess the Effects of Cure Regime.

Crystal Type	Cure Regime (days, °C)	Test Regime	Time (min) to 300°C	Time (min) to 400°C	Duration (min)	Maximum Extent of Intumescence (mm)
Small needles		850° - 900°C				
$(C_3H_6N_6)_{1.2}.H_3PO_4$	2d, 20°C		8½	15	18	voluminous
(roll milled)	7d, 20°C		8½	14	17	voluminous
coating weight	14d, 20°C		8½	14	17	voluminous
~ 70g						
Small block plates		750° - 800°C				
$(C_3H_6N_6)_{1.2}.H_3PO_4$	1d, 20°C		8½	22	24	10
coating weight	7d, 20°C		8	17	20	40
~ 42g	23d, 20°C		5¼	17½	26½	30
	23d, 55°C		8	17	19	35
Thin plates		750° - 800°C				
$(C_3H_6N_6)_{1.3}.H_3PO_4$	1d, 20°C		12	23	27	40
coating weight	23d, 20°C		7½	20	20	35
~ 43g	23d, 55°C		13	-	26½	25

Plate 5.16 : Extrusion Rheometer in use.

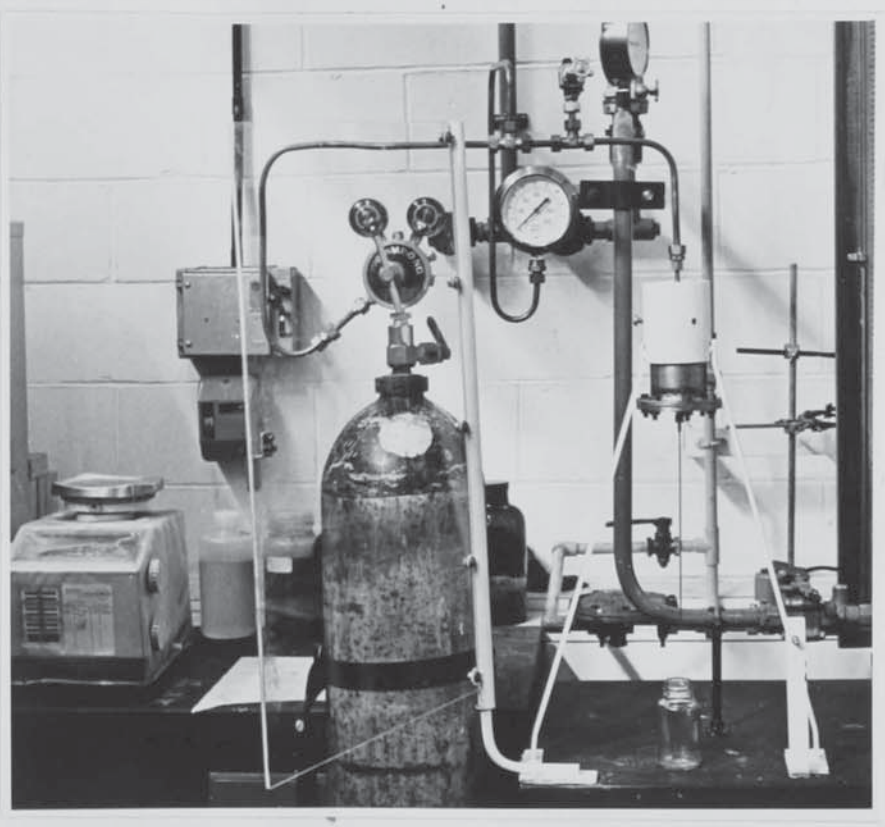

Plate 5.17 : Extrusion Rheometer, disassembled, showing all four extrusion tubes

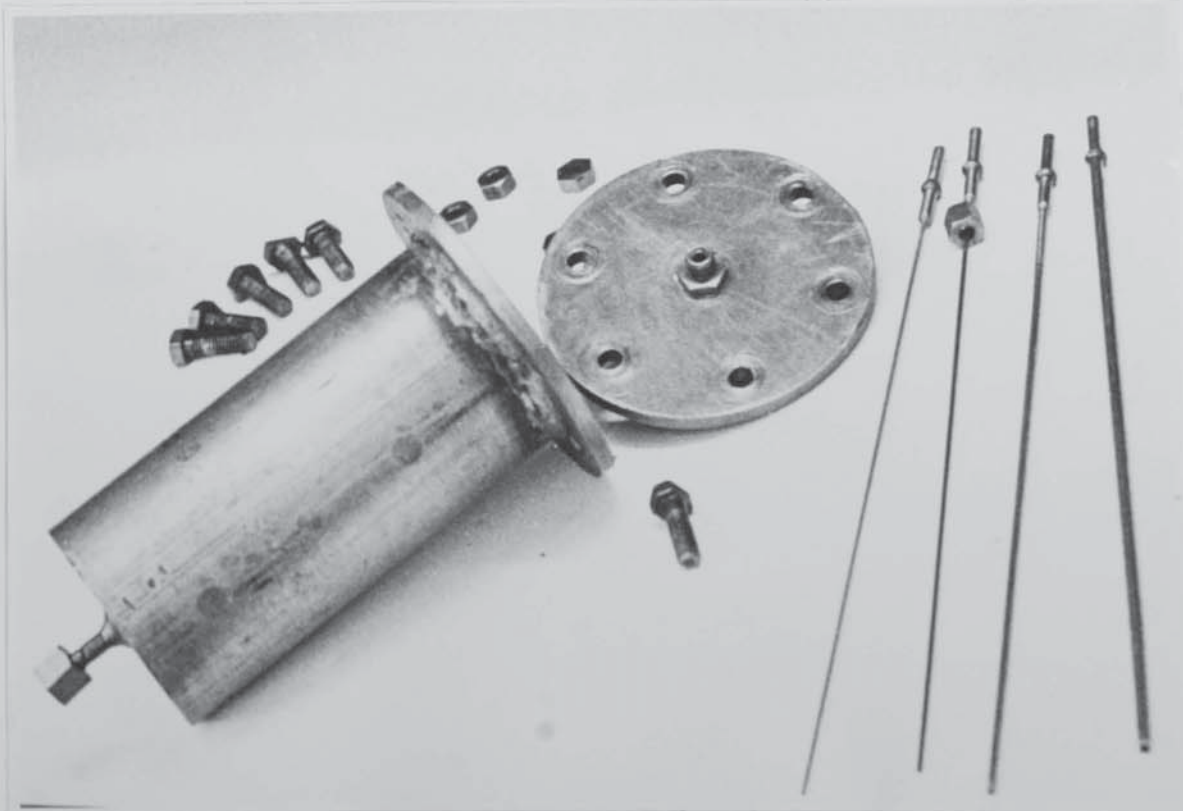

at a range of pressures, but for experimental purposes the mass flow rates and the density of the mixtures were measured.

5.3.2 Theory

For time-independent behaviour of certain fluids, the Power Law model is applicable, viz :

$$\tau_{rz} = \kappa (\dot{u})^n \tag{5.1}$$

At the wall of the tube

$$\tau_R = \kappa (\dot{u}_w)^n \tag{5.2}$$

But

$$\tau_R = \frac{R.\ \Delta P}{2L} \tag{5.3}$$

from the definition of shear stress. For round pipes, it can also be shown (59) that

$$Q = \frac{\pi R^3}{\tau_R^3} \int_0^R \tau_{rz}^2 \left(\frac{\tau_{rz}}{\kappa}\right)^{1/n} d\tau_{rz} \tag{5.4}$$

$$= \frac{\pi R^3}{\tau_R^3 \kappa^{1/n}} \left[\frac{\tau_{rz}^{3+1/n}}{3 + 1/n}\right]_0^R$$

$$= \pi R^3 \cdot \frac{n}{3n+1} \left(\frac{\tau_R}{\kappa}\right)^{1/n} \tag{5.5}$$

But, from the Power Law expression, $\dot{u}_w = \left(\frac{\tau_R}{\kappa}\right)^{1/n}$

Therefore $Q = \pi R^3 \cdot \frac{n}{3n+1} \cdot \dot{u}_w$ (5.6)

From this an expression for $\dot{u}_w$ is available, but cannot be used directly as n is an unknown. However the apparent shear rate at the wall

$$\dot{u}_w \text{ (apparent)} = \frac{4Q}{\pi R^3} = \frac{4m}{\pi \rho R^3} \qquad (5.7)$$

By substitution of expressions (5.3) and (5.7) in the Power Law expression, the apparent viscosity and power can be obtained, viz.

$$\frac{R.\ \Delta P}{2L} = \kappa' \left(\frac{4m}{\pi \rho R^3} \right)^{n'} \qquad (5.8)$$

therefore $\log \Delta P = n' \log m + \text{constant}$

A plot of $\log \Delta P$ vs. $\log m$ will have a gradient equal to n'. For fluids obeying the Power Law

$n = n'$.

From expressions (5.6) and (5.7)

$$\dot{u}_w = \frac{4n}{3n+1} \cdot \dot{u}_w \text{ (apparent)} \qquad (5.9)$$

Thus a further plot may now be undertaken of $\log \tau_R$ vs. $\log \dot{u}_w$, i.e. $\log \left(\frac{R\ \Delta P}{2L} \right)$ vs. $\log \left(\frac{3n+1}{4n} \cdot \frac{4m}{\pi \rho R^3} \right)$ to obtain the actual viscosity, κ , when $\log \dot{u}_w = 0$.

The following effects may cause corrections to be necessary:

(a) Head of fluid above the tube exit

(b) Kinetic energy effects

(c) Tube entrance effects

(d) Effective slip near tube walls.

The first three may be corrected by a consideration of the total mechanical energy balance for the flow in the reservoir and tube. However Bagley's empirical method is frequently used in correcting for tube entrance effects. For any constant $\dot{u}_w$ (apparent) the ratio L/R is plotted against the pressure differential ΔP, and the intercept at $\Delta P = 0$ gives a value of $L/R = -N_f$ where $N_f R$ is a fictional extra

length of tube to account for the entrance effects. Substitition in the expression

$$\tau_R = \frac{R.\ \Delta P}{2(L+N_f R)} \qquad (5.9)$$

gives a value of τ_R free from tube entrance effects. Correction for effective slip may be carried out by means of experiments on tubes of constant L and varying R, whereby a coefficient of effective slip, β , may be derived from a plot of

$\frac{Q}{\pi R^3 \tau_R}$ vs τ_R for each tube. This is then substituted in the expression:

$$Q \text{ (corrected)} = Q \text{ (measured)} - \beta\tau_R\pi R^2 . \qquad (5.10)$$

5.3.3 Experimental

Initial experiments to commission the instrument were carried out with epoxy resin alone, and with a mixture of resin and two sizes of needles of melamine phosphate in a ratio of five to three.

A further series of experiments was carried out on other types to investigate the effects of crystal size and shape on the viscosity of the material. The large needles used in the initial experiments and the very large needles used in the further series were incorporated into the epoxy resin under low shear on an orbital mixer at low mixing speed. It was however found to be impossible to break down the very large agglomerates of small crystals in an orbital mixer and obtain a sufficiently uniform mixture to carry out rheological studies. Small needles, medium needles and thin reflective plates were all therefore incorporated by roll milling. Those materials tested in the second series of experiments were incorporated at levels of one part and three

parts melamine phosphate to five parts epoxy resin to simulate the viscosities of uncured mixtures containing 12½% and 30% melamine phosphate.

The inverted reservoir was filled with fluid, and the base bolted on. An extrusion tube was then screwed onto the base, and the instrument bolted into place in its frame, the gas supply pipeline screwed in and mass flow rates measured at not less than four pressures up to 150 pounds per square inch. The procedure was repeated for the other tubes (although only in the initial series were all the tubes used). Densities of the materials were measured using density bottles.

The graphical interpretation of results was carried out by plotting $\log \tau_R = \log \left(\frac{R.\ \Delta P}{2L}\right)$ vs.

$\log \dot{u}_w$ (apparent) $= \log \frac{4m}{\pi \rho R^3}$. The gradient of this plot is n, which was then used in a plot of

$$\log \tau_R = \log \left(\frac{R.\ \Delta P}{2L}\right) \text{ vs. } \log \dot{u}_w = \log \left(\frac{4m}{\pi \rho R^3} \cdot \frac{3n+1}{4n}\right).$$

The intercept at $\log \dot{u}_w = 0$ is $\log \kappa$, where κ is the actual viscosity. Different results were obtained from the tubes, and therefore corrections were investigated. To use Bagley's correction, ΔP was plotted against the tube length to radius ratio L/R at constant shear rate. However these points were not in linear arrangements, although by exclusion of Tube 2 an approximately linear result could be obtained. Some curvature was nevertheless apparent, suggesting the presence of time dependence and effective slip. The Bagley correction factor, N_f was obtained in a few cases, and the viscosities were obtained using

the corrected values of τ_R for each tube. However the magnitude of N_f was in all cases small, typically around 20 and the corrected values of viscosity not very different from the original values. Likewise the coefficient of effective slip, β was small, and the correction in the mass flow only around 0.03g min^{-1} for Tube 1, which is insignificant. It is believed that the main sources of error are instrumental, Tube 2 being especially affected. Each tube however gives self consistent results, suitable for comparative studies.

5.3.4 Results

Table 5.3 illustrates the results obtained from the experimental work and includes a mean value for viscosity for each mixture (excluding the results from Tube 2). Most of the calculations were carried out using a computer program by linear regression analysis on $\ln \tau_R$ and $\ln \dot{u}_w$ (apparent) to obtain n, and then on $\ln \tau_R$ and $\ln \dot{u}_w$ (actual) to obtain the actual viscosity, κ .

It appears that pure epoxy resin exhibits Newtonian behaviour, whereas the mixtures become increasingly pseudoplastic or thixotropic with increasing concentration of melamine phosphate. At concentrations of 60 parts melamine phosphate per 100 parts epoxy resin, all the mixtures were of the order of 35 N s m^{-2}; whereas at the lower concentration of 20 parts melamine phosphate per 100 parts of epoxy resin, the mixture incorporating very large needles was similar in viscosity to pure epoxy resin, at around 5 N s m^{-2}, whereas incorporation of smaller crystals gave rise to a higher viscosity of around 8 N s m^{-2}. In practice use of an orbital mixer causes aeration which increases the viscosity of mixtures containing small to medium size crystals considerably, but does so to a negligible extent to very large crystals.

TABLE 5.3 : Viscosities of Epoxy Resin and Mixtures With Melamine Phosphate Obtained by Extrusion Rheometry.

Material (pts. melamine phosphate per 100 pts. epoxy resin)	Density (kg m^{-3})	Tube	Power n	Actual Viscosity K (N s m^{-2})	Optimum Value of K (N s m^{-2})
-	1.147×10^3	1	0.99	5.97	5
		2	1.00	6.60	
		3	1.01	3.83	
		4	0.99	4.73	
60 small needles	1.32×10^3	1	0.97	30.5	25
		2	0.96	19.8	
60 large needles	1.32×10^3	1	0.95	20.6	30
		2	0.90	45.0	
		3	0.87	33.5	
		4	0.92	28.3	

Material (pts. melamine phosphate per 100 pts. epoxy resin)	Density (kg m^{-3})	Tube	Power n	Actual Viscosity K (N s m^{-2})	Optimum Value of K (N s m^{-2})
60	1.32×10^3	1	0.88	35.8	36
very large needles		2	0.80	64.4.	
20	1.205×10^3	1	0.94	4.96	5
very large needles		2	0.97	6.06	
60	1.32×10^3	1	0.86	36.8	38
medium needles		2	0.91	40.9	
20	1.205×10^3	1	0.93	8.05	8
medium needles		2	0.90	12.75	
		3	0.93	8.15	
60	1.32×10^3	1	0.86	34.1	35
thin reflective plates		2	0.88	40.3	
20	1.205×10^3	2	0.93	12.7	12
thin reflective plates					

CHAPTER 6

THE FIRE TESTING PROGRAMME

CHAPTER 6

THE FIRE TESTING PROGRAMME

Nomenclature

h	:	film coefficient of heat transfer from substrate to environment behind substrate
K	:	coefficient of thermal conductivity of char (mean value across char)
l	:	thickness of substrate
m	:	mass of substrate
t	:	time (general)
x	:	thickness of char
A	:	cross-sectional area of substrate
C_p	:	specific heat capacity of substrate
G, H	:	computer predictions for h used in calculation of same
T	:	temperature in British Standard 476 : 1972 Part 8 time-temperature curve
T_o	:	initial temperature in above
T_a	:	temperature of environment behind substrate
T_p	:	face temperature of char
T_q	:	substrate temperature
ΔT	=	$T_q - T_a$
ΔT^o	:	experimental standard for ΔT
θ	:	time (specific)
θ^o	:	experimental standard for θ
ρ	:	density of substrate
[ ]	:	experimentally determined values
{ }	:	values calculated from model

6.1 The Fire Test Regimes

Fire testing was carried out by placing a cured sample into position in the sindagno frame, and placing a protecting board of Sindagno over it. The wires of the thermocouple reading substrate temperature were led away from the lower edge of the sample. The back of the substrate was uninsulated as no means of achieving effective insulation at high substrate temperature could be found. Thus the heat balance for the substrate at any time θ during a fire test may be given by, in general terms for a fully developed char:-

$$\left(\frac{K}{x}\right)_\theta A(T_p - T_q)_\theta = m C_p \left(\frac{dT_q}{dt}\right)_\theta + h A (T_q - T_a)_\theta \qquad (6.1)$$

Heat flux conducted through char	Rate of increase of internal energy of substrate	Heat flux lost from back of substrate

It may be assumed that for tests carried out under similar conditions the heat loss term will be similar. This has been shown experimentally to be true (see Section 6.4). Thus groups of tests carried out under the same test regime are internally comparable. All substrate temperature readings, T_q, are the resultant of heat input through the char, and heat loss from the back surface of the substrate. This may occassionally lead to a decrease for a short time in the substrate temperature. An accurate assessment of the film coefficient of heat transfer from the back surface of the substrate has been carried out (see Section 6.4), thus allowing an assessment of $\left(\frac{x}{k}\right)$, the resistance to heat flow through the total thickness of a char as it develops under the conditions of a specific test. This was used to gather information of a quantitative nature, and was not required for a comparative assessment of the relative performance of coatings

incorporating different varieties of melamine phosphate crystals.

Three fire testing regimes were used; their time-temperature profiles are illustrated in Figure 6.1. Temperature measurement was by the two side mounted mineral insulated thermocouples in the frame, which were shown to be at a slightly lower temperature than the centre of the sample at a given range - the front of an expanded char would be at an even higher temperature. Obstruction of these thermocouples by voluminous char and reradiation from chars also affected the readings of these thermocouples. True sample face temperatures have been established by calibration tests (see Section 4.2).

(a) 850° - 900°C

By using a standard distance of 125 mm between the sample and the burner source and air and gas flow rates of 370 litre min^{-1} and 26 litre min^{-1} respectively, a face temperature of 850°C would be attained within five minutes as measured by the mineral insulated thermocouples. Temperatures up to, and occasionally above 900°C are indicated in such tests due to radiation from the char - during the later stages of such a test the temperature usually stabilises at around 850°C.

(b) 750° - 800°C

Such a test temperature was achieved using a distance of 190 mm of the sample from the burner source and similar air and gas flow rates as above. A temperature of 775° $\pm$ 25°C is attained within ten minutes, and remains fairly steady thereafter. This test regime proved the most useful for distinguishing behavioural differences between samples.

(c) British Standard Time-Temperature Curve Simulation Test

British Standard 476 : 1972, Part 8 for the fire testing of

FIGURE 6.1 : The Fire Testing Regimes

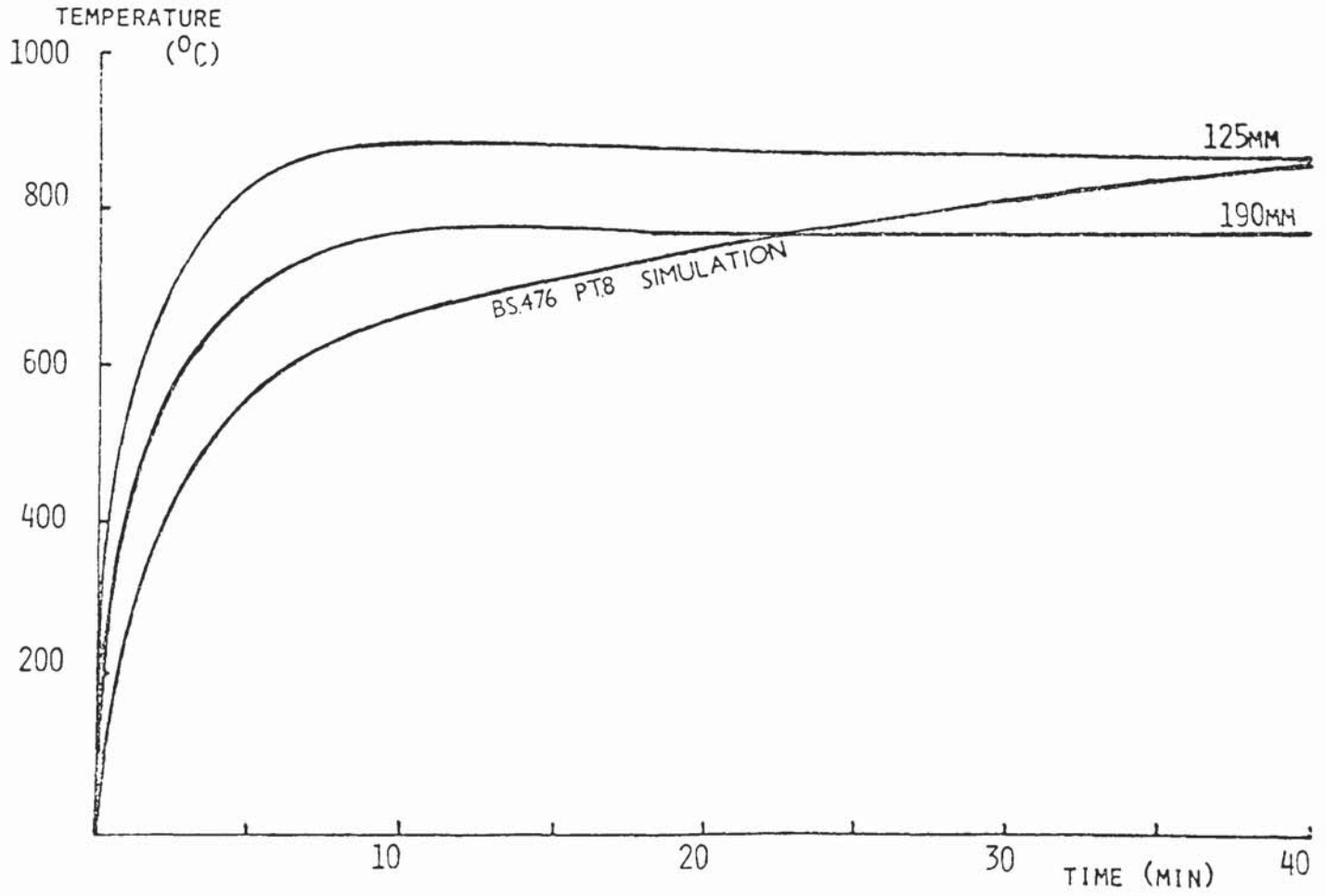

structural members specifies a time-temperature curve for the furnace which follows the equation:

$T - T_o = 345 \log_{10} (8t + 1)$

The temperature difference $(T - T_o)$ reaches 556°C after five minutes, 719°C after 15 minutes, 820°C after 30 minutes, etc. The test used in this work is not analagous to the British Standard Test, since no structural member is involved; however the above time-temperature curve was applied to the sample face temperature T_p, to enable the sample to be heated more slowly than in the above tests, but ultimately exposed to a temperature in excess of 900°C in many tests. This was accomplished by manually moving the sample in its frame towards the burner source during the course of a test. However slight differences inevitably occured between tests in the rate of rise of face temperature, and in the tables giving the results of these tests, the face temperature attained at a specified time is always given. In fact most tests were somewhat more severe than the British Standard time-temperature curve. Due to cross-currents the temperatures measured by the mineral-insulated thermocouples on either side of the sample frequently differed. The higher value of the two readings was used and the sample frame moved towards the burner source in accordance with this value.

6.2 An Historical Note

This section briefly sets out the information gained from early fire tests which led to the selection of tests for the main experimental series described in the next section.

The fire test regime almost universally used in the early tests was at 850° - 900°C, the sample being at a distance of 125 mm from the burner source. Using small needles $(C_3H_6N_6)_{1.2}.H_3PO_4$ at a 30% level of

incorporation, near the upper limit specified in British Patent 1,373,908, (54) in this fire test led to voluminous intumescence, which, not being able to push out very far directly ahead, would grow at a variety of angles and in a variety of directions, and continue to form new char until the material was exhausted and the substrate exposed. No quantitative data and little qualitative data could be obtained from such behaviour, and a search began to produce a formulation wherein the differences, if any, between different types of melamine phosphate and different treatments, such as incorporation under low shear compared with roll milling would be evidenced in the physical nature of the char. In these early tests, protection was due to dynamic factors, the production of cooling gas on a continuous basis. A stable char giving protection due to its inherent low thermal conductivity never survived. However by testing at the lower temperature of 750° - 800°C, at a distance of 190 mm from the burner source, such durable chars were formed from samples containing only melamine phosphate, epoxy resin, and hardener. The protection afforded to a substrate by such a char after the initial reaction producing it had subsided is a function of the physical structure, thermal conductivity and resistance to ablation of the char.

Nevertheless attempts to obtain a more durable char in tests at 850° - 900°C were also carried out, by the addition of such materials as titanium dioxide, cure accelerator, and bentone, materials commonly included in commercial formulations of this type; and by reduction in the level of incorporation of melamine phosphate. The effects of the cure regime on performance were also investigated (Section 5.2.3), leading ultimately to the standard cure regime of 24 hours at ambient temperature followed by nine days at 55°C.

For samples of coating weight around 70 g, tested at 850° - 900°C, a 12½% level of incorporation proved to give the optimum performance in the series containing 5%, 12½%, 20%, 25% and 30% loadings of melamine phosphate. Higher levels of melamine phosphate gave better protection in the early stages of the tests; however their durability was less than that of a sample containing only 12½% melamine phosphate, which after the formation and rapid destruction of a voluminous char during the first eight minutes of a test, retained some hardened char which would ablate slowly, eventually breaking down at around twenty minutes into the test. This residue giving extra protection did not occur at levels above 20% melamine phosphate. A similar sample containing 30% melamine phosphate lasted only 16 minutes. A 5% level of incorporation proved totally inadequate - much epoxy resin burned brightly, intumescence was patchy and breakdown occured in around five minutes. A 12½% level of incorporation was therefore chosen, together with a 30% level, for the main series of tests.

The addition of titanium dioxide led to severely restricted intumescence even at 850° - 900°C with 30% small needles $(C_3H_6N_6)_{1.2}.H_3PO_4$ (with respect to the total weight of resin, hardener and melamine phosphate, excluding titanium dioxide). Levels as low as 2% titanium dioxide with 12½% melamine phosphate caused deterioration in performance giving a restricted powdery char of poor structure; the deleterious effects became more pronounced as the quantity of titanium dioxide increased. For the purposes of this test, titanium dioxide could not be considered a suitabile additive. Addition of 2% triamyl ammonium phenate (Ciba-Geigy accelerator Araldite DY063) caused no noticeable change in performance compared to samples without this accelerator. Likewise a one per cent level of bentone incorporated by

roll milling together with a polar additive to cause plate separation (2% of a mixture of 20 parts methanol and one part water) caused no deleterious change in fire test performance. Bentone is normally added to provide thixotropic properties considered desirable during application of coatings.

Amongst these early tests were the first trials using crystal forms other than small needles, such as thin plates $(C_3H_6N_6)_{1.3}.H_3PO_4$ and large block plates $(C_3H_6N_6)_{2.0}.H_3PO_4$, and the more restricted intumescence provided by these materials first noted.

Amongst the early tests were included also several trials comparing crystals roll-milled into epoxy resin with samples in which low shear incorporation had been used. The voluminous intumescence of samples incorporating 30% melamine phosphate small needles at 850° - 900°C masked any small differences which might have existed. Trials with thin reflective plates at 12½% and 30% levels of incorporation at 850° - 900°C suggested that roll-milled samples gave slighly improved performance, but although giving this result at both levels of incorporation, the differences were not sufficiently large to be definitive, and further evidence concerning the effects of roll-milling contradicts these early findings (see Section 6.3.3).

The main series of fire tests was then carried out, using samples incorporating 12½% and 30% melamine phosphate. Tests at 750° - 800°C, considered to be the test providing the most information were always duplicated; the other tests were duplicated if it was felt that more information would be provided thereby. Further tests were carried out, with small changes in the processing when the results were not unequivocal - this was especially the case with samples incorporating thin plates. Originally melamine phosphate produced from equimolar

proportions of reagents was used; this had a melamine to phosphate ratio of 1.2 to 1.3. Then dimelamine phosphate and material with a melamine to phosphate ratio of approximately 1.0 was also tested. Finally a few mixtures of crystal types were used, being tested at the 30% level of incorporation.

A further series of experiments looked in less detail at the effects of further processing parameters - encapsulation of the particles of melamine phosphate, heat treatment of selected crystal types at 210°C for 48 hours, the effects of adding sodium hydrogen orthophosphate to the formulations. The latter two highlighted the need for further detailed investigation.

A portable mass spectrometer was used to analyse the gases evolved by burning of these samples. The only obviously detectable gases were oxides of carbon and ammonia. Considerable quantities of smoke were however also evolved; this would render these materials, especially when reacting quickly under high temperature conditions, unsuitable for use in the protection of personnel. They are best suited to the protection of buildings, capital equipment, and stores of flammable materials.

A full listing of the results of each individual fire test appears in Appendix A.4. Mean (typical) results are shown in Tables 6.1 to 6.9. The appearance of a typical voluminous char, around 100mm thick and of a typical restricted char, around 25 mm thick, obtained in the first ten minutes in tests at 750° - 800°C are shown in plates 6.1 and 6.2.

Plate 6.1 : Typical voluminous char, around 100 mm obtained after around ten minutes in a test at 750° - 800°C.

Plate 6.2 : Typical restricted char, around 20 mm; obtained after around ten minutes in a test at 750° - 800°C.

6.3 The Fire Test Programme

6.3.1 Materials Incorporating 12½% Melamine Phosphate

6.3.1.1 Tests at 750° - 800°C

The results from these tests are summarised in Table 6.1, which indicates the progress of a test by means of the times taken from the start of a test for the thermocouple situated centrally on the inner face of the substrate to register 300°C and 400°C respectively; the total duration of the test, ie. the time taken for 10% of the surface of the substrate to become exposed, or the substrate temperature to reach 500°C, whichever occured earlier; the maximum extent of intumescence and the time taken to reach this extent of intumescence. Figure 6.2 illustrates these results graphically. Each test was carried out twice to investigate reproducibility. In some cases further repetitions were carried out as a part of, for example, investigations into the effects of varying the cure regime.

The results are analysed below in decreasing order of performance:

Medium Needles $(C_3H_6N_6)_{1.0}\cdot H_3PO_4$

This material gave voluminous intumescence, which resisted ablation to a greater extent than samples containing $(C_3H_6N_6)_{1.2}\cdot H_3PO_4$, and gave excellent performance.

Very Large Needles $(C_3H_6N_6)_{1.0}\cdot H_3PO_4$

This material performed similarly to medium needles $(C_3H_6N_6)_{1.0}\cdot H_3PO_4$, but with less intumescence.

Large Needles $(C_3H_6N_6)_{1.2}\cdot H_3PO_4$

Of the materials of this stoichiometry, large needles gave the best performance, with as much intumescence as very large needles of $(C_3H_6N_6)_{1.0}\cdot H_3PO_4$. There was a degree of variation between the two tests conducted.

FIGURE 6.2 : Typical Substrate Time-Temperature Responses at 750° - 800°C; 12½% melamine phosphate.

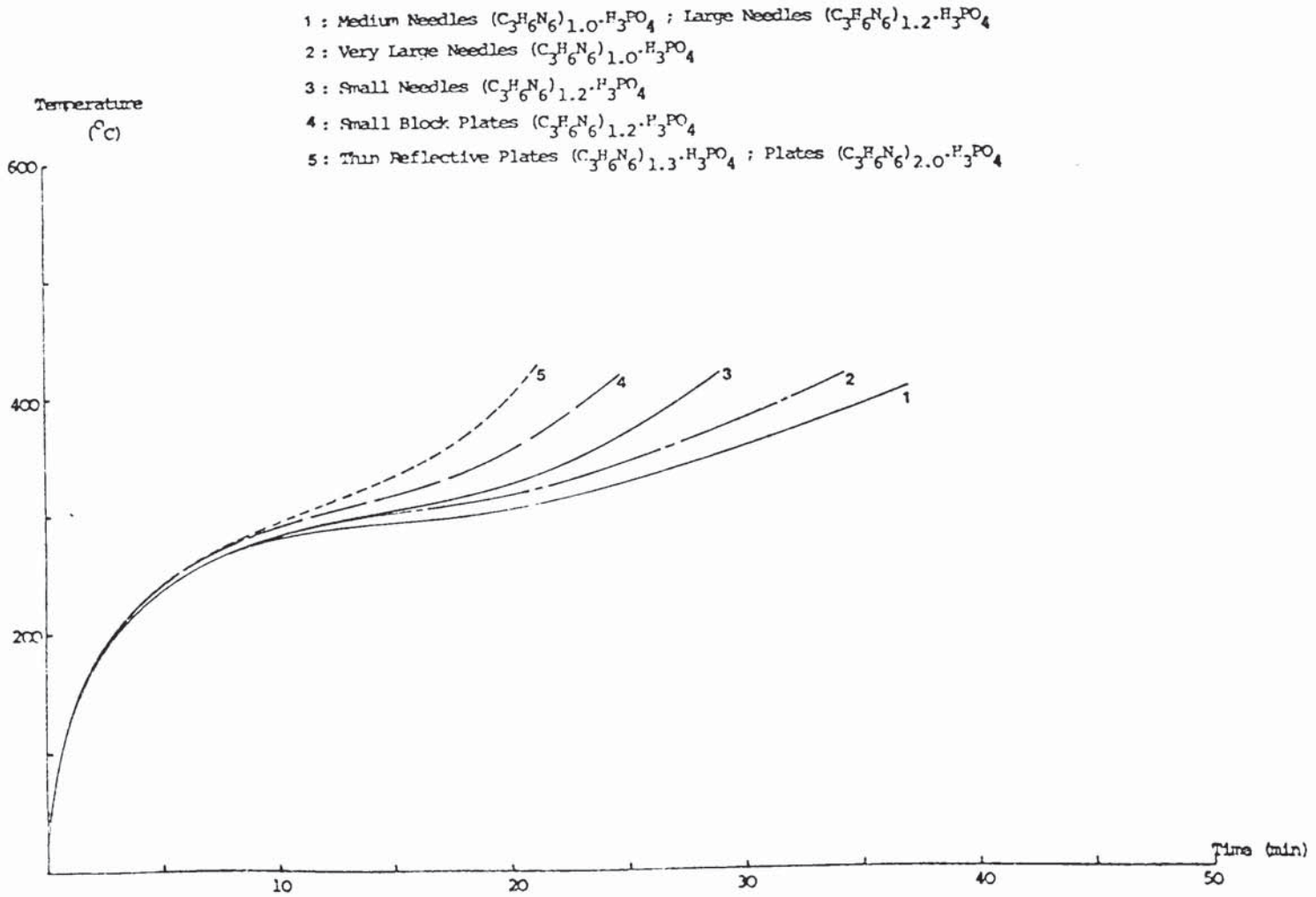

Small Needles $(C_3H_6N_6)_{1.2}\cdot H_3PO_4$

Intumescence was reduced with respect to large needles of $(C_3H_6N_6)_{1.2}\cdot H_3PO_4$.

Small Block Plates $(C_3H_6N_6)_{1.2}\cdot H_3PO_4$

Largely comparable to small needles, or slightly inferior.

Thin Reflective Plates $(C_3H_6N_6)_{1.3}\cdot H_3PO_4$

This material behaved in an almost consistently considerably inferior manner to the foregoing materials. Intumescence was normally more restricted than for the foregoing materials, but not consistently so. However when intumescence of a similar degree to e.g. small needles occurred, around 55 mm, the char structure was very poor, with large voids allowing convection currents to develop. Thus performance was as poor as in cases where only 20 to 30 mm of intumescence had developed.

The ablative characteristics of this material were also unusual. Rather than a constant reduction in the extent of the intumescence as surface ablation took place, with this material ablation would occur behind a brittle and hard outer skin, leaving a gap of up to 5 mm behind the skin. At this stage, the skin would break up, exposing the new surface, whereupon ablation would continue in like manner.

Thirteen tests were carried out with thin plates at a 12½% level of incorporation under this fire test regime. Two had a formula $(C_3H_6N_6)_{1.1}\cdot H_3PO_4$ - one of these gave a considerably improved performance, but the other was not significantly different in performance from the remainder. Cure regime was varied from the standard 9 days at 55°C, allowing from one day at ambient temperature to four weeks at 55°C.

Roll milled material, containing agglomerates of average diameter around 20 μm, and material mixed under low shear containing agglomerates of visible size, were tested, and despite differences in weight - an average of 60 g for roll milled samples, and 45g for other samples - no systematic differences were noted, although individual samples varied somewhat in the extent of intumescence, and overall performance occasionally. Surprisingly a sample cured for only one day at ambient temperature intumesced to 40 mm and gave a better than average performance! A full listing of the results appears in Appendix A.4.

Dimelamine Phosphate - medium and large plates

These samples all showed restricted intumescence and poor performance, comparable to that of thin plates of $(C_3H_6N_6)_{1.3}.H_3PO_4$, but inferior to that of other crystal types of such stoichiometry.

6.3.1.2 Tests on a British Standard Time-Temperature Curve Simulation

A consistent feature of these tests was the restricted extent of intumescence, compared to that occuring when heating quickly to 750° - 800°C, though in general those samples which intumesced to the greatest extent in the former test did likewise in this test. In nearly all cases imperfect matching of the constituents of the intumescent system led to melting prior to hardening of the char, thus reducing the quantity of material actually protecting the substrate. Each test was repeated.

The order of performance was similar to that in the test regime at 750° - 800°C. Table 6.2 summarises the results, which are illustrated graphically in Figure 6.3.

TABLE 6.1 : Typical Performance Of Samples Containing Melamine Phosphate Incorporated At A Level Of 12½% And Of Total Weight Of Coating 45 - 50g, Tested At 750° - 800°C. N.B. The Results Are Averaged, And Do Not Represent Any One Specific Test.

Crystal Type	Time To -(min)		Duration	Maximum Extent	Time to Attain
	300°C	400°C	(min)	of Intumescence (mm)	Maximum Extent (min)
Medium Needles $(C_3H_6N_6)_{1.0}\cdot H_3PO_4$	16	34	34	85	6
Very Large Needles $(C_3H_6N_6)_{1.0}\cdot H_3PO_4$	12	31	34	50 - 70	7
Large Needles $(C_3H_6N_6)_{1.2}\cdot H_3PO_4$	10 - 17	25 - 35	30 - 38	70	3 - 4
Small Needles $(C_3H_6N_6)_{1.2}\cdot H_3PO_4$	11	28	33	30 - 50	6½
Small Block Plates $(C_3H_6N_6)_{1.2}\cdot H_3PO_4$	8 - 10	17 - 22	20 - 27	30 - 50	6 - 9

Table 6.1 (cont)

Crystal Type	Time To -(min)		Duration	Maximum Extent	Time to Attain
	300°C	400°C	(min)	of Intumescence (mm)	Maximum Extent (min)
Thin Reflective Plates $(C_3H_6N_6)_{1.3}\cdot H_3PO_4$	5	18	21	20 - 40	3 - 5
Medium Block Plates $(C_3H_6N_6)_{2.0}\cdot H_3PO_4$	5	20	21	15	5½
Large Block Plates $(C_3H_6N_6)_{2.0}\cdot H_3PO_4$	5	20	24	40	6

TABLE 6.2 : Typical Performance of Samples Containing Melamine Phosphate Crystal Types Incorporated At A Level Of 12½% And Total Weight Of Coating 45 - 50g, In British Standard Time-Temperature Curve Simulation Tests.

Crystal Type	Times (min) to Reach Stated Substrate Temperature, & Face Temperature At This Time (in Brackets, °C)		Extent of Intumescence (mm)
	300°	400°	
Medium Needles $(C_3H_6N_6)_{1.0}\cdot H_3PO_4$	15 (745°)	28 (855°)	25
Very Large Needles $(C_3H_6N_6)_{1.0}\cdot H_3PO_4$	10½ (685°)	-	25
Large Needles $(C_3H_6N_6)_{1.2}\cdot H_3PO_4$	16½ (740°)	27 (815°)	20
Small Needles $(C_3H_6N_6)_{1.2}\cdot H_3PO_4$	12 (675°)	22 (780°)	35
Small Block Plates $(C_3H_6N_6)_{1.2}\cdot H_3PO_4$	17 (745°)	-	25
Thin Reflective Plates $(C_3H_6N_6)_{1.3}\cdot H_3PO_4$	8 (645°)	16 (755°)	10
Medium Block Plates $(C_3H_6N_6)_{2.0}\cdot H_3PO_4$	10 (675°)	17½ (770°)	10
Large Block Plates $(C_3H_6N_6)_{2.0}\cdot H_3PO_4$	8 (655°)	17 (760°)	10

FIGURE 6.3 : Typical Substrate Time-Temperature Responses under British Standard 476 Pt. 8 Time-Temperature Curve Simulation conditions; 12½% melamine phosphate.

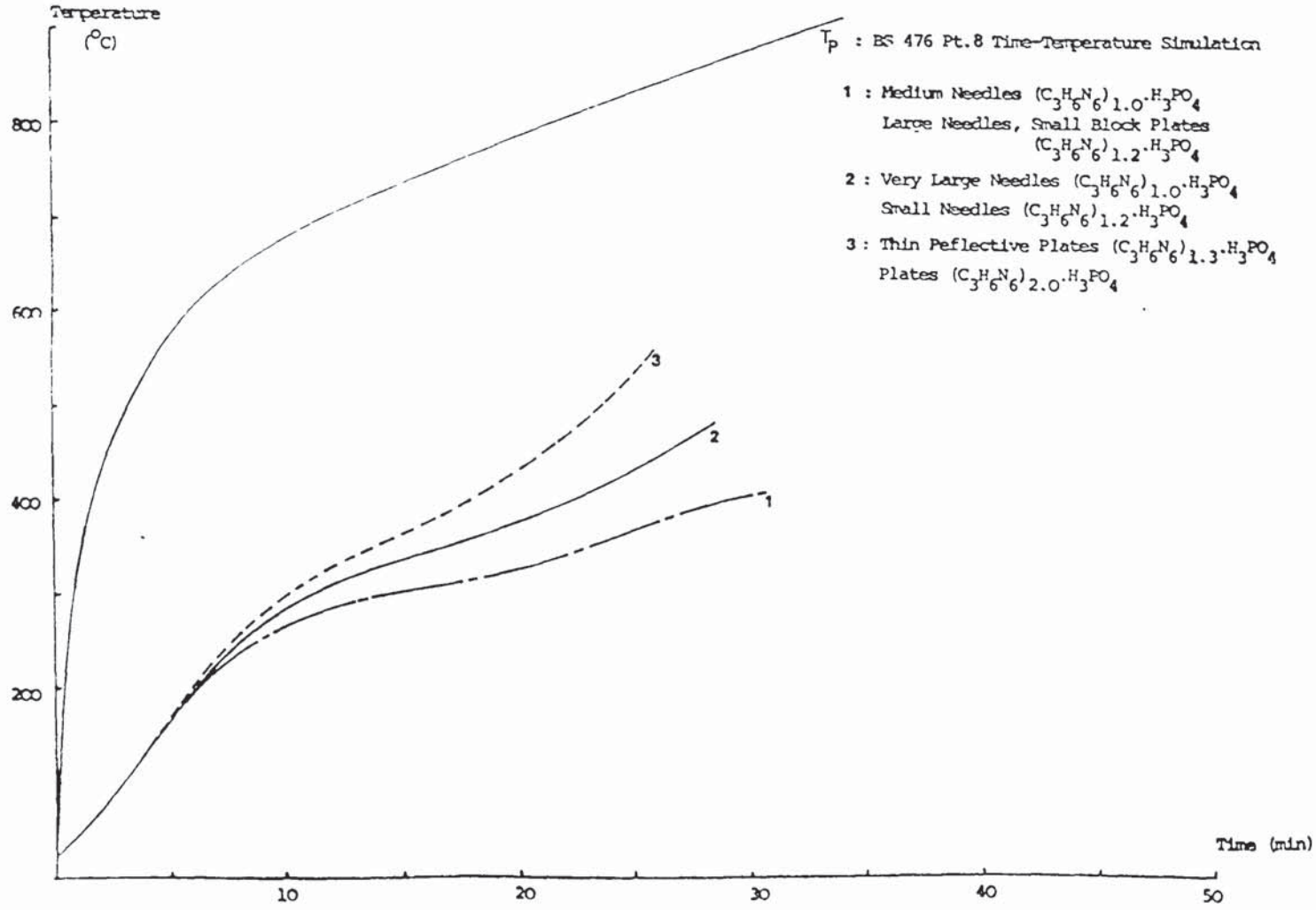

6.3.1.3 Tests at 850° - 900°C

Intumescence in this test was uniformly more voluminous than in a test at 750° - 800°C although the extent of intumescence was still less for thin reflective plates of $(C_3H_6N_6)_{1.3}.H_3PO_4$ and for dimelamine phosphate. The disadvantages of such voluminous intumescence for obtaining information have been discussed.

It does appear however that the less voluminous intumescence of the latter two types is not consumed so quickly and thus samples produced with thin reflective plates or dimelamine phosphate may perform better than the other crystal types - a reverse of the order experienced in the other tests. However at a 12½% level of incorporation those samples which did intumesce voluminously in the first eight minutes, or thereabouts were still normally left with some harder char, if the sample weight exceeded 50g, and their temperature was maintained at a low level by the voluminous intumescence during this stage. Whether a sample giving restricted intumescence would give superior performance than one giving voluminous intumescence in its early stages would depend upon the weight per unit surface area and the thickness of the coating, and upon the resistance to ablation of the voluminous char in a large scale test.

Results of individual tests are given in Appendix A.4. General conclusions of a more quantitative nature cannot be drawn from these results on this scale of test.

6.3.2 Materials Incorporating 30% Melamine Phosphate

6.3.2.1 Tests at 750° - 800°C

The results from these tests are summarised in Table 6.3, and the nature of their time-temperature responses illustrated graphically

TABLE 6.3 : Typical Performance Of Samples Containing Melamine Phosphate Incorporated At A Level of 30%, And Of Total Weight Of Coating Around 55g, Tested at 750° - 800°C. N.B. Where Two Figures Are Given, These Refer To Upper And Lower Temperature Response Patterns.

Crystal Type	Time To - (mins)		Duration	Maximum Extent	Time to Attain
	300°C	400°C	(min)	of Intumescence (mm)	Maximum Extent (min)
Medium Needles $(C_3H_6N_6)_{1.0}\cdot H_3PO_4$	24	45	50	80	10
Very Large Needles $(C_3H_6N_6)_{1.0}\cdot H_3PO_4$	20	40	50	100	7½
Plates $(C_3H_6N_6)_{1.1}\cdot H_3PO_4$	15	35	47	80	12
Large Needles $(C_3H_6N_6)_{1.2}\cdot H_3PO_4$	18, 24	32, 46	38, 54	95, 45	7½
Small Needles $(C_3H_6N_6)_{1.2}\cdot H_3PO_4$	15, 22	34, 38½	40, 42	100, 75	7

Crystal Type	Time To - (mins)		Duration (min)	Maximum Extent of Intumescence (mm)	Time To Attain Maximum Extent (min)
	300°C	400°C			
Small Block Plates $(C_3H_6N_6)_{1.2}\cdot H_3PO_4$	17, 25	30, 43	39, 44	80, 60	8
Thin Reflective Plates $(C_3H_6N_6)_{1.3}\cdot H_3PO_4$	8	17	20, 34	45, 20	8
Medium Block Plates $(C_3H_6N_6)_{2.0}\cdot H_3PO_4$	5	13	29	12	6
Large Block Plates $(C_3H_6N_6)_{2.0}\cdot H_3PO_4$	8	17	26	35	6½
Small Amorphous Material $(C_3H_6N_6)_{2.0}\cdot H_3PO_4$	8	19	25	35	8½

in Figure 6.4. All tests were carried out twice.

The crystal types of melamine phosphate fell into two distinct categories under this type of exposure. In that consisting of the samples giving better performance were all the samples containing needles and small block plates, being of stoichiometry $(C_3H_6N_6)_{1.0}.H_3PO_4$ to $(C_3H_6N_6)_{1.2}.H_3PO_4$. Among these an unusual phenomenon was observed, whereby at around thirteen minutes into the test the temperature of the substrate either began to rise slowly or else maintained a steady state for several minutes longer. This results in two families of curves, the members of which are almost superimposed until around thirty minutes into the tests, into either of which any sample produced from any of the above crystal types might fall. Thus at 28 minutes into the tests those samples on the lower family of curves were all within the temperature range 300° - 320°C, whilst those on the upper family of curves were within the range 370° - 395°C. It was only after around thirty to thirty five minutes that differences within samples on the lower family of curves appeared, and needles of stoichiometry $(C_3H_6N_6)_{1.0}.H_3PO_4$ and large needles of stoichiometry $(C_3H_6N_6)_{1.2}.H_3PO_4$ proved to give the best performance, continuing to give protection, whilst the other samples, small needles and small block plates of $(C_3H_6N_6)_{1.2}.H_3PO_4$ began to break up. The majority of samples on the upper family of curves however lasted no longer than 43 minutes. Statistical analysis of tendencies to follow a particular response pattern can only be highly tentative with a population of this size; it does however appear that slightly over half of all the samples produced with crystals of stoichiometry $(C_3H_6N_6)_{1.2}.H_3PO_4$ followed the upper temperature response pattern, where-

FIGURE 6.4 : Typical Substrate Time-Temperature Responses at 750° - 800°C; 30% Melamine Phosphate.

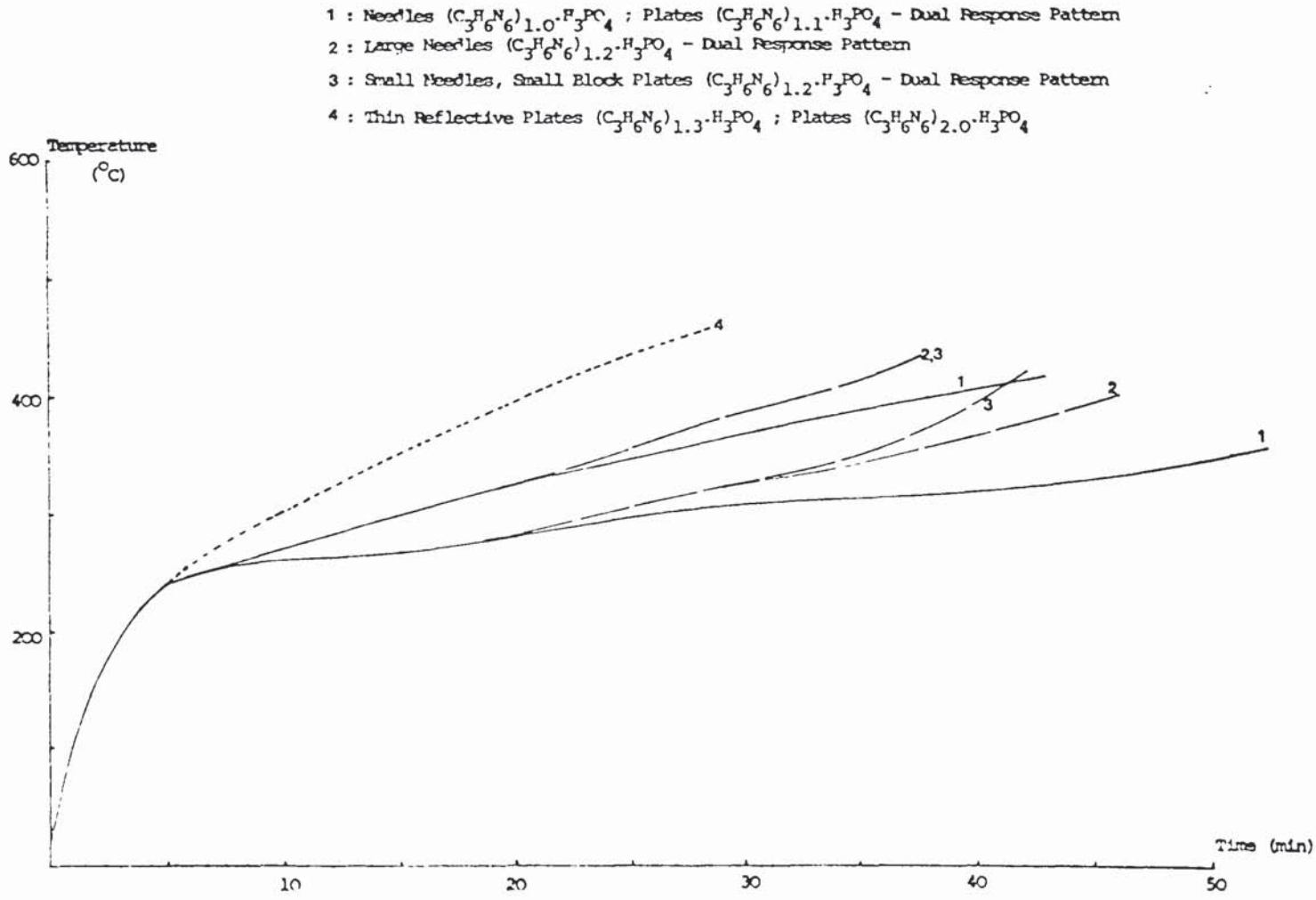

as the reverse was true for those samples produced with crystals of stoichiometry $(C_3H_6N_6)_{1.0}.H_3PO_4$.

On examination of the degree of intumescence obtained it appeared that some samples intumesced considerably more voluminously than others during the early stages of the tests. Thereafter ablation took a greater toll of these samples, which had spent more of their substance in the early stages, and these samples constituted the upper temperature response pattern, failing earlier than the samples which intumesced less voluminously and were thus able to give protection for a longer period of time. These latter followed the lower response pattern. For example, the tests involving samples incorporating large needles of stoichiometry $(C_3H_6N_6)_{1.2}.H_3PO_4$ provided respectively 95 mm and 45 mm of intumescence at 7½ minutes, but by the time 30 minutes had elapsed these had but 10 mm and 20 mm respectively, the latter having earlier produced less intumescence still giving more protection after this time. Small needles and small block plates similarly yielded samples each following a separate response pattern (the difference in char production being rather smaller for the latter). The remaining materials produced samples both following the same response pattern. A single sample incorporating plates of stoichiometry $(C_3H_6N_6)_{1.1}.H_3PO_4$ was also tested, and followed the upper temperature response pattern.

Those samples containing thin reflective plates of stoichiometry $(C_3H_6N_6)_{1.3}.H_3PO_4$ and any crystal size of dimelamine phosphate performed in considerably inferior fashion with respect to duration and substrate temperature response pattern. It appears that these samples may also exhibit a dual temperature response pattern similar to that noted above. In all cases intumescence was more restricted than was

the case with the samples giving superior performance. Small amorphous dimelamine phosphate was produced by mixing melamine in suspension and phosphoric acid in appropriate proportions, stirring and filtering prior to the formation of plates. It probably actually consists of "ordinary" melamine phosphate and melamine; a sample containing this material, produced as a dimelamine phosphate crystal size analogue to small needles of $(C_3H_6N_6)_{1.2}.H_3PO_4$, gave a performance fairly similar to the other true dimelamine phosphate samples.

6.3.2.2 Tests on a British Standard Time-Temperature Curve Simulation

Due to the problems encountered with melting of the coating and variations in the time-temperature curve actually followed due to the problems of manual control of the distance of the sample from the burner heat source, only one British Standard time-temperature curve simulation test was carried out on each sample. The results are recorded in Table 6.4 and in Appendix A.4 and illustrated graphically in Figure 6.5.

In summary, it was found that an order of performance exists somewhat similar to that for a test at 750° - 800°C, viz:

Medium Needles $\doteq$ Small Needles $>$ Large Needles $\doteq$

$(C_3H_6N_6)_{1.0}.H_3PO_4$ $(C_3H_6N_6)_{1.2}.H_3PO_4$ $(C_3H_6N_6)_{1.2}.H_3PO_4$

Small Block Plates $\gg$ Thin Reflective Plates $\doteq$ Small Amorphous Material $>$

$(C_3H_6N_6)_{1.2}.H_3PO_4$ $(C_3H_6N_6)_{1.3}.H_3PO_4$ $(C_3H_6N_6)_{2.0}.H_3PO_4$

Large Block Plates

$(C_3H_6N_6)_{2.0}.H_3PO_4$

TABLE 6.4 : Typical Performance Of Samples Containing Melamine Phosphate At A 30% Level of Incorporation And Total Weight Of Coating Around 55g, In British Standard Time-Temperature Curve Simulation Tests.

Crystal Type	Times (min) To Reach Stated Substrate Temperature, & Face Temperature At This Time (In Brackets, °C)		Extent of Intumescence (mm)
	300°C	400°C	
Medium Needles $(C_3H_6N_6)_{1.0}.H_3PO_4$	30 (865°)	-	25
Large Needles $(C_3H_6N_6)_{1.2}.H_3PO_4$	20 (790°)	29½ (850°)	28
Small Needles $(C_3H_6N_6)_{1.2}.H_3PO_4$	25 (840°)	-	50
Small Block Plates $(C_3H_6N_6)_{1.2}.H_3PO_4$	20½ (780°)	31 (885°)	33
Thin Reflective Plates $(C_3H_6N_6)_{1.3}.H_3PO_4$	17 (775°)	23½ (820°)	15
Large Block Plates $(C_3H_6N_6)_{2.0}.H_3PO_4$	9½ (675°)	18½ (775°)	15
Small Amorphous Material $(C_3H_6N_6)_{2.0}.H_3PO_4$	12 (715°)	25 (805°)	25

FIGURE 6.5 : Typical Substrate Time-Temperature Responses under British Standard 476 Pt. 8 Time-Temperature Curve Simulation conditions; 30% melamine phosphate.

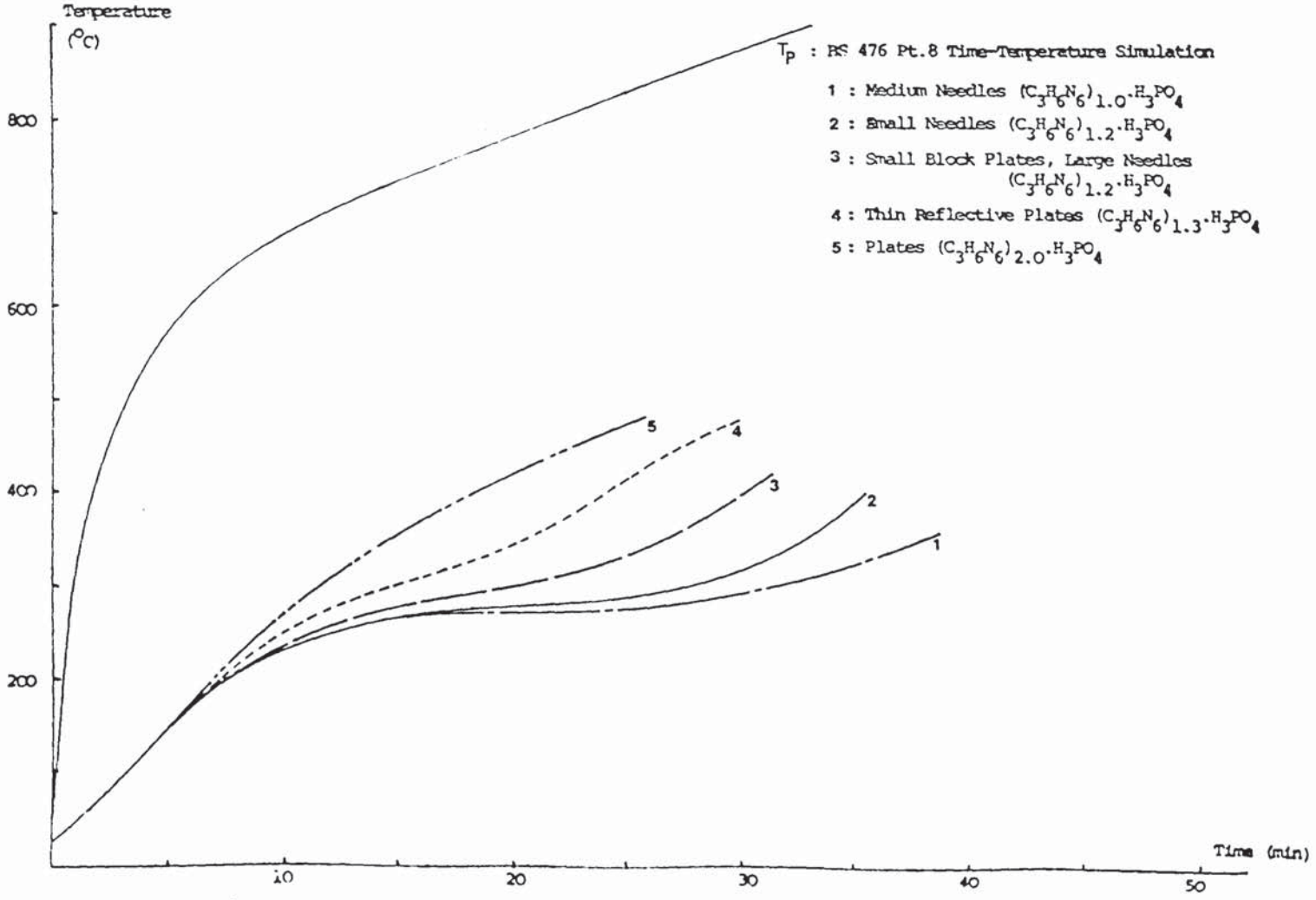

However with this amount of testing, the crystal types may only be definitively placed into two categories : dimelamine phosphate and thin reflective plates $(C_3H_6N_6)_{1.3}.H_3PO_4$ gave inferior performance to the other crystal types. Other differences within each of these categories may not be significant, but simply due to the vagaries of the tests, and slight differences in the weights of the samples.

6.3.2.3 Tests at 850° - 900°C

Those samples incoporating crystal types giving good performance and a higher degree of intumescence in the foregoing tests intumesced voluminously in a manner totally unsuitable for obtaining quantitative information. Early samples produced from thin reflective plates gave restricted intumescence, a roll-milled sample giving a slightly improved substrate temperature response than a sample with the crystals mixed in under low shear. However a further sample intumesced fairly voluminously whilst dimelamine phosphate incorporation led to much more restricted intumescence (100 - 150 mm total). As in the case of the samples containing 12½% melamine phosphate, a larger scale test would probably be required to assess performance in this test regime adequately, but it seems likely that a product containing one of the crystal types giving a high level of intumescence would give better protection for short periods, whilst incorporation of thin reflective plates might lead to a slightly longer life for the coating in a fire at this temperature. Full results are listed in Appendix A.4.

6.3.3 The Effect of Crystal Type on Performance in a Fire Test - A Summary

The foregoing results show that there are essentially two categories of performance according to the crystal type incorporated.

Within each category there appears to be a further ranking of performance. Incorporation of thin reflective plates or dimelamine phosphate leads to an inferior performance - a lower extent of intumescence in most cases and a shorter period of protection - than is the case with other crystal types (except perhaps in a LPG fuelled fire where the temperature rise is sudden and high, and the intumescence of the majority of crystal types may be too voluminous and insufficiently strong to avoid detachment by the high wind speeds encountered in such fires).

The ratio of melamine to phosphate appears to be very important; where this is 1.0 a longer period of protection at 750° - 800°C or in a British Standard Time-Temperature Curve Simulation test situation may be expected than where this ratio is around 1.2. The use of Dimelamine phosphate leads to considerably inferior performance.

Tests were carried out at 12½% and 30% levels of incorporation. In the tests at 750° - 800°C and British Standard simulations the 30% materials always gave considerably improved performance and had a longer life than the 12½% materials, by normally around 50%. At the lower level of incorporation there appears to be insufficient phosphate to react with all the epoxy resin, as is required to allow the endothermic dehydration route of combustion to take place. Some of the resin therefore burns exothermically, and flames play across the surface of the char. At the 30% level of incorporation any such flaming is very temporary and minor. Such flaming of course increases the temperature of the front of the char. Flames were also often seen during a sudden spurt of intumescence issuing from the newest intumescence at the back where the material was still shining and semi-molten. If excessive melting occured during a test, flames were often

associated with the drops of melt falling onto the working surface - this happened frequently especially with the British Standard simulation tests, suggesting poor matching of the epoxy resin and melamine phosphate when the rate of heating was slow.

At 850° - 900°C however a 12½% level of incorporation was an advantage especially with those crystal types which tend to give very voluminous intumescence. At a 30% level, reaction tends then to be so vigorous that the coating is consumed within around seven minutes (45g weight) to twelve minutes (65g weight). However 65g of coating with 12½% melamine phosphate will give initially a voluminous intumescence, but after around eight minutes a residue of char will be left which may protect the substrate for up to a further twelve minutes.

Crystal size for a particular crystalline type appears to have some effect on the course of a fire test. A large crystal size will result in a smaller contact area with epoxy resin per unit volume of melamine phosphate.than a small size. As a result the reaction is less vigorous and may be slightly more prolonged. However a slower reaction also leads to more epoxy resin being burned exothermically before it has a chance to react with phosphate, and thus to increased flaming. This may tend to reduce the life of the coating. Large needles $(C_3H_6N_6)_{1.2}.H_3PO_4$ appeared to perform better than small needles of the same stoichiometry, but there appeared to be no such difference, or possibly a slight reverse effect, in the case of very large needles and medium needles $(C_3H_6N_6)_{1.0}.H_3PO_4$. The advantages of a more restrained reaction may be greatest when the particle size differential is between 10 μm and 80 μm rather than between 50 μm and 300 μm. Some observations on the effects of roll milling

TABLE 6.5 : A Comparison Of The Performance Of Specific Samples Containing Melamine Phosphate Incorporated Respectively Under Low Shear And By Roll-Milling.

Test No. (see Appendix A.4)	Weight (g)	Times (min) to: 300°C	400°C	Duration (min)	Maximum Extent of Intumescence (mm)
Thin Reflective Plates, 12½% Level of Incorporation					
(1) Low Shear Incorporation					
4	45	5½	17½	21	35
29	50	8	21½	25½	15
(2) Roll Milled					
110	55.6	4½	16	20½	40
112	50.8	6	19	26	55
Small Needles,, 30% Level of Incorporation					
(1) Low Shear Incorporation					
35	54.9	15	34	42	150
43	62	22	38½	41½	75
(2) Roll Milled					
144	63.2	10	20½	29	40
145	53.8	6½	19½	30	48

appear to confirm this. All milling was done with very closely set rolls and the mixture passed several times over the rolls. The particle sizes were considerably reduced thereby. A comparison of the behaviour of roll-milled samples with material containing a similar crystalline type of melamine phosphate incorporated under low shear shows the former normally to have fared considerably worse than the latter, even if the weight of the former was greater, in tests at 750° - 800°C. Some typical test results appear below in Table 6.5, illustrating this point.

In the case of small block plates, tests carried out with this material incorporated at a 12½% level did not show such an effect: the heavier roll milled samples performed better. However a blocky plate is considerably less likely to agglomerate than a small needle or thin plate, and consequently roll milling is unlikely in the former to cause as great a change in the particle characteristics.

Examination of some of these results reveals that it is not always true that a sample with a greater weight of coating performs better. In some cases, e.g. comparing tests 92 and 94, or tests 144 and 145, the difference in weight is insufficient to prevent other factors overriding that parameter. It is often the case that the sample which intumesces most in the early stages is less durable.

6.3.4 Encapsulation of Melamine Phosphate

Tests were conducted using samples where the particles of melamine phosphate, small needles of $(C_3H_6N_6)_{1.2}.H_3PO_4$, were encapsulated in part of the epoxy resin/hardener mixture to ensure thorough wetting, before finally mixing with the rest of the resin/hardener mixture, to a final composition of 30% melamine phosphate. About one third of the total quantities of epoxy resin and hardener to

be used were diluted with acetone, and Ciba-Geigy accelerator DY 063 added, equivalent to around 2% of the combined weight of resin and hardener. This solution was added dropwise to the melamine phosphate being agitated in a Kenwood Major mixer; evaporation of the acetone leads to fast cure of the resin on the surfaces of the melamine phosphate. The dry coated melamine phosphate was then mixed in the normal way under low shear with the remainder of the resin and hardener.

The process of encapsulation caused almost total quenching of intumescence, which was very restricted, even in a test at 850° - 900°C, and in all three test regimes, substrate temperature response was worse than for any other material tested! Table 6.6 shows the results obtained.

6.3.5 Coatings Containing a Mixture of Crystal Types

The performances of coatings in which two types of melamine phosphate crystals, which had been shown to behave in a different manner alone, were incorporated to a total loading of 30% melamine phosphate, were investigated. Two formulations were investigated to the same extent as previous 30% formulations, i.e. two tests at 750° - 800°C, and one test each at 850° - 900°C and by the British Standard time-temperature curve simulation. These contained equal weights of medium needles of $(C_3H_6N_6)_{1.0}.H_3PO_4$ and thin reflective plates of $(C_3H_6N_6)_{1.0}.H_3PO_4$, and small needles of $(C_3H_6N_6)_{1.2}.H_3PO_4$ and dimelamine phosphate medium block plates respectively. Briefer investigations were carried out on a few other formulations, where a single sample only was produced and tested at 750° - 800°C. One of these contained equal weights of medium block plates of $(C_3H_6N_6)_{2.0}.H_3PO_4$ and medium

TABLE 6.6 : The Performance Of Samples, Of Approximate Coating Weight 50g, Of Melamine Phosphate 30% Encapsulated In Epoxy Resin.

*Face temperature attained at the stated times given in brackets, °C.

Test Regime	Times (min) To:-		Duration (min)	Maximum Extent Of Intumescence (mm)
	300°	400°C		
750° - 800°C	6	13	22	8
BS Simulation*	9¼ (645°)	16¾ (745°)		10
850° - 900°C	3½	6¾	8½	70

needles of $(C_3H_6N_6)_{1.0}.H_3PO_4$, which were the dominant forms in the other mixtures. The others contained medium needles of $(C_3H_6N_6)_{1.0}.H_3PO_4$ and thin reflective plates of $(C_3H_6N_6)_{1.3}.H_3PO_4$ in weight ratios of 1 : 3 and 1 : 8 respectively.

The result of these tests are shown in Table 6.7, and illustrated graphically in Figure 6.6 in the case of the tests at 750° - 800°C. In the first named mixture, medium needles of $(C_3H_6N_6)_{1.0}.H_3PO_4$ totally dominated thin reflective plates of $(C_3H_6N_6)_{1.3}.H_3PO_4$, the substrate time-temperature response not being substantially different from that of a sample containing only 30% medium needles of $(C_3H_6N_6)_{1.0}.H_3PO_4$. Progressive reduction of the quantity of medium needles with respect to thin reflective plates led to a progressive reduction in performance. The second named mixture was however dominated by the crystals of dimelamine phosphate, although the presence of small needles of $(C_3H_6N_6)_{1.2}.H_3PO_4$ improved the performance slightly. A mixture of these dominant forms performed in a manner intermediate between that of the other mixtures of equal weights of both components (and less well than a 1 : 8 mixture of medium needles of $(C_3H_6N_6)_{1.0}.H_3PO_4$ and thin plates of $(C_3H_6N_6)_{1.3}.H_3PO_4$).

Likewise in the British Standard time-temperature simulation curve tests, the first named mixture performed better than the second.

In the tests at 850° - 900°C, however, one of the best performances encountered in a fire test at this temperature occured in the case of the mixture of small needles of $(C_3H_6N_6)_{1.2}.H_3PO_4$, and medium block plates of $(C_3H_6N_6)_{2.0}.H_3PO_4$. The dimelamine phosphate restricted intumescence somewhat but the char structure was better than this

TABLE 6.7 : Typical Performances Of Samples Containing Mixtures Of Crystal Types To A 30% Level Of Incorporation, Total Weight Of Coating Around 55g.

Mixture I : medium needles $(C_3H_6N_6)_{1.0}.H_3PO_4$ and thin reflective plates $(C_3H_6N_6)_{1.3}.H_3PO_4$

Mixture II : small needles $(C_3H_6N_6)_{1.2}.H_3PO_4$ and medium block plates $(C_3H_6N_6)_{2.0}.H_3PO_4$ - ratio 1 : 1.

Mixture III : medium needles $(C_3H_6N_6)_{1.0}.H_3PO_4$ and medium block plates $(C_3H_6N_6)_{2.0}.H_3PO_4$ - ratio 1 : 1

Table 6.7a : Tests at 750° - 800°C

Mixture	Time (min) To:- 300°C	400°C	Duration (min)	Maximum Extent of Intumescence (mm)	Time To Maximum Intumescence (min)
Mixture I					
Ratio 1 : 1	19	60	60	80	10
Ratio 1 : 3	15	43	55	100	8
Ratio 1 : 8	10½	43	49	25	10 - 22
Mixture II	6	21	27	35	6½
Mixture III	7½	28	36	80	7¼

Table 6.7b : British Standard Time-Temperature Curve Simulation Tests. Temperatures in brackets indicate face temperatures attained at the stated times, °C.

Mixture I (Ratio 1 : 1)	27½ (845°)	-	30
Mixture II	10 (675°)	20 (750°)	17

Table 6.7c : Tests at 850° - 900°C

Mixture	Time (min) To:-		Duration (min)	Maximum Extent of Intumescence (mm)
	300°	400°		
Mixture I (Ratio 1 : 1)	-	7	7½	voluminous
Mixture II	-	7¾	8	voluminous

FIGURE 6.6 : Typical Substrate Time-Temperature Responses at 750° - 800°C; Mixtures of crystal types, total loading 30% melamine phosphate.

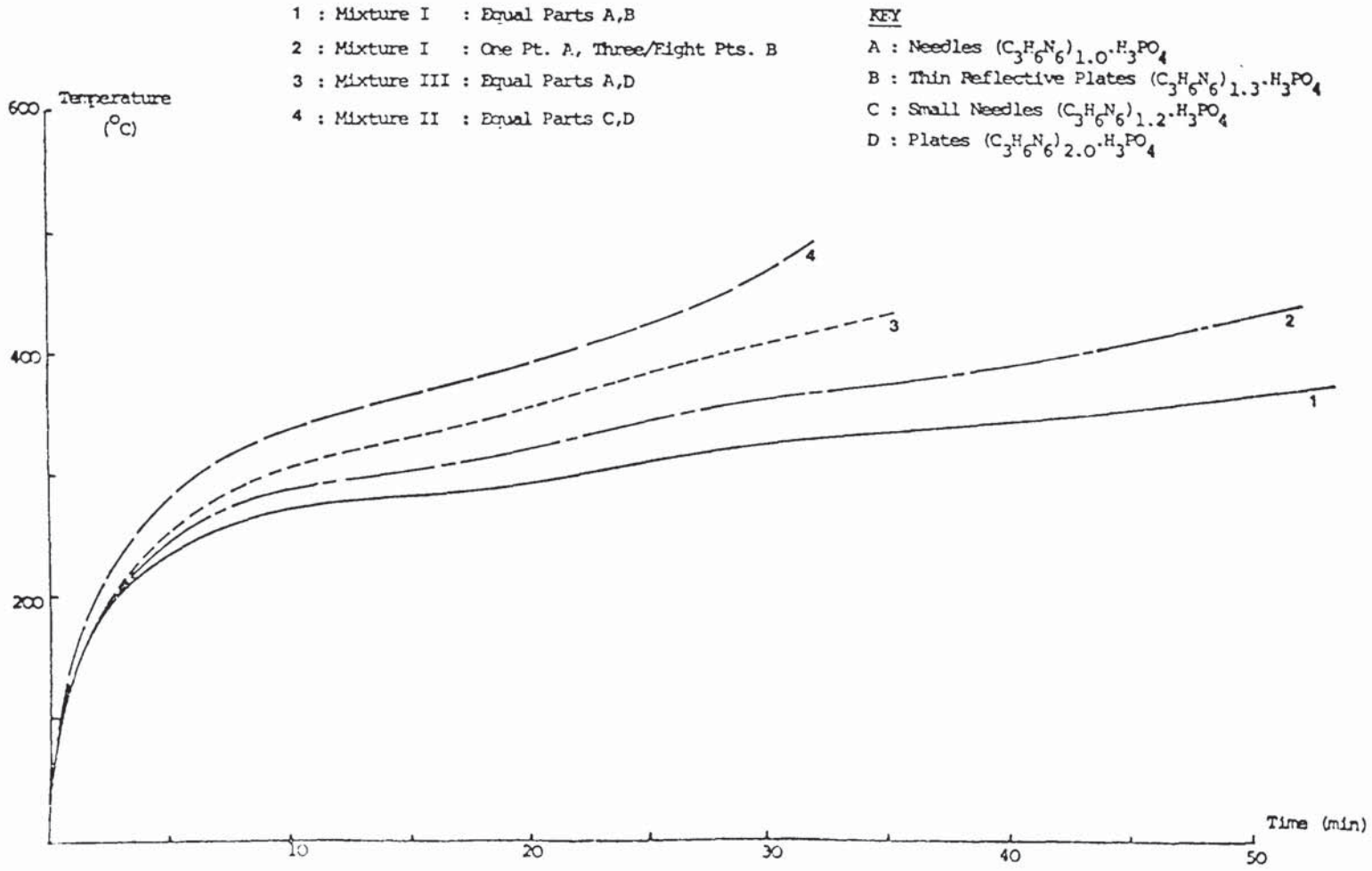

material alone normally provides, presumably due to the presence of small needles.

6.3.6 Coatings Incorporating Melamine Phosphate Treated at 210°C

Six crystal types of melamine phosphate were treated at 210°C for 48 hours in trays, a process designed to reduce the solubility of the melamine phosphate. They were then incorporated at a 30% level in samples for testing at 750° - 800°C.

The crystal types tested are listed below, with the number of samples of each tested in brackets.

(a) Medium Needles $(C_3H_6N_6)_{1.0}.H_3PO_4$ (one sample)

(b) Very Large Needles $(C_3H_6N_6)_{1.0}.H_3PO_4$ (one sample)

(c) Small Block Plates $(C_3H_6N_6)_{1.2}.H_3PO_4$ (two samples)

(d) Thin Reflective Plates $(C_3H_6N_6)_{1.3}.H_3PO_4$ (two samples)

(e) Plates $(C_3H_6N_6)_{1.1}.H_3PO_4$ (one sample)

(f) Medium Block Plates $(C_3H_6N_6)_{2.0}.H_3PO_4$ (two samples)

Dimelamine phosphate incorporation led, as expected, to very poor performance. Small block plates led to good performance, similar to or improving slightly upon the performance of samples containing untreated crystals of this type. The remaining crystal types however behaved in a manner totally different from their untreated analogues, both thin reflective plates $(C_3H_6N_6)_{1.3}.H_3PO_4$ and plates $(C_3H_6N_6)_{1.1}.H_3PO_4$ giving excellent performance. Contrary to this the needles, although rich in phosphate gave considerably poorer performances than their untreated analogues. It thus appears that within a range of melamine to phosphate ratio from 1.0 to 1.3 the crystal shape influences performance in a fire test to a far greater extent than this ratio.

In summary the order of decreasing performance was as follows:

thin reflective plates $(C_3H_6N_6)_{1.3}\cdot H_3PO_4$ ≐ plates $(C_3H_6N_6)_{1.1}\cdot H_3PO_4$ > small block plates $(C_3H_6N_6)_{1.2}\cdot H_3PO_4$ >

medium needles $(C_3H_6N_6)_{1.0}\cdot H_3PO_4$ ≐ very large needles $(C_3H_6N_6)_{1.0}\cdot H_3PO_4$ > medium block plates $(C_3H_6N_6)_{2.0}\cdot H_3PO_4$

Full results are shown in Table 6.8, and illustrated graphically in Figure 6.7.

It is noteworthy also that all the plate samples intumesced to a greater extent than their untreated counterparts, although this did not necessarily cause better performance to occur, viz. dimelamine phosphate plates. The needles samples intumesced to the same extent as untreated samples, but the char was not as resistant to ablation as that produced by their untreated counterparts. The thin reflective plate samples (and perhaps the other plate samples) appear to be susceptible to the dual time-temperature response patterns discussed earlier for tests at 750° - 800°C. The char structure of that produced by heat treated thin plates was excellent compared to the poor structure with large voids obtained from untreated samples. Ablation of this char during the course of a test was steady, unlike the unusual ablative characteristics encountered for untreated samples.

6.3.7 The Effect of Adding Sodium Orthophosphate to Coatings

It has been noted that the ratio of melamine to phosphate is of crucial importance in determining performance in a fire test (with the partial exception of samples produced with heat treated melamine phosphate). It was decided to investigate the effect of adding excess phosphate to the system in the form of sodium orthophosphate.

TABLE 6.8 : Typical Performance Of Samples Containing 30% Heat Treated Melamine Phosphate, Of Coating Weight Around 60g, Tested at 750° - 800°C.

Crystal Type	Time (min) To:- 300°C	400°C	Duration (min)	Maximum Extent of Intumescence (mm)	Time To Maximum Intumescence (min)
Medium Needles $(C_3H_6N_6)_{1.0}\cdot H_3PO_4$	9¾	24½	33½	100	8
Very Large Needles $(C_3H_6N_6)_{1.0}\cdot H_3PO_4$	-	-	32	80	6½
Plates $(C_3H_6N_6)_{1.1}\cdot H_3PO_4$	21½	48	48	100	6
Small Block Plates $(C_3H_6N_6)_{1.2}\cdot H_3PO_4$	21	40	41	150	7½
Thin Reflective Plates $(C_3H_6N_6)_{1.3}\cdot H_3PO_4$	14, 22	36½, 47	45, 55	40, 85	8
Medium Block Plates $(C_3H_6N_6)_{2.0}\cdot H_3PO_4$	10½	23	28	120	4½

FIGURE 6.7 : Typical Substrate Time-Temperature Responses at 750° - 800°C; 30% Melamine Phosphate, treated at 210°C.

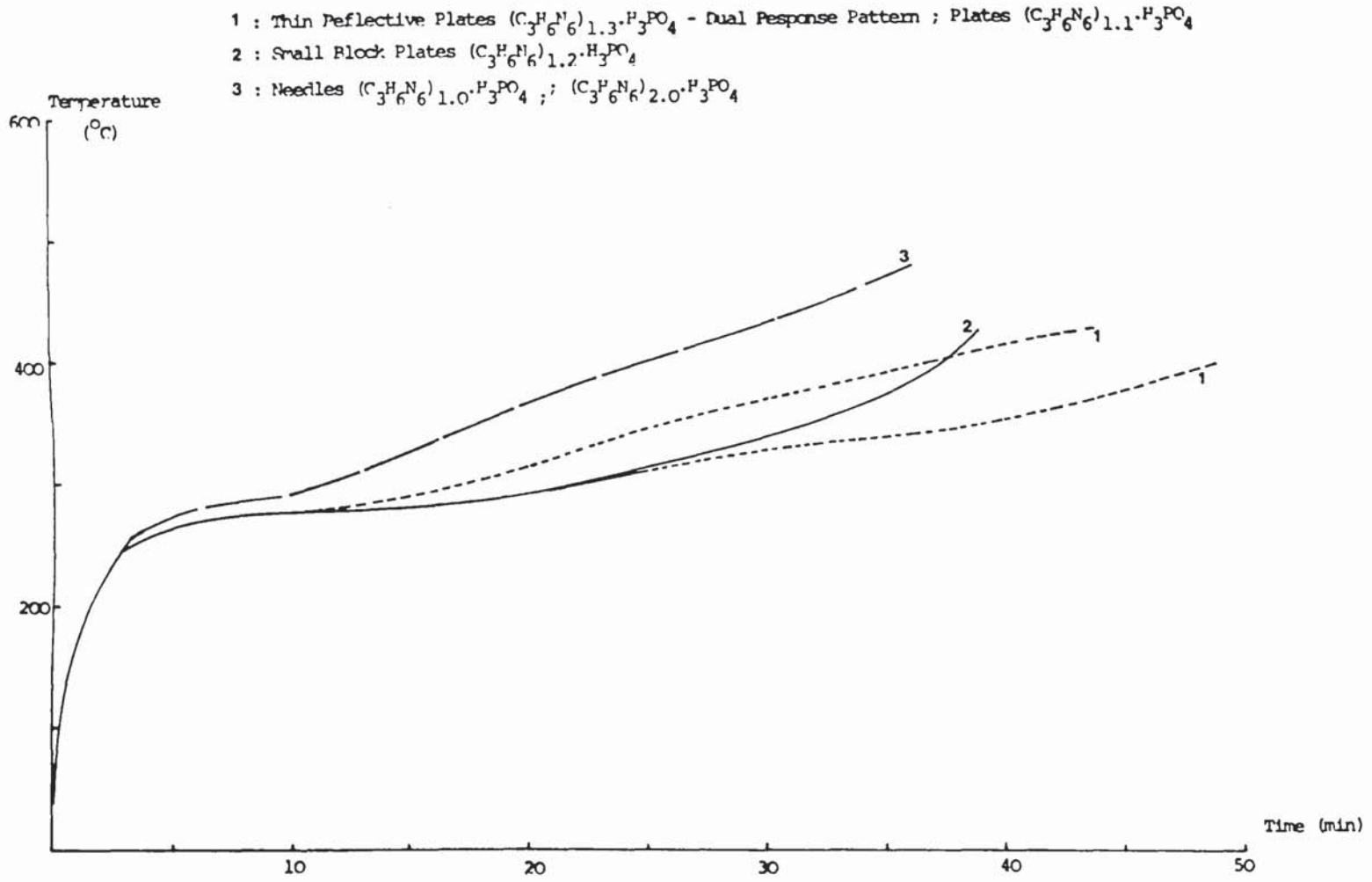

A preliminary pair of tests was carried out on samples containing 12½% small needles of $(C_3H_6N_6)_{1.2}.H_3PO_4$ (with respect to the total weight of epoxy resin, hardener, and melamine phosphate) to which were added a quantity of $NaH_2PO_4.2H_2O$ and Na_3PO_4 respectively, by weight 30% of the total weight of the resin, hardener, and melamine phosphate. The formulation containing $NaH_2PO_4.2H_2O$ performed excellently, giving 40 mm of durable intumescence which ablated slowly, protecting the substrate for in excess of 40 minutes. However addition of Na_3PO_4 totally quenched intumescence, and consequently the sample deteriorated very quickly. It is apparent that an acid phosphate specifically is required to enhance the performance of these intumescent coatings.

A more detailed investigation was then undertaken with two crystal types of melamine phosphate, small needles of $(C_3H_6N_6)_{1.2}.H_3PO_4$ and thin reflective plates of $(C_3H_6N_6)_{1.3}.H_3PO_4$, both incorporated at a level of 30% by weight with respect to the total weight of resin, hardener and melamine phosphate. The small needles had been roll milled into the mixture, the thin reflective plates incorporated under low shear. Six different samples were produced with each of these basic formulations by adding respectively one sixth, one third, and two thirds mole $NaH_2PO_4.2H_2O$ and the same quantities of $Na_2HPO_4.2H_2O$ per mole melamine phosphate incorporated. The samples were then tested at 750° - 800°C. It was hypothesised that the effect of a given molar quantity of dihydrogen phosphate might be approximately equivalent to twice that molar quantity of monohydrogen phosphate.

In effect the pattern proved to be considerably more complex than this simple hypothesis suggested. It is difficult to draw definite conclusions from a test sample of this size, with its range of formulations; in addition the increasing quantity of phosphate

tends to result in a denser coating, and sample weights tended to increase somewhat for the standard thickness of 6 mm as the quantity of phosphate added was increased.

The stated hypothesis was however decisively disproved. For the monohydrogen salt there proved to be an optimum quantity above which a steady deterioration in performance occured. At the lowest level of a molar ratio of one sixth with respect to melamine phosphate, intumescence was voluminous in the case of both samples. The sample of small needles gave the greatest expansion ever encountered in a test at 750° - 800°C. As progressively more monohydrogen phosphate was added intumescence was progressively restricted. However counterbalancing this is the tendency for an increasing quantity of phosphate to increase the durability and resistance to ablation of the char. The optimal concentrations of monohydrogen phosphate occured at molar ratios of one third in the case of thin plates, and one sixth in the case of small needles.

All the samples containing the dihydrogen phosphate performed in a superior fashion to any of the samples containing the monohydrogen phosphate with respect to durability and rate of rise of substrate temperature. It does appear however that similar factors operate in both cases, i.e. progressive reduction in the extent of intumescence counterbalanced by increasing durability of the char as the phosphate concentration is increased. Within the small needles series performance improved through the series, despite the lower maximum extent of intumescence in the sample containing the highest concentration of dihydrogen phosphate. However in the case of the thin plates, the sample containing the highest concentration performed less well, although intumescing to a greater extent, than the other two samples

which performed in equivalent manner. This behaviour appears to be anomalous.

The great importance of the availability of acid has been proved. Valuable research giving an insight into the mechanism of intumescence could be carried out by investigating the exact nature of the relationship between acid concentration and performance - it appears not to be linear - and how acid concentration and phosphate concentration are linked. An increasing weight of inorganic salt progressively restricts intumescence - this has been shown in the case of sodium chloride and titanium dioxide also. Thus there appears to be an optimal concentration of acid phosphate. Full details of performance are given in Table 6.9.

6.3.8 Discussion of the Fire Test Results - a Mechanistic Analysis

The factors which influence the nature and durability of an intumescent char are the nature of the constituents of the coating and the relative timing of three independent reactions occurring during the process of intumescence. These are the softening of the epoxy resin at 330° - 360°C, the evolution of gaseous products, mainly from the decomposition of melamine, and the esterification of the hydroxyl groups of the cured epoxy resin by phosphate, leading to dehydration and the ultimate formation of a carbon-phosphorous char. Loss of phosphorus from the char at temperatures in excess of 700°C leads to ablation of the char.

The nature of the fire is likely to affect the relative timing of the above reactions. A fast heating rate to a high temperature is likely to cause early softening of epoxy resin which remains soft at exactly the right time for esterification and dehydration to lead to the formation of a solid char, which is thus evolved very voluminously.

TABLE 6.9 : Performances Of Samples Incorporating Melamine Phosphate And Sodium Hydrogen Phosphates, Tested At 750° - 800°C.

Crystal Type	Sodium Phosphate:- Molar Ratio To Melamine Phosphate	Times (min) To:- 300°C	400°C	Duration (min)	Maximum Extent Of Intumescence (mm)
Small Needles	$Na_2HPO_4.2H_2O$				
	1/6	12½	26½	37	>200
$(C_3H_6N_6)_{1.2}.H_3PO_4$	1/3	9	26½	32	85
	2/3	5¼	20	24	70
	$NaH_2PO_4.2H_2O$				
	1/6	10½	32	41½	82
	1/3	13½	33	46½	100
	2/3	27	67	67	35
Thin Reflective Plates	$Na_2HPO_4.2H_2O$				
	1/6	5¾	15	25	200
$(C_3H_6N_6)_{1.3}.H_3PO_4$	1/3	8	28	35½	50
	2/3	4	14½	40	18

TABLE 6.9 (cont.)

Crystal Type	Sodium Phosphate:- Molar Ratio To Melamine Phosphate	Times (min) To:- 300°C	400°C	Duration (min)	Maximum Extent of Intumescence (mm)
Thin Reflective Plates	$NaH_2PO_4.2H_2O$				
$(C_3H_6N_6)_{1.3}.H_3PO_4$	1/6	17	45	64½	75
	1/3	17	44	64½	40
	2/3	7	27	45½	70

Intumescence is less voluminous if the ultimate temperature is slightly lower, and the heating rate less fast. A considerably slower rate of heating, as in the British Standard 476 Part 8 curve simulation tests, is likely especially in the front layer to lead to esterification and char formation before the resin has been able to soften. A skin is thus formed on the forward surface of the char. Behind this some softening does occur, and this may lead to melting of the coating if the gases are unable to penetrate the forward skin. However gas bubbles are being formed in a considerably different environment to that occurring during fast heating, leading to restricted intumescence of a considerably stronger type than fast heating to 900°C causes.

In a given fire test three characteristics of melamine phosphate are likely to influence the performance of a coating containing this material. These are the chemical constitution of the melamine phosphate, its thermal degradation behaviour, and its physical nature. The following comments apply to fire tests at 750° - 800°C. For materials dried at 110°C only, the chemical constitution and thermal degradation behaviour appear to be the major factors influencing performance. A high ratio of phosphate to melamine endows a char with resistance to ablation, probably because more phosphate is present initially and needs to be lost before ablation can take place. This has been demonstrated with the addition of sodium hydrogen phosphate. Thus needles of $(C_3H_6N_6)_{1.0}.H_3PO_4$ give slightly superior performance to crystals of $(C_3H_6N_6)_{1.2}.H_3PO_4$, which in turn are superior to thin reflective plates and dimelamine phosphate. The sharp decrease in performance of thin reflective plates must however be explained in terms of its thermal degradation behaviour. Alone of all the samples

tested by differential thermal analysis, this had no peak maximum in the range 300° to 350°C, the peak normally occurring at around 350°C in other samples being found at the higher temperature of 360°C. In many respects the thermal behaviour of thin reflective plates was closer to that of dimelamine phosphate than to the types of stoichiometry $(C_3H_6N_6)_{1.0-1.2}.H_3PO_4$. For materials heat treated at 210°C however, the physical characteristics of the material are the major influence upon performance, with the exception of dimelamine phosphate which performed poorly. Overlapping plates in such a configuration that their surfaces face the fire may be expected to give a more uniform structure to a foamed char than needles, and the excellent performance of the plate types vindicates this hypothesis. The thermal degradation behaviour of these materials was fairly similar, all, except thin reflective plates and, to some extent, dimelamine phosphate, having lost those peaks below 325°C. Thin reflective plates appear not to show significantly different thermal degradation characteristics after treatment at 210°C except that its intermediate peak then occurs at 345°C; this accords with the low decrease in the solubility with such treatment, where a temperature of at least 220°C was required to achieve conversion. Particle size does however affect all the materials, whether dried at 110°C or heat treated. Roll milling of small needles and thin reflective plates has been found to be disadvantageous, whereas large needles of $(C_3H_6N_6)_{1.2}.H_3PO_4$ perform in superior fashion to small needles. The optimum size range for particles (whether agglomerates or individual crystals) appears to be 50 - 100 μm. Such particles presumably have the optimum contact area with epoxy resin for reaction to take place at a controlled rate.

It is noteworthy that in fire tests at 900°C a lower quantity of melamine phosphate, especially if of a crystal type which normally gives poor performance at 750° - 800°C or preferably of a mixture of crystal types, such as small needles with dimelamine phosphate, gives rise to a slower and more controlled reaction and thus better performance than the use of a formulation suited to a test at 750° - 800°C.

6.4 Quantitative Determination of Resistance to Heat Flow Through Chars

6.4.1 Introduction

As mentioned in Section 6.1, the heat flow balance for the substrate at time θ is given by expression (6.1), the subscripted terms varying with the progression of the test.

$$\left(\frac{K}{x}\right)_\theta A\,(T_p - T_q)_\theta = mC_p\left(\frac{dT_q}{dt}\right)_\theta + hA(T_q - Ta)_\theta \qquad (6.1)$$

Heat flux conducted through char	Rate of Increase of internal energy of substrate	Heat flux lost from back of substrate

The heat flux through the char is shown as purely conductive; however since the char is porous radiation and convection across the voids are also responsible for heat transfer. The above is however a reasonable model, in which $(\frac{x}{K})$ represents the resistance to heat flow by any method across the char. To obtain a quantitative determination of $(\frac{x}{K})_\theta$ for a fire test it is necessary to calculate the film coefficient for heat loss from the substrate. If it can be shown that this is substantially similar in all tests carried out at the same range, the values of h obtained from cooling curves may be applied to the fire tests described in Section 6.3, thus enabling $(\frac{x}{K})_\theta$

to be calculated.

6.4.2 Determination of Cooling Curves

Due to the variation in temperature across the surface of a normal substrate measuring 95 mm x 95 mm, a smaller target substrate was designed to be substituted for the normal substrate, for the determination of cooling curves. A standard container was adapted by the removal of a disc of diameter 25 mm from its centre. Into the centre of the gap thus produced was placed a precisely weighed aluminium alloy disc of diameter 12.5 mm insulated from the mild steel container by an annulus of Pyruma (R) fire-clay. The assembly of this was aided by placing adhesive tape under the container, but this was removed from the sample prior to fire testing. A Ni-Cr/Ni-Al thermocouple was peened into the inner surface of the aluminium substrate and the wires led out through a hole in the base of the container as in a standard fire test sample. The aluminium disc and thermocouple were weighed separately before being joined, and again after peening in, thus enabling an accurate weight for the disc alone with the thermocouple in place to be obtained. The containers were then filled to a depth of 6 mm with a typical composition containing 30% melamine phosphate by weight. Small needles were usually used, but the material used is not of great importance.

After a standard cure the samples were placed in the frame on the fire testing device. In addition to thermocouples reading face temperature at the sides of the sample, and the substrate temperature, further thermocouples were placed in the film of air behind the substrate to obtain values of T_a, the temperature of the air to which heat from the substrate is transferred. These were mineral insulated

(R) Pyruma is a registered trade mark of British Sisalkraft, Ltd.

thermocouples of thickness 1 mm. It is difficult to define exactly the air temperature T_a: it is the temperature of air which comes into contact with the substrate at a point shortly before that contact. However heat transfer proceeds down through an appreciable film thickness of air, and the temperature measured by a thermocouple close to the substrate may be influenced by radiation as well as convection. Since the absorption coefficient for radiant energy is greater for the metal sheath of the thermocouple than for air this leads to an inaccuracy in such a reading. Although in some tests only one thermocouple measuring air temperature was used close up to the substrate, in two tests three thermocouples at increasing distances from the substrate were used. Figures 6.8 and 6.9 illustrate schematically the constitution of the samples and the arrangement for fire testing.

The samples were placed at a distance of 190 mm from the burner, and a char developed under normal gas and air flow conditions (750° - 800°C). When the substrate temperature had reached a value between 250°C and 300°C, after around fifteen minutes, the test was abruptly stopped by closing off air and therefore, automatically, gas supplies, and the substrate and air temperatures monitored for around forty minutes to obtain cooling curves. The fume extraction fan remained operational during the cooling phase.

6.4.3 Calculation of the Film Coefficient of Heat Transfer to the Environment

Immediately after closing off air and gas supplies some heat is still being transferred through the char, but after around five minutes it may be assumed that the char is an effective thermal barrier in either direction. Figure 6.10 illustrates a typical cooling curve, from which the point of inflexion is assumed to mark the

FIGURE 6.8 : Rear View of Sample used for determination of cooling curves.

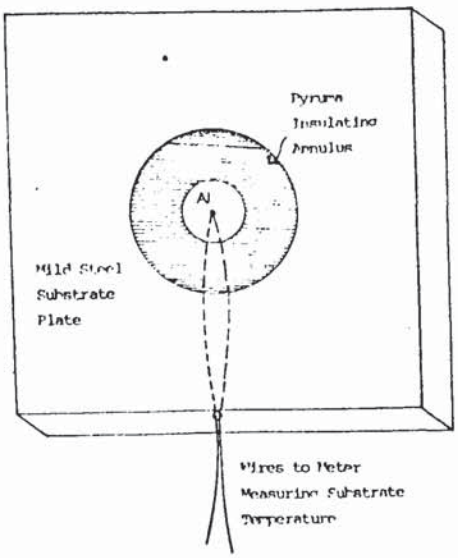

FIGURE 6.9 : Configuration for determination of cooling curves prior to fire test.

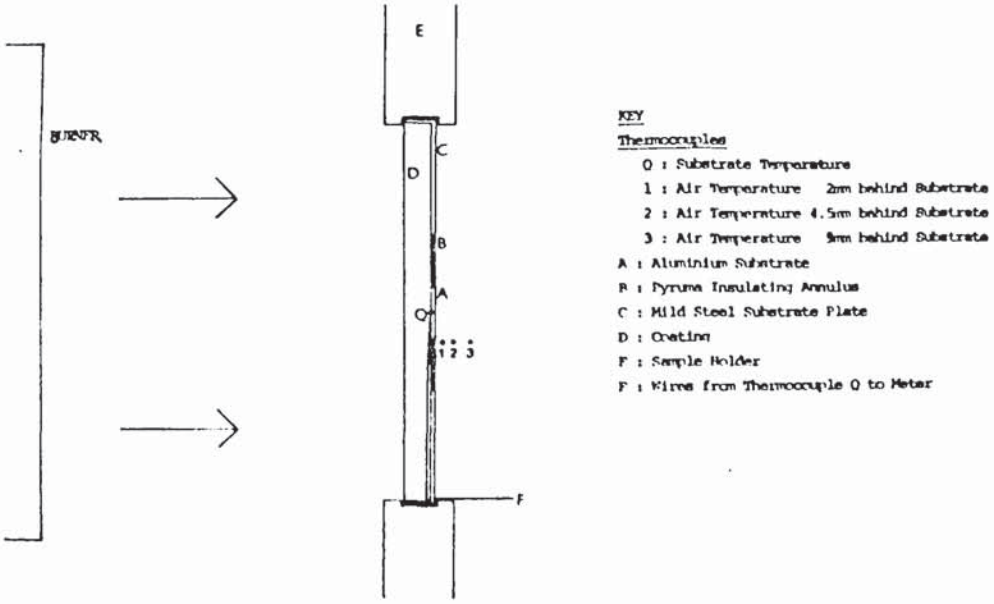

FIGURE 6.10 : Cooling Curves from one sample.

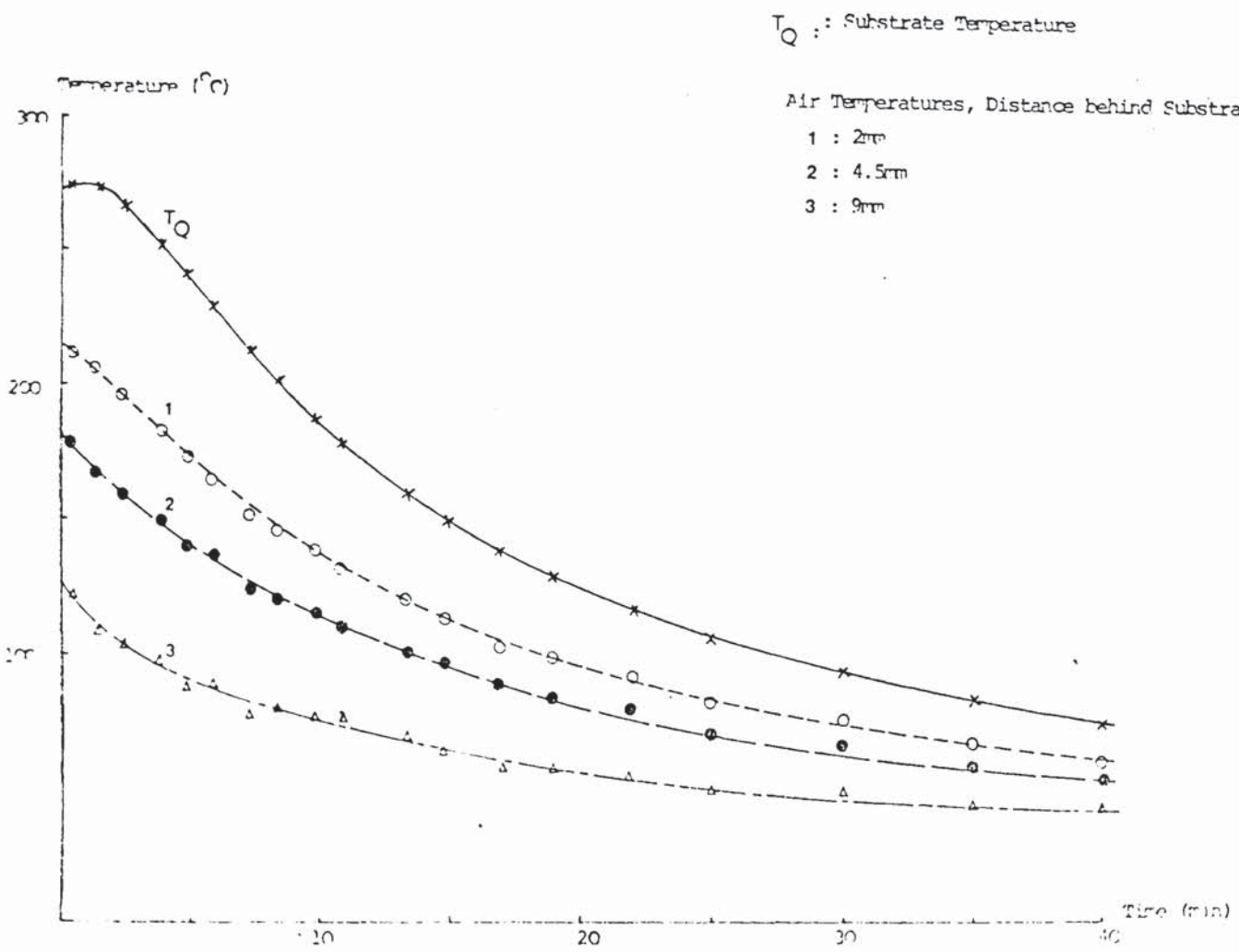

establishment of zero heat flow through the char.

Therefore assuming that $(\frac{K}{x})A(T_p-T_q) = 0$ on cooling,

$$-mC_p\left(\frac{dT_q}{dt}\right)_\theta = hA(T_q-T_a)_\theta \qquad (6.3)$$

An integrative approach was now used due to the problems in obtaining accurate values of $\left(\frac{dT_q}{dt}\right)_\theta$ (60).

$$\int_{T_1}^{T_2} \frac{dT_q}{(T_q-T_a)_\theta} = \int_{\theta_1}^{\theta_2} -\frac{hAdt}{mCp} \qquad (6.4)$$

The integration of the left hand side is mathematically not entirely rigorous, since T_a is not constant. It has however been shown that the values of T_a do not influence the decay rate $\frac{d(T_q-T_a)}{dt}$ significantly, as for instance, exemplified for the three positions of the thermocouples reading T_a on some tests. The integration may therefore be performed, substituting ΔT for (T_q-T_a), and using square brackets for experimental observations and scrolled brackets for calculated values. Let the lower limit of integration be an experimental standard at time θ^o, where $(T_q-T_a) = \Delta T^o$; the point of inflexion on the cooling curve was used for this standard. Then:

$$\ln \{\Delta T\}_2 - \ln \Delta T^o = \frac{hA}{mC_p}(\theta_2 - \theta^o) \qquad (6.5)$$

$$\text{Therefore } \{\Delta T\}_2 = \Delta T^o.\exp\left(\frac{hA(\theta_2-\theta^o)}{mC_p}\right) \qquad (6.6)$$

The value $\{\Delta T\}_2$ represents a calculated value obtained from the model, which may be compared with the experimental value $[\Delta T]_2$. An optimisation technique to obtain the most accurate value of h was carried out by summing the squares of the differences between calculated and experimental values of ΔT over all observations beyond the standard, and minimising this sum for different suggested values of h substituted into the model,

i.e.

$$\sum_{\theta} \left(\{\Delta T\}_{\theta} - [\Delta T]_{\theta} \right)^2 \qquad (6.7)$$

is minimised for different values of h.

A computer program was written to carry out the above calculation. Its input consisted of all experimental values of T_q and T_a (two input formats being provided according to whether one or three values of T_a were available - in the latter cases, three independent values of h were calculated); H, the initial guess at the film coefficient of heat transfer; and m. A and C_p, being constant for all the tests were incorporated into the program itself. The calculation proceeded in three stages as follows:

(a) Determination of the standard values θ^o, ΔT^o from the point of inflexion on the cooling curve.

(b) By means of a Function subprogram SUMSQ which calculates the value of expression (6.7) for any value of h, initial values of the sum of the squares of the differences are calculated for H, (H+1), and (H-1). If SUMSQ (H) has the lowest value of these, the program proceeds to the next stage; otherwise it continues to calculate SUMSQ for values of h increasing or decreasing in steps of 1.0 until

the value of SUMSQ has reached a minimum. Let the value of h at which this minimum occurs be labelled G.

(c) A procedure to reduce further the inaccuracy in the value of h is then instituted. On a DO loop from i = 1 to 15, values of H3 and H4 are calculated as follows:

$H3 = G + 2^{1.2-i}$

$H4 = G - 2^{1.2-i}$

and SUMSQ calculated for both. The loop is then repeated with the value giving the minimum SUMSQ substituted for G.

The output enumerates the above stages, gives an optimum value of h, the film coefficient of heat transfer to the environment, and calculates $\{T_q\}$ at the times of the experimental observations, based on the experimental values of T_a.

The values of h obtained from the various cooling curves were broadly similar within the limits of experimental error. They are of a magnitude to be expected for natural convection. Furthermore the values of h obtained from using different values of T_a for the same test were broadly similar, and are as follows:

Test 1 : 3.84 W m^{-2} K^{-1}

Test 2 : 3.95 W m^{-2} K^{-1}

Test 3 : 3.89, 3.84, 3.72 W m^{-2} K^{-1}

Test 4 : 4.31, 4.39, 4.27 W m^{-2} K^{-1}

A program listing and output is given in Appendix A.5.1.

6.4.4 Calculation of the Thermal Resistance of Chars for Several Fire Tests

From equation (6.1), it is apparent that the heat flow balance is independent of area; viz.

$$\left(\frac{K}{x}\right)_\theta \quad (T_p - T_q)_\theta = l\rho C_p \left(\frac{dT_q}{dt}\right)_\theta \quad + h\,(T_q - T_a)_\theta \qquad (6.8)$$

The following values were used for the constants in the above equation:

thickness of substrate, l = 1.65 mm, a mean value as measured with a micrometer;

density of mild steel, ρ = 7,860 kg m^{-3}

specific heat capacity of mild steel, C_p = 420 J kg^{-1} K^{-1}

film coefficient of heat transfer for heat losses to the environment from the substrate, h = 3.9 W m^{-2} K^{-1}

These values are those relevant to the mild steel substrates used in the ordinary fire tests. The equation simplifies to:

$$\left(\frac{K}{x}\right)_\theta = \frac{5447 \left(\frac{dT_q}{dt}\right)_\theta + 3.9\,(T_q - T_a)_\theta}{(T_p - T_q)_\theta} \qquad (6.9)$$

Equation (6.9) has been applied computationally to several fire tests to enable the calculations of resistances to heat flow throughout the tests. The variables were obtained by the following techniques:-

(a) T_q : obtained at intervals of one minute from the graphed time-temperature substrate response patterns of each test.

(b) T_p : obtained from the model of char face temperatures illustrated in Section 4.2, taking account of the actual char face to burner distances (rather than the sample to burner distances). The model gives curves for T_p vs. Range for a char position several centimetres in front of the frame, and very close to the frame - interpolation from either model or a mixture of both was used according to the thickness of the char at a given time. The accuracy of the

model, taking into account the above interpolation and the use of a thermocouple junction to model the char face is expected to be around $\pm$ 20°C.

(c) $\frac{dT_q}{dt}$: for evenly spaced observations from the graphed results of fire tests

$$\left(\frac{dT_q}{dt}\right)_i = \frac{1}{2\,\Delta t} \left([T_q]_{i+1} - [T_q]_{i-1}\right)$$

For the observations used ΔT = 60 seconds.

(d) $(T_q - T_a)$: in the case of a few fire tests, direct measurements of T_a were obtained throughout the test. However the problems in defining accurately T_a have led to the use also of two empirical models, derived from observations on the cooling curves used for the determination of the film coefficient of heat transfer accounting for heat losses from the substrate.

These were:

(a) $(T_q - T_a) = 0.49\ T_q - 20$

(b) $(T_q - T_a) = 0.34\ T_q - 14.5$

obtained from the two positions of the thermocouples recording T_a on cooling curves at distances of 4.5 mm and 2.0 mm from the substrate respectively.

It is in the calculation of $(T_q - T_a)$ that the greatest error in the determination of $\left(\frac{x}{K}\right)$ lies. The use of the above models render results which differ by around 50%. It is believed that the former is the better model; the latter appears to add an insufficient contribution, resulting in some cases, where $\left(\frac{dT_q}{dt}\right) < 0$, in a negative value for $\left(\frac{K}{x}\right)$ also. The models are also based on observations for T_q

up to 280°C only, and it is possible that at substrate temperatures above 300°C the loss is greater than suggested by either model.

Analyses were carried out on several test results, representing the typical superior performances of most needle crystal types and the inferior performances of thin reflective plates and dimelamine phosphate, at 12½% and 30% levels of incorporation, conducted at 750° - 800°C. A summary of the results appears in Table 6.10, giving thermal resistances. Typical computer print-outs for a superior performance in a material incorporating 30% melamine phosphate, and an inferior performance in a material incorporating 12½% melamine phosphate appear in Appendix A.5.2. These show profiles of $\left(\frac{K}{x}\right)$ as calculated by all three methods for evaluating $(T_q - T_a)$. The values of $\left(\frac{K}{x}\right)$ obtained using model (a) to supply values of $(T_q - T_a)$ were normally the highest, and these values have been accepted as suitable in most cases. The problems in direct measurement of T_a are such that no greater accuracy should be ascribed to values obtained by this means, which were however frequently similar to those obtained using model (a), though occasionally considerably less.

Approximate values of the mean thermal conductivity across their thickness of the chars were calculated using the approximate char thicknesses assessed during fire tests. These compare with the conductivity of fibrous insulators, such as Kapok (0.03 $W\ m^{-1}\ K^{-1}$) and are somewhat lower than that of concrete (0.1 $W\ m^{-1}\ K^{-1}$) (61). A slight decrease during the later stages of tests is spurious, being due to an insufficiently large heat loss correction in the equation used to obtain $\left(\frac{K}{x}\right)$. Values are listed in Table 6.11.

TABLE 6.10 : Thermal Resistances Of Selected Chars In Fire Tests

Test. No.	Material	Variation in Thermal Resistance $\left(\frac{x}{K}\right)$	Time Periods (min)	Comments
		$\left(\frac{x}{K}\right)$ $(W\ m^{-2}\ K^{-1})^{-1}$		
46	30% level of large needles $(C_3H_6N_6)_{1.2}\cdot H_3PO_4$	Rises to 1.4	9	Superior performance in pair showing dual substrate time temperature response pattern (see Section 6.3.2)
		then 1.1	10 - 15	
		falls to 0.7 maintained	18 - 24	
		and then to 0.33	44	
51	30% level of large needles $(C_3H_6N_6)_{1.2}\cdot H_3PO_4$	A very high maximum	9	Inferior performance in above pair
		then 0.75	12 - 17	
		falls to 0.35 maintained	24 - 26	
		and then to 0.22	37	

Table 6.10 (cont.)

Test No.	Material	Variation in Thermal Resistance $\left(\frac{x}{K}\right)$	Time Periods (min)	Comments
		$\left(\frac{x}{K}\right)$ $(W\ m^{-2}\ K^{-1})^{-1}$		
34	30% level of thin reflective plates $(C_3H_6N_6)_{1.3}\cdot H_3PO_4$	Rises to 0.58 falls to 0.22 maintained before failure	9 16 - 27 29	Thin reflective plates give a lesser thickness of char, and thus exhibit lower thermal resistance.
119	30% level of medium needles $(C_3H_6N_6)_{1.0}\cdot H_3PO_4$	Rises to 1.0 maximum 1.1 falls to 0.77 maintained falls to 0.26 on failure	9 - 16 14 16 - 26 45	Similar to test 46
7	12½% level of thin reflective plates $(C_3H_6N_6)_{1.3}\cdot H_3PO_4$	Rises to 0.4 then falls and fails at 0.2	5 - 12 19	Tests 7 and 29 show the variations obtained with thin reflective plates

Table 6.10 (cont)

Test No.	Material	Variation in Thermal Resistance $\left(\frac{x}{K}\right)$ $(W\ m^{-2}\ K^{-1})^{-1}$	Time Periods (min)	Comments
				incorporated into coatings.
29	12½% level of thin reflective plates $(C_3H_6N_6)_{1.3}\cdot H_3PO_4$	Rises to 0.7 (momentary maximum) and falls to 0.3 maintained then fails shortly thereafter.	6 14 - 19	
114	12½% level of medium needles $(C_3H_6N_6)_{1.0}\cdot H_3PO_4$	Rises to 1.0 falls to 0.6 maintained and then falls quickly to failure at 0.2	5 - 13 15 - 29 32	

TABLE 6.11 : Approximate Thermal Conductivities Of Chars, Eleven Minutes From The Beginning Of The Tests.

Test No.	Material	Thickness of Char (mm)	Thermal Conductivity ($W\ m^{-1}\ K^{-1}$)
46	Large needles, 30%	40	0.035
51	Large needles, 30%	65	0.060
34	Thin reflective plates, 30%	20	0.045

CHAPTER 7

CONCLUSIONS AND RECOMMENDATIONS

CHAPTER 7

CONCLUSIONS AND RECOMMENDATIONS

7.1 Conclusions

Conclusions have been drawn from four aspects of the research into melamine phosphate as a component of intumescent coatings. These are detailed below.

7.1.1 Elucidation of the Crystallisation Processes of Melamine Phosphate

Melamine orthophosphate has been shown to exist in several crystallographically distinct crystal forms, as does melamine pyrophosphate. It also exhibits a continuously variable stoichiometry according to the conditions of crystallisation. The thermal degradation of these forms differs.

7.1.2 Construction and Use of a Calibrated Small Scale Fire Testing Facility

A reasonable degree of reproducibility has been shown under circumstances where this is notoriously problematical, and the facility has demonstrated its utility for testing large numbers of coating formulations at low cost and with high throughput. However the facility is essentially a research instrument, and large scale fire testing would be required for further developmental work.

7.1.3 Coatings Containing Melamine Phosphate in Fire Tests

An extensive investigation has demonstrated the importance in melamine phosphate of a high phosphate to melamine ratio on performance in the above fire testing facility. The importance of acid as well as phosphate has also been demonstrated. Differences in crystal form and particle size and shape have been shown to lead to differences in

behaviour. It has been found preferable not to break down agglomerated materials, such as small needles, by excessive roll milling. Thin reflective plates have been shown to result in inferior performance compared to other materials of similar stoichiometry, unless treated at 210°C. Such heat treatment has been shown drastically to alter the performance of coatings incorporating melamine phosphate. Encapsulation of melamine phosphate in part of the epoxy resin, to protect the melamine phosphate from possible leaching, has been shown to quench intumescence. In mixtures of crystal types, some forms appear to dominate others in affecting performance. A loading of 30% melamine phosphate has been shown to give a longer duration of protection than lower loadings except when the coating is exposed to very high temperatures very quickly, as may occur in a petroleum fuelled fire. In such cases, a loading level of only 12½% gives more controlled intumescence, which is burned away more slowly than the char formed from a higher loading.

The best material at 750° - 800°C was medium needles of stochiometry $(C_3H_6N_6)_{1.0}.H_3PO_4$, dried at 110°C. Very large needles of the same material were slightly inferior.

Thin reflective plates treated at 210°C, and large needles of $(C_3H_6N_6)_{1.2}.H_3PO_4$, dried at 110°C, also gave excellent performance; small block plates of $(C_3H_6N_6)_{1.2}.H_3PO_4$. treated at 210°C, were amongst the best of the heat treated materials. All these materials would be used at loadings of 30%. In a fire developing more slowly a similar order of performance occurs, but intumescence is reduced, and some melting of the char occurs as it is formed. At 850° - 900°C a material that gave excellent performance was a mixture of equal weights

of dimelamine phosphate and small needles of $(C_3H_6N_6)_{1.2}.H_3PO_4$, in which the former restrains excessive intumescence whilst the latter gives rise to a better char structure than dimelamine phosphate alone promotes. This would presumably be best used at a loading of 12 - 15%.

7.1.4 Optimisation of the Production Route to Melamine Phosphate

The melamine phosphate product must exhibit good weatherability, be easy to incorporate into a coating and then apply to suitable substrates, and give protection against fires. From the foregoing it is apparent that under different fire conditions different types and loadings of melamine phosphate may be most suitable; furthermore, the addition of other materials, such as metal oxides and fibres, is likely to affect the development of intumescence. Higher loadings of melamine phosphate may then be necessary to ensure optimum performance in a fire.

Heat treatment is necessary to reduce the solubilities of all types of melamine phosphate to around 0.05% at 28°C. Unfortunately the water uptake of most types begins to increase dramatically after treatment at 210°C for prolonged periods, only $(C_3H_6N_6)_{1.0}.H_3PO_4$ being almost unaffected. This material, treated at 210°C, exhibits the best weatherability of any melamine phosphate. However its performance in fire tests is poor. Small block plates or thin reflective plates are to be preferred for performance in a fire. Of these, small block plates exhibit the lower water uptake tendency, as water uptake for heat treated materials appears to rise with the ratio of melamine to phosphate. Treatment at 200°C for at least twenty four hours appears sufficient to reduce the solubility of this material whilst not having too adverse an effect upon water uptake.

The recommended production route to this material is by means of the hydrochloride or acetate, using monosodium phosphate to precipitate the required product. The acetate intermediate is to be preferred, for although acetic acid is slightly more costly than hydrochloric acid, problems arising from the highly gelatinous nature of the hydrochloride are avoided. Assuming that prices for bulk supplies of the acids are in a similar ratio to those for laboratory supplies, general purpose grade hydrochloric acid of 36% strength costs £2.25 per 2.5 litre, equivalent to £0.078 per mole, whereas glacial acetic acid costs £3.92 per 2.5 litre, equivalent to £0.090 per mole. The acetic acid, after prior dilution with three volumes of water, is added slowly to a well stirred suspension of melamine at ambient temperature, and stirring maintained for one hour. The acetate consists of large plates which do not form gelatinous structures such as the hydrochloride, although it is important to stir continuously. The solution is supersaturated, and cessation of stirring has led to the precipitation of a network of fine needles. The problem of encapsulation of unreacted melamine in a network of needles, such as occurs with the hydrochloride at ambient temperature, is thus avoided, and the costs of heating to dissolve the hydrochloride and ensure complete reaction saved. The major problem in using the acetate intermediate is foaming of the reaction mixture. A solution of monosodium phosphate is then added while stirring. By using an excess of monosodium phosphate a higher yield of melamine phosphate may be obtained, due to the common ion effect. After further stirring, the product may be filtered and washed. The filtrate mainly contains sodium acetate and sodium phosphate, which may be recovered. It is

obviously preferable to use as concentrated media as possible, but increasing the total bulk concentration does tend to increase the aspect ratio of the product somewhat. It has been found suitable on a pilot scale to use 100 g melamine with an appropriate quantity of acetic acid in a total volume of one litre, and then to add slowly a solution of 150g $NaH_2PO_4 .2H_2O$ dissolved in the minimum volume of water at ambient temperature or up to 40°C. The material is stirred for a further hour, filtered, dried initially at 110°C, and then treated at 200°C for twenty four hours. It may be incorporated into a coating under conditions of moderate shear.

7.2 Recommendations for Further Work

In both major areas of interest in this research, production and fire testing of melamine phosphate, there exists scope for further work. Recommendations are given for each of these areas.

7.2.1 Production of Melamine Phosphate

A full investigation into the kinetics and solution thermodynamics of the reaction between melamine and phosphate, which appears to be a multi-stage reaction involving considerable mass transfer after the initial crystal formation, is recommended. The present research has provided only a qualitative assessment of the crystallisation processes, sufficient to show the existence of several crystal types, and give information on how they may be manufactured. An investigation of the kinetics may explain the contributions made by such parameters as concentrations, rates of cooling, stirring, and relative proportions of the reactants. Such processes of mass transfer leading to changes in crystal type may continue for long periods after initiation of the reaction, and appear also to occur in the production of certain pyrophosphates, such as tetramelamine pyrophosphate.

A full study of the crystalline structure and variations due to the variable stoichiometry would appear also to be warranted. Although differential thermal analysis has led to the elucidation of differences between the materials, it is known that thermogravimetry may give apparently contradictory results (49), because the latter is carried out in an atmosphere of air, whereas the former has been carried out in quartz crucibles which do not allow fast escape of the gases produced by degradation. Thermogravimetry was able to detect differences in the degradation of the different types of melamine pyrophosphate (14), not detected by differential thermal analysis; it may also elucidate more fully the tentative conclusions concerning the degradation of thin reflective plates compared to the other crystal types, as well as revealing inherent differences in crystal form. Such a study of the crystalline structure would be most suited to a researcher in a Department of Chemistry.

The production processes for melamine phosphate have been investigated only on a laboratory scale. Scale-up studies are required to ensure, for instance, that unsuspected gel formation does not then occur. Suitable drying and heat treatment processes, perhaps by a fluid-bed method, require investigation.

7.2.2 Fire Tests

Several major areas of research utilising the Aston University fire testing facility are apparent.

Further research into formulations incorporating melamine orthophosphate would yield valuable information. A fuller investigation of the effects of prior heat treatment on performance in a fire test, and the correlation of such performance with the thermal

breakdown characteristics of the melamine phosphate is required. The effects on performance of materials treated at a range of temperatures from 180° to 240°C might then be correlated with structural changes over this temperature range, over which the performance of thin reflective plates may be expected to improve, and that of needles to deteriorate. The temperature at which these changes take place, and the width of the changeover zone might be compared to changes in solubility and water uptake. Heat treatment of mixtures requires investigation, especially since one such mixture appears to give outstanding performance at 850° - 900°C.

A deeper investigation into the relationship between available phosphate and acid linked to performance may give rise to fundamental insight into the mechanism of intumescence. Since the addition of sodium dihydrogen phosphate was beneficial, a search for a suitable insoluble acid phosphate should be instituted. $Al_2O_3.3P_2O_5.3H_2O$, an amorphous material of low solubility and water uptake characteristics, produced from $Al(H_2PO_4)_3$ by treatment at 250°C may be suitable (62). The latter is not suitable due to its hygroscopic nature.

The present investigation has looked at fundamental issues concerning melamine phosphate. The effects of other components normally present in commercial formulations, such as fibres, metal oxides, and thixotropic agents require investigation. A variety of formulations containing melamine phosphate, using different carbonific agents and binders, formulated as paints as well as mastics should be tested, to determine whether the results obtained in the present study still apply generally. It is likely that performance will be linked to individual correlations between the thermal breakdown of the carbonific agent and melamine phosphate.

Commercially sponsored investigations into entirely new intumescent agents could also be conducted. This tends however to be a lengthy process involving a large extent of guesswork. Comparisons between melamine orthophosphate and pyrophosphate or polyphosphate in fire test performances might be undertaken.

The nature of the test itself might be altered. Different substrates could be investigated. Configuration is an important aspect in determining fire development. A configuration of especial interest when using intumescent coatings is that of fire passing through a narrow gap the sides of which have been coated with an intumescent paint. A typical example is the gap between a door and its frame.

It is hoped that the fire testing facility will be extensively used on such investigations as those detailed above.

APPENDICES

APPENDIX A.1

Experimental Analytical Techniques

A.1.1 Chemical Analyses

Analytical techniques were developed for melamine and sodium cations, and orthophosphate and chloride anions. These are described below.

A.1.1.1 Melamine Cation, $C_3H_7N_6^+$

A simple far ultraviolet spectroscopic technique is available for the melamine cation, which has two peaks at 210 nm and 236 nm respectively (63). The ratio of the peak heights is approximately 3.2 at a pH of around 2, at which all samples should be analysed. A higher peak ratio indicates insufficient acidity, as melamine itself has a larger extinction coefficient at 210 nm, but does not absorb at all at 236 nm. A lower peak ratio is usually obtained when the absorbance of a particular sample at 210 nm exceeds 1.40, as above this value a linear relationship between absorbance and concentration is no longer maintained. Recalibration was not found to be necessary after the initial calibration had been carried out. Samples were diluted and sufficient acid added, normally around 0.5% v/v 'AnalaR' hydrochloric acid 31.5% as a proportion of the total solution volume, to obtain absorbances of between 0.1 and 0.9 at 236 nm, at which wavelength analysis took place. A Pye-Unicam SP 1800 spetrophotometer was used.

A.1.1.2 Phosphate Anion, $H_2PO_4^-$

This was measured colorimetrically by the method of Barnard and Chayen (64). Samples require dilution to the range 0.02 mg to 0.20 mg phosphorus.

To an aliquot of the test sample in a 25 cm^3 volumetric flask were added successively 1 cm^3 hydrochloric acid 31.5% (in preference to perchloric acid as suggested by Barnard and Chayen), 2 cm^3 amidol solution (1% diaminophenol hydrochloride + 20% sodium metabisulphite, filtered, and kept refrigerated and away from light; used within 36 hours), and 1 cm^3 ammonium molybdate 8.3% solution (to which a little ammonia was added to aid solubilisation), and the volume made up to 25 cm^3. The absorbance was read after twelve minutes.

The blue colouration produced is due to a precipitate of molybdenum "blue" oxide, and the intensity of colouration is time dependent. The absorbance was read at 700 nm, the upper wavelength limit of the Pye-Unicam SP 1800 spectrophotometer used. Calibration was carried out using solutions of monosodium orthophosphate dihydrate, the instrument being recalibrated on each occasion of use. The method is suitable for orthophosphate, having an error of around $\pm$ 5%, greater than that in the determination of melamine cation. To use the method for total phosphorus determination, oxidation and hydration to orthophosphate is first necessary as described by Barnard and Chayen, but such analyses were not within the province of this project.

A.1.1.3 Sodium Cation, Na^+

This was measured using atomic absorbtion spectroscopy. Samples were diluted to concentrations of 0.05 - 0.9 $\mu g/cm^3$.

A.1.1.4 Chloride Anion, Cl^-

This was measured volumetrically by titration against standardised silver nitrate solution using a chloride sensitive electrode to indicate the end-point, attained at a chloride concentration of 10^{-5}M (the solubility product of silver chloride being approximately 10^{-10} $mole^2$ $litre^{-2}$). The silver nitrate solution used had first been

standardised against a standard solution of potassium chloride to the same end-point. Some samples were also analysed by the analytical service of the Chemistry Department, Aston University.

A.1.2 Solubility Determination

Accurate determination of solubility has four major requirements: a constant temperature environment, the attainment of equilibrium between a solution and excess solid, a means of transfer of the solution without contamination with solid or other bodies, and a method of analysis for the solution.

A thermostatically controlled heated water bath, accurate to within 0.2°C and of internal height 380 mm was used for solubility determinations at temperatures up to 75°C. Especially at elevated temperatures, transfer of solution by means of a pipette is impractical as crystallisation may occur from a hot solution in the pipette. A method was therefore devised, based on that of Robinson (65) as described by Zimmerman (66), whereby transfer under pressure took place of solution from the equilibration vessel to a receiving vessel through a short length of PVC tubing, at the entrance to which a cotton wool filter was placed, the whole apparatus being submersed in the bath. Both vessels, conical flasks of capacity 250 cm^3, were fitted with condensers, which in addition to preventing loss by evaporation, acted as suitable points for clamping the system. All glassware was fitted with Clearfit ground glass joints. Pressure was applied to the equilibration vessel to achieve transfer. The apparatus is shown schematically in Figure A.1.1.

It is important to ensure that equilibrium has been attained before a transfer of solution is undertaken. Around 2g melamine phosphate and 100 cm^3 distilled water were mixed together using a

FIGURE A.1.1 : Apparatus for determining the solubility of a material over the temperature range 10° - 80°C

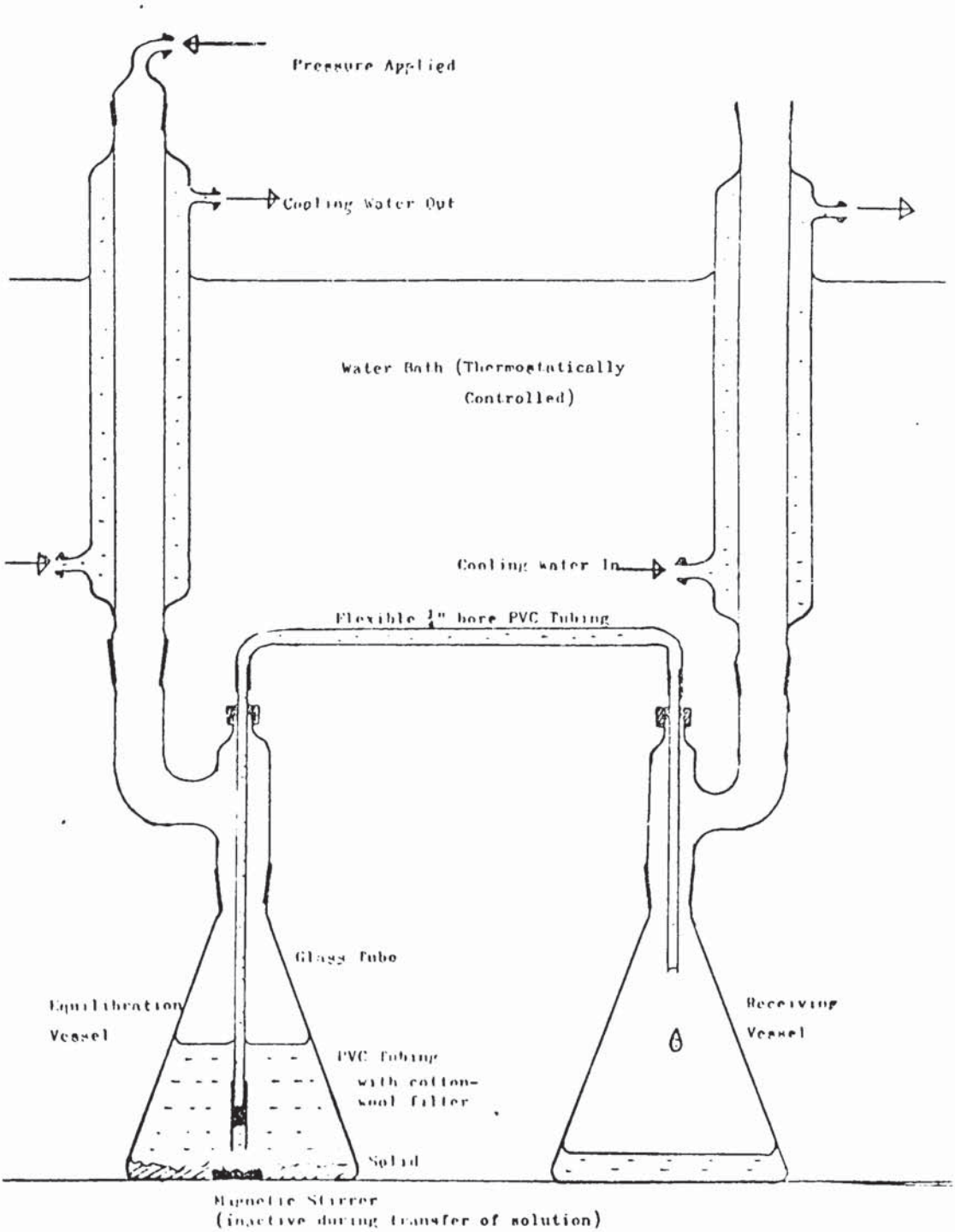

submersible magnetic stirrer for a minimum of 24 hours. A useful check to ensure that equilibrium has been attained is to prepare two samples with water at temperatures initially above and below that of the water bath respectively. After equilibration at the temperature of the water bath, both solutions should be similar.

Once transfer had occurred analysis was by either gravimetric or chemical techniques. The gravimetric technique involved evaporation to dryness of a weighed quantity of solution in a 20 cm^3 vial. Chemical analyses were by the techniques described in Appendix A.1.1, but when chemical techniques were used, the solutions were diluted immediately after transfer to prevent crystallisation occurring prior to analysis.

A.1.3 Measurement of Water Uptake

Nomenclature

m : weight of sample

m_o : weight of sample on removal from hydrostat

m_f : weight of sample an 'infinite' time after removal from hydrostat

m_θ : weight of sample at time θ

t : time (general)

F : computational common weighting factor

W : individual computational weighting

H : rate constant for first order loss of weight after removal of sample from hydrostat

θ : time (specific)

The water uptake of a dry powder in a humid atmosphere may be used as an indication of the hydrophilic nature, or otherwise, of the sample. A hydrophilic material, even if insoluble in water, may be

leached out of a coating through long exposure to water. The measurement of water uptake presents several problems. Powders should be finely divided, and particle sizes of samples being compared should be similar. The experiment should be designed in such a way that all parts of a sample have equal access to water vapour. It must be ensured that the humidity is similar for different trials. It is very difficult to ensure that all these conditions are absolutely met, and therefore the accuracy of the results may be low. However general trends may easily be discerned. All measurements were repeated at least once, and in many cases several times.

In the case of melamine phosphate particle sizes are somewhat dissimilar, and differences in shape may lead to differences in susceptibility to water uptake due to the varying volume to surface area ratio. The latter is a real consideration which this investigation sought to take account of. Quantities of the order of 200 mg were weighed into polystyrene boats and spread over the inside. This ensures as far as possible reasonable access of water vapour to most particles, but does not fulfil the condition absolutely. It is one of the main inaccuracies in the method. Up to three boats were placed into hydrostats and held at 28°C $\pm$ 1°C and 100% relative humidity for between sixty and sixty five hours. The hydrostats were vessels, with lids sealed by means of a greased flange, in which the boats were placed on a wire mesh above a little water. A constant temperature environment was provided in an incubator constructed from an insulated box with a controller monitoring temperature by means of a resistance thermometer. This was proved to give excellent control to within $\pm$ 1°C.

After removal from the controlled environment into the atmosphere, weight loss was found to be immediate. In some cases the total weight loss, even after standing in the atmosphere for several hours, was small, whereas in others there was total loss of the water taken up, thus restoring in about one hour the original dry weight. In most cases however intermediate behaviour occurred and the final weight obtained after standing in the atmosphere for twenty four hours was greater than the original dry weight, but with nevertheless considerable loss of weight. There appeared to be no systematic cause to account for these differences in behaviour. However due to the immediate weight loss, it proved impossible to obtain an accurate result for water uptake in the 100% relative humidity environment. A model extrapolating back to the time of removal of samples from this environment was devised, utilising successive weight measurements over a period of around 4 hours. A computer program was written using this model to give percentage water uptake directly, and this was used except in cases where the water loss was sufficiently small to be able to deduce the original water uptake measurement by observation.

It is assumed that the rate of loss of water vapour after removal from a 100% relative humidity environment is first order, and is at any time proportional to the quantity of water left in excess of that still present at 'infinite' time, i.e.

$$-\frac{dm}{dt} = H\,(m - m_f) \qquad \text{(A.1.3.1.)}$$

Integrating between time θ and zero time:

$$\int_{m_o}^{m_\theta} \frac{dm}{(m - m_f)} = \int_{o}^{\theta} -H\,dt \qquad \text{(A.1.3.2)}$$

Therefore $[\ln (m - m_f)]_{m_o}^{m_\theta} = - H\theta$

Therefore $\ln\left(\frac{m_o - m_f}{m_\theta - m_f}\right) = - H\theta$

Therefore $m_o = (m_\theta - m_f) \exp (H\theta) + m_f$ (A.1.3.3)

With three unknowns : m_o, H, m_f, it is theoretically possible to obtain values for these from a minimum of three values of m_θ vs. θ. However, the arithmetic is needlessly complex, and it is preferable to have m_f as an experimental value. The weight twenty four hours after removal from the controlled environment was used.

From equation (A.1.3.2)

$\ln (m_\theta - m_f) = - H\theta + \ln (m_o - m_f)$ (A.1.3.4)

which is of linear form. By plotting $\ln (m_\theta - m_f)$ vs. θ, the intercept on the ordinate gives a value $\ln (m_o - m_f)$, from which m_o may be deduced. The gradient -H is a measure of the rate of loss of weight after removal from the controlled environment.

The applicability of the model was verified graphically on a trial experiment. By determining $\frac{dm}{dt}$ and m at two points on a linear plot, a value of H was obtained at each point i, since

$$H = \frac{\dot{m}_i}{m_i - m_f} \quad (A.1.3.5)$$

where $\dot{m}_i = \frac{dm_i}{dt}$.

From a logarithmic graph of equation (A.1.3.4) H may also be obtained by direct measurement.

An experimental value of m_f was used in equation (A.1.3.5) but m_f may also be deduced graphically from the two points:

$$m_f = \frac{m_2\dot{m}_1 - m_1\dot{m}_2}{\dot{m}_1 - \dot{m}_2} \quad (A.1.3.6)$$

Table A.1.1 illustrates the closeness of agreement for a set of trial samples (small needles treated at 220°C).

In utilising linear regression analysis for points obeying a law of the type of equation (A.1.3.4), an error in ln $(m_\theta - m_f)$ will be dependent upon the absolute value of $(m_\theta - m_f)$. It is necessary to weight points in such a way as to reflect this dependency, thus:

$$W = F\,(m_\theta - m_f) \qquad (A.3.1.7)$$

W, F being integers, where F is a constant weighting factor set arbitrarily at 6000 (in early trials at 700). Any reading for which the expression $F\,(m_\theta - m_f) < 1$ was ignored.

The program was constructed using a linear regression analysis NAG library subroutine (53), capable of printing information on the regression errors. After input of information on weight and time, the readings were weighted and new arrays of both elements formed, for linear regression analysis. Printed output included the extrapolated value of percentage water uptake at 100% relative humidity, and the final percentage increase in weight over the dry weight at 'infinite' time after the conclusion of the experiment. A specimen print-out is included in Figure A.1.2.

A.1.4 Differential Thermal Analysis

Differential thermal analysis detects any physical or chemical changes occurring to a material as it is heated, which are either of an endothermic or exothermic nature. A sample of the test material, tightly packed into a crucible to ensure good contact, and a reference material, such as alumina, are heated at the same rate in a heating block. The temperatures of both crucibles are monitored by thermo-couples in contact with their bases. Any endothermic or exothermic change in the sample leads to a temperature difference between the

TABLE A.1.1 : Model Verification For A Trial Set Of Samples. All Weights Include The Weight Of Polystyrene Boats.

Time of heat treatment (hours)	5	24	48
m_f			
Experimental	1.2858	1.2280	1.3749
Graphical	1.2832	1.2239	1.3714
(using equation (A.1.3.6))			
H			
Graphical, point 1	0.1245	0.0650	0.0749
Graphical, point 2	0.1250	0.0651	0.0750
From Logarithmic Graph	0.156	0.075	0.094
Computational	0.172	0.0782	0.1043
% water uptake			
Graphical	13.86	17.96	16.42
Computational	14.10	18.14	16.77

sample and the reference material. A thermogram may thus be obtained showing peaks for temperature difference and the relevant furnace temperature. The thermal masses of sample and reference material should be similar; any degradation leading to a change in weight of the sample will lead to drift of the base line. The rate of heating and the actual masses of sample (and reference) do affect the trace also; it is desirable for comparative work to keep these as similar as possible (49).

A Stanton-Redcroft Analyser was used, with long-stemmed quartz crucibles to prevent contamination of the instrument by subliming material, which condenses further up the stem of the crucible. Determinations were carried out in static air, but the atmosphere in the vicinity of any sample which decomposes thermally with the evolution of gaseous products will consist of those gaseous products at temperatures above the minimum decomposition temperature. Thus the course of the further decomposition is then likely to take a somewhat different course to that which would occur if the decomposition products were being continuously removed and replaced with fresh air.

FIGURE A.1.2 : Computer program and sample results for obtaining the water uptake of samples of melamine phosphate.

```
      MASTER MELPHOS
C WT LOSS AT END OF WATER UPTAKE EXPT BY LINEAR REGRESSION
C ANALYSIS
C N DATA POINTS MAX 10
C NTOT WEIGHTED DATA POINTS
C MT IS WEIGHT AT TIME T SECS, MF IS FINAL WT
      REAL MF, MT(10), TIME(10), M(10), LN(10), TIME2(999),
     1LEN(999), RESULT(20), INITM
      INTEGER V, T, U, IW(10)
    5 READ (1,10) N, MF, TABLE, WT
      IF (N .LE. 0) STOP
      READ (1,20) (TIME(I),MT(I),I=1,N)
      IFAIL = 0
      WRITE (2,9999)
      DO 100 I = 1,N
      M(I) = MT(I) - MF
      LN(I) = ALOG(M(I))
      IW(I) = 6000*M(I)
      WRITE (2,22) TIME(I), MT(I)
  100 CONTINUE
   52 V = IW(1)
      DO 200 J =1,V
      LEN(J) = LN(1)
      TIME2(J) = TIME(1)
  200 CONTINUE
      DO 600 I =2,N
      IF (IW(I) .EQ. 0) GO TO 700
      IP = I - 1
      IT = 0
      DO 300 JT =1,IP
      IT = IT + IW(JT)
  300 CONTINUE
      T = IT + 1
      U = 0
      DO 400 JU =1,I
      U = U + IW(JU)
  400 CONTINUE
      DO 500 J =T,U
      LEN(J) = LN(I)
      TIME2(J) = TIME(I)
  500 CONTINUE
  600 CONTINUE
  700 NTOT = 0
      DO 800 JN =1,N
      NTOT = NTOT + IW(JN)
  800 CONTINUE
      IF (NTOT .LE. 2 ) GO TO 6
      CALL G02CAF (NTOT, TIME2, LEN, RESULT, IFAIL)
   53 INITM = EXP(RESULT(7)) + MF
```

```
C CALCULATE PERCENTAGE WATER UPTAKE PER
      PER = (INITW - WT)*100/(WT - TARE)
    6 PERF = (MF - WT)*100/(WT - TARE)
      DO 6001 L = 1,10
      WRITE (2,50) L, RESULT(L)
 6001 CONTINUE
      WRITE (2,9998)
      WRITE (2, 30) N, TARE, WT, MF, INITW
      WRITE (2,9997)
      WRITE (2,32) PER, PERF
      GO TO 5
   10 FORMAT (I5, 3F10.0)
   20 FORMAT (F5.3, F10.0)
   25 FORMAT (1X, F9.0, F10.5)
   30 FORMAT (1X, I4, 4F10.5/)
   32 FORMAT (1X,2F15.3///)
   50 FORMAT (1X,7HRESULT( ,I2, 2H)= , 1PE15.5 /)
 9997 FORMAT (3X,11HINITIAL PER,4X,9HFINAL PER)
 9998 FORMAT (4X, 1HN, 6X, 4HTARE, 4X, 6HDRY WT, 2X,
     2&HFINAL WT,3X,8H DIST WT)
 9999 FORMAT (6Y, 4HTIME, 4X, 6HWEIGHT /)
      END
      FINISH
```

Thin reflective plates

$(C_3H_6N_6)_{1.3}\cdot H_3PO_4$

treated at 220°C for 48 hours.

TIME	WEIGHT
60.	1.32120
120.	1.31970
180.	1.31790
270.	1.31610
495.	1.31300
1110.	1.30870

RESULT(6) = -2.5[illegible]48E-05

RESULT(7) = -4.1[illegible]36E 00

RESULT(8) = 2.411[illegible]4E-05

RESULT(9) = 5.7[illegible]38E-03

RESULT(10) = -1.0[illegible]97E 02

RESULT(11) = -7.25994E 02

RESULT(12) = 4.10655E 01

RESULT(13) = 1.00000E 00

RESULT(14) = 4.10655E 01

RESULT(15) = 1.1[illegible]70E 04

RESULT(16) = 1.01419E 00

RESULT(17) = 2.79000E 02

RESULT(18) = 3.[illegible]-03

N	TARE	DRY WT	FINAL WT	MOIST WT
6	1.10220	1.30[illegible]0	1.30820	1.32375

INITIAL PER	FINAL PER
11.723	5.[illegible]3

TIME	WEIGHT
113.	1.21390
170.	1.21180
225.	1.20920
295.	1.20760
360.	1.20670
435.	1.20490
500.	1.20350
570.	1.20190
855.	1.19820
2115.	1.19570

Dimelamine Phosphate treated

at 210°C for 48 hours.

RESULT(6)= -2.0?461E-03

RESULT(7)= -?.?8106E 00

RESULT(8)= 7.24342E-06

RESULT(9)= 2.69823E-03

RESULT(10)= -2.?51740 02

RESULT(11)= -1.401328 03

RESULT(12)= 1.0?143E 02

RESULT(13)= 1.000008 00

RESULT(14)= 1.031438 02

RESULT(15)= 8.?02165 04

RESULT(16)= 7.?1721E-01

RESULT(17)= 5.??0003 02

RESULT(1?)= 1.29?24?-03

N	TARE	DRY WT	FINAL WT	MOIST WT
10	1.01340	1.1?560	1.1?530	1.21810

INITIAL PER	FINAL PER
1?.734	5.510

APPENDIX A2

SOLUBILITY AND WATER UPTAKE OF MELAMINE PHOSPHATE - A FULL LISTING

A.2.1 Solubility Measurements

Table A.2.1 gives a full listing of solubility measurements for melamine phosphate, dried at 110°C, and treated at 210°C for 48 hours, including, where relevant, measurements from an investigation of the effects of temperature and duration of heat treatment, obtained both by spectroscopic and gravimetric methods. Table A.2.2 gives a full listing of results from this investigation.

A.2.2 Water Uptake Measurements

Tables A.2.3 and A.2.4 give full listings of water uptake measurements for materials dried at 110°C, and treated at 210°C for 48 hours; and from an investigation of the effects of temperature and duration of heat treatment.

TABLE A.2.1 : Solubility Measurements For Melamine Phosphate; (a) Dried at 100°C; (b) Treated at 210°C For 48 Hours.

Crystal Type	Dried at 110°C Analytical Technique	Melamine (mole l^{-1})	Phosphate (mole l^{-1})	% (w/w)	Treated at 210°C Analytical Technique	Melamine (mole l^{-1})	% (w/w)	
Large Needles	S	0.0193	0.0217	0.456	G	[illegible]	0.068	N.B. No phos-
$(C_3H_6N_6)_{1.0}.H_3PO_4$	S	0.0212	0.0258	0.521	S	0.00252		phate as the
	S	0.0271	0.0428	0.76				analytical
Small Needles	S			0.347				technique is
$(C_3H_6N_6)_{1.2}.H_3PO_4$	G			0.357				invalid for
	S	0.0244	0.0364	0.664				partially
Small Block Plates	S			0.363	G		0.054	condensed
$(C_3H_6N_6)_{1.2}.H_3PO_4$	G			0.365	S	0.00242		phosphate
	S	0.0228	0.0399	0.678				content.
	S	0.0230	0.0279	0.564				
Thin Reflective Plates	S			0.320	G		0.260	
$(C_3H_6N_6)_{1.3}.H_3PO_4$	G			0.267	S	0.01139		
	S	0.0167	0.0159	0.366	S	0.0071		

Table A.2.1 (cont).

Crystal Type	Analytical Technique	Melamine (mole l^{-1})	Phosphate (mole l^{-1})	% (w/w)	Analytical Technique	Melamine (mole l^{-1})	% (w/w)
Thin Reflective Plates	S	0.0148	0.0134	0.318			
$(C_3H_6N_6)_{1.3}.H_3PO_4$	S	0.0158	0.0150	0.346			
	S	0.0152	0.0126	0.315			
Block Plates	S	0.0133	0.0096	0.262	G		0.008
$(C_3H_6N_6)_{2.0}.H_3PO_4$	S	0.0142	0.0077	0.254	S	0.0036	(≡ 0.0496)

Key S : spectroscopic analysis

G : gravimetric analysis

TABLE A.2.2 : Solubility Measurements For Melamine Phosphate Treated At A Variety Of Temperatures For Different Durations, % (w/w).

S = spectroscopic analysis, G = gravimetric analysis

		Small Needles $(C_3H_6N_6)_{1.2}\cdot H_3PO_4$			Small Block Plates $(C_3H_6N_6)_{1.2}\cdot H_3PO_4$			Thin Reflective Plates $(C_3H_6N_6)_{1.3}\cdot H_3PO_4$		
		5^h	24^h	48^h	5^h	24^h	48^h	5^h	24^h	48^h
170°	S	0.342	0.367	0.388	0.326	0.332	0.334	0.296	0.290	0.294
	G	0.316	0.345	0.364	0.316	0.335	0.339	0.267	0.257	0.246
195°	S	0.425	0.327	0.403	0.317	0.125	0.106			
	G	0.446	0.300	0.374	0.312	0.128	0.113			
220°	S	0.040	-	0.056	0.099	0.056	0.057	0.061	0.055	0.058
	G	-	0.033	0.057	0.077	0.031	0.033	0.051	0.032	0.018
252°	S	-	0.047	-	0.056	0.067	0.075			
	G	-	0.018	-	0.028	0.026	0.031			

TABLE A.2.3 : Water Uptake % (w/w), By Melamine Phosphate : A) Dried At 110°C; (B) Treated At 210°C For 48 Hours.

Crystal Type	Dried At 110°C		Treated At 210°C
Large Needles	1.2		4.1
$(C_3H_6N_6)_{1.0}.H_3PO_4$	0.0		1.1
	0.0		0.4
	0.0		0.4
Small Needles	0.6	4.2	
$(C_3H_6N_6)_{1.2}.H_3PO_4$	1.2	5.5	
	3.2		
Small Block Plates	2.3	3.7	8.2
$(C_3H_6N_6)_{1.2}.H_3PO_4$	6.3	6.5	10.6
	3.4		
Thin Reflective Plates	5.0	3.9	18
$(C_3H_6N_6)_{1.3}.H_3PO_4$	1.1	5.6	10.3
	6.2		
Block Plates	6.5		11.2
$(C_3H_6N_6)_{2.0}.H_3PO_4$	5.9		17.3
			18.7

TABLE A.2.4 : Water Uptake, % (w/w), By Melamine Phosphate Treated At A Variety Of Temperatures For Different Durations.

	Small needles $(C_3H_6N_6)_{1.2}.H_3PO_4$			Small block plates $(C_3H_6N_6)_{1.2}.H_3PO_4$			Thin reflective plates $(C_3H_6N_6)_{1.3}.H_3PO_4$		
	5^h	24^h	48^h	5^h	24^h	48^h	5^h	24^h	48^h
170°	1.5	1.8	1.2	1.7	1.9	1.9	7.4	3.2	3.0
	2.0	2.8	2.0	5.4	6.4	4.2			
				6.4	6.8	7.9			
195°	1.9	1.8	3.3	2.1	2.8	3.5			
	4.2	2.0	3.4	2.6	8.1	5.1			
						5.9			
220°	4.4	4.3	3.0	3.2	6.3	2.6	6.6	8.8	5.3
	4.8	5.7	9.1	4.1	7.4	4.5		9.7	11.7
252°		7.0		6.5	1.5	2.3			
		3.0		11.9	9.4	5.4			

APPENDIX A3

Computer Program to obtain the Parameters of a bizonal Exponential Decay Model of the Incident Heat with respect to Range in the Fire Testing Device.

The Data for this program were obtained at a height of 175 mm above the working surface, with normal air and gas flow rates of 370 litre min^{-1} and 26 litre min^{-1} respectively.

```
      MASTER BOUNDARY
C TWO CURVE REGRESSION ANALYSIS EXPONENTIAL DECAY
C BOUNDARY 50*M
      REAL R(45),W(45),T(45),RJ(45),TJ(45),WJ(45),RK(45),
     1TK(45),RKT(45),WK(45),SW(12),GW(12),ST(12),GT(12),
     2SKW(12),GKW(12),SKT(12),GKT(12)
    5 READ (1,100) N,(R(I),W(I),T(I),I=1,N)
      IF (N.EQ.1) STOP
      WRITE (2,99)
      WRITE (2,100) N,    (R(I),W(I),T(I),I=1,N)
      DO 200 J=1,12
      GW(J)=1E20
      GT(J)=1E20
  200 CONTINUE
      DO 9 M=2,12
      J=1
      DO 8 I = 1,N
      IF (IFIX(R(I)).GT.50*M) GO TO 8
      RJ(J) = R(I)
      WJ(J) = ALOG(W(I))
      TJ(J) = ALOG(T(I))
      J = J+1
    8 CONTINUE
      WRITE (2,500)
      CALL REGRESS (J,RJ,WJ,SW,GW,M)
      WRITE (2,501)
      CALL REGRESS (J,RJ,TJ,ST,GT,M)
    9 CONTINUE
C MINIMUM SOURCE AND GRADIENT
      CALL MINIM (GW,MW)
      CALL MINIM (GT,MT)
      MW50 = MW*50
      MT50 = MT*50
      K=1
      KT=1
      DO 7 I =1,N
      IF (IFIX(R(I)).LE.50*MW) GO TO 6
      RK(K) = R(I)
      WK(K) = ALOG(W(I))
      K = K+1
    6 IF(IFIX(R(I)).LE.50*MT) GO TO 7
      RKT(KT) = R(I)
      TK(KT)  =ALOG(T(I))
      KT = KT + 1
    7 CONTINUE
      WRITE (2,101) MW50,MT50
      WRITE(2,502)
      CALL REGRESS (K,RK,WK,SKW,GKW,MW)
      WRITE (2,503)
```

```
      CALL REGRESS (KT,WKT,TK,SKT,GKT,NT)
      WRITE (2,505)
      DO 26 L=100,400,50
      WM=SW(MW)*EXP(GW(MW)*FLOAT(L))
      TM=ST(MT)*EXP(GT(MT)*FLOAT(L))
      WKM=SKW(MW)*EXP(GKW(MW)*FLOAT(L))
      TKM=SKT(MT)*EXP(GKT(MT)*FLOAT(L))
      WRITE (2,102)L,WM,TM,WKM,TKM
   26 CONTINUE
      WRITE (2,504)
      GO TO 5
   99 FORMAT(5X,'R',11X,'W',7X,'T',9X,'R',11X,'W',7X,'T')
  100 FORMAT (I5/(6F10.2))
  101 FORMAT (1X,'OPTICAL BOUNDARY - IRRADIANCE    ',
     3'TEMPERATURE'/20X,2I10)
  102 FORMAT (1X,I5,4F12.3)
  500 FORMAT (1X ,20HIRRADIANCE,LOW RANGE)
  501 FORMAT (1X ,21HTEMPERATURE,LOW RANGE)
  502 FORMAT (1X ,21HIRRADIANCE,HIGH RANGE)
  503 FORMAT (1X ,22HTEMPERATURE,HIGH RANGE)
  504 FORMAT (1H1)
  505 FORMAT (13X,9HLOW RANGE,15X,10HHIGH RANGE/1X, 5HRANGE,7X,
     41HW,11X,1HT,11X,1HW,11X,1HT)
      END

      SUBROUTINE REGRESS (NZ,X,Y,SOURCE,GRAD,M)
      REAL X(45),Y(45),RESULT(20),SOURCE(12),GRAD(12)
      M50 =M*50
      IF (NZ.LE.3) RETURN
      IFAIL = 0
      N=NZ-1
      CALL G02CAF (N,X,Y,RESULT,IFAIL)
      SOURCE(M) = EXP(RESULT(7))
      GRAD(M)   = RESULT(6)
      WRITE (2,900) M50,N,SOURCE(M),(RESULT(L),L=6,9)
      RETURN
  900 FORMAT (1X,'BOUNDARY',I5,3X,'VALUES IN RANGE',I5/
     97H SOURCE,F15.3,3X,9HGRADIENT,1PE15.6/1X,
     8'INTERCEPT ',1PE15.6/1X,'STD ERRORS ',2(1PE15.6)//)
      END

      SUBROUTINE MINIM (S,MIN)
      REAL S(12)
      MIN = 2
      DO 171 I = 3,12
      IF (ABS(S(I)).LE.ABS(S(MIN))) MIN=I
  171 CONTINUE
C S(MIN) CONTAINS MINIMUM VALUE
      RETURN
      END
      FINISH
```

P	W	T	P	W	T
42					
297.00	1.79	655.00	407.00	1.00	455.00
373.00	1.24	590.00	375.00	1.59	590.00
307.00	1.78	640.00	277.00	2.01	679.00
248.00	2.15	716.00	227.00	2.33	750.00
320.00	1.67	631.00	365.00	1.31	540.00
405.00	1.00	452.00	445.00	0.64	349.00
485.00	0.47	258.00	525.00	0.34	197.00
497.00	0.46	242.00	463.00	0.64	310.00
422.00	0.92	405.00	312.00	1.10	500.00
353.00	1.40	553.00	320.00	1.72	620.00
287.00	1.92	665.00	258.00	2.12	707.00
227.00	2.35	749.00	202.00	2.55	785.00
172.00	2.79	814.00	163.00	2.98	842.00
140.00	3.43	862.00	303.00	1.70	675.00
415.00	0.90	472.00	350.00	0.88	490.00
305.00	1.46	650.00	270.00	1.71	700.00
192.00	2.31	758.00	437.00	0.85	415.00
348.00	1.53	588.00	265.00	2.00	685.00
223.00	2.50	776.00	177.00	2.92	838.00
135.00	3.49	935.00	117.00	4.26	980.00
292.00	1.91	702.00	357.00	1.16	540.00

IRRADIANCE,LOW RANGE
TEMPERATURE,LOW RANGE
IRRADIANCE,LOW RANGE
BOUNDARY 150 VALUES IN RANGE 3
SOURCE 11.309 GRADIENT -8.256296E-03
INTERCEPT 2.425569E 00
STD ERRORS 3.572562E-03 4.621465E-01

TEMPERATURE,LOW RANGE
BOUNDARY 150 VALUES IN RANGE 3
SOURCE 1727.934 GRADIENT -4.787475E-03
INTERCEPT 7.454682E 00
STD ERRORS 2.422923E-03 3.174985E-01

IRRADIANCE,LOW RANGE
BOUNDARY 200 VALUES IN RANGE 7
SOURCE 10.267 GRADIENT -7.473174E-03
INTERCEPT 2.328525E 00
STD ERRORS 7.512272E-04 1.197798E-01

TEMPERATURE,LOW RANGE
BOUNDARY 200 VALUES IN RANGE 7
SOURCE 1371.103 GRADIENT -2.976745E-03
INTERCEPT 7.223881E 00
STD ERRORS 4.473661E-04 7.133049E-02

IRRADIANCE,LOW RANGE
BOUNDARY 250 VALUES IN RANGE 12
SOURCE 7.063 GRADIENT -4.983233E-03
INTERCEPT 1.957733E 00
STD ERRORS 5.205649E-04 9.284077E-02

```
TEMPERATURE,LOW RANGE
BOUNDARY  250    VALUES IN RANGE    12
SOURCE          1215.028    GRADIENT  -2.158432E-03
INTERCEPT      7.102522E 00
STD ERRORS      2.185773E-04    4.152273E-02


IRRADIANCE,LOW RANGE
BOUNDARY  300    VALUES IN RANGE    19
SOURCE             6.271    GRADIENT  -4.275707E-03
INTERCEPT      1.835944E 00
STD ERRORS      3.033846E-04    7.026251E-02


TEMPERATURE,LOW RANGE
BOUNDARY  300    VALUES IN RANGE    19
SOURCE          1167.035    GRADIENT  -1.922630E-03
INTERCEPT      7.063222E 00
STD ERRORS      1.198752E-04    2.640106E-02


IRRADIANCE,LOW RANGE
BOUNDARY  350    VALUES IN RANGE    27
SOURCE             6.031    GRADIENT  -4.548836E-03
INTERCEPT      1.891751E 00
STD ERRORS      3.354839E-04    8.724550E-02


TEMPERATURE,LOW RANGE
BOUNDARY  350    VALUES IN RANGE    27
SOURCE          1217.838    GRADIENT  -2.130263E-03
INTERCEPT      7.104432E 00
STD ERRORS      1.206621E-04    3.293960E-02


IRRADIANCE,LOW RANGE
BOUNDARY  400    VALUES IN RANGE    32
SOURCE             6.507    GRADIENT  -4.459543E-03
INTERCEPT      1.872926E 00
STD ERRORS      2.509115E-04    7.039345E-02


TEMPERATURE,LOW RANGE
BOUNDARY  400    VALUES IN RANGE    32
SOURCE          1251.500    GRADIENT  -2.258304E-03
INTERCEPT      7.132092E 00
STD ERRORS      1.059974E-04    2.970961E-02


IRRADIANCE,LOW RANGE
BOUNDARY  450    VALUES IN RANGE    38
SOURCE             7.046    GRADIENT  -4.796742E-03
INTERCEPT      1.952396E 00
STD ERRORS      2.030515E-04    6.239072E-02
```

```
TEMPERATURE,LOW RANGE
BOUNDARY  450    VALUES IN RANGE    32
SOURCE          1363.430    GRADIENT   -2.623927E-03
INTERCEPT      7.217759E 00
STD ERRORS      1.176623E-04    3.615357E-02


IRRADIANCE,LOW RANGE
BOUNDARY  500    VALUES IN RANGE    41
SOURCE             7.756    GRADIENT   -5.177215E-03
INTERCEPT      2.047494E 00
STD ERRORS      2.024967E-04    6.545820E-02


TEMPERATURE,LOW RANGE
BOUNDARY  500    VALUES IN RANGE    41
SOURCE          1538.131    GRADIENT   -3.101493E-03
INTERCEPT      7.336324E 00
STD ERRORS      1.670362E-04    5.399539E-02


IRRADIANCE,LOW RANGE
BOUNDARY  550    VALUES IN RANGE    42
SOURCE             8.163    GRADIENT   -5.371605E-03
INTERCEPT      2.099585E 00
STD ERRORS      2.099204E-04    6.916830E-02


TEMPERATURE,LOW RANGE
BOUNDARY  550    VALUES IN RANGE    42
SOURCE          1621.286    GRADIENT   -3.301823E-03
INTERCEPT      7.390975E 00
STD ERRORS      1.819837E-04    5.996320E-02


IRRADIANCE,LOW RANGE
BOUNDARY  600    VALUES IN RANGE    42
SOURCE             8.163    GRADIENT   -5.371605E-03
INTERCEPT      2.099585E 00
STD ERRORS      2.099204E-04    6.916830E-02


TEMPERATURE,LOW RANGE
BOUNDARY  600    VALUES IN RANGE    42
SOURCE          1621.286    GRADIENT   -3.301823E-03
INTERCEPT      7.390975E 00
STD ERRORS      1.819837E-04    5.996320E-02
```

OPTIMUM BOUNDARY - IRRADIANCE TEMPERATURE
300 300

IRRADIANCE,HIGH RANGE
BOUNDARY 300 VALUES IN RANGE 23
SOURCE 14.757 GRADIENT -6.347454E-03
INTERCEPT 2.691741E 00
STD ERRORS 4.568702E-04 1.400861E-01

TEMPERATURE,HIGH RANGE
BOUNDARY 300 VALUES IN RANGE 23
SOURCE 3269.101 GRADIENT -5.052744E-03
INTERCEPT 8.092271E 00
STD ERRORS 2.901858E-04 1.143235E-01

	LOW RANGE		HIGH RANGE	
RANGE	W	T	W	T
100	4.039	962.904	7.441	1972.360
150	3.302	874.647	5.284	1532.045
200	2.667	794.478	3.752	1190.016
250	2.153	721.658	2.664	924.344
300	1.739	655.513	1.892	717.984
350	1.404	595.430	1.343	557.694
400	1.134	540.854	0.954	433.189
450	0.916	491.281	0.677	336.479
500	0.739	446.251	0.491	261.360
550	0.597	405.349	0.342	203.011
600	0.482	368.195	0.243	157.689

APPENDIX A4

THE RESULTS OF THE FIRE TEST PROGRAMME - A FULL LISTING

The results of the Fire Test Programme, including early tests to determine the test formulation to use in evaluating differences between crystal types of melamine phosphate are shown in Tables A.4.1 to A.4.7.

All test samples, unless otherwise specified, consist only of epoxy resin Araldite MY753, hardener Versamid 125 in a ratio of five parts to two by weight, and Melamine Phosphate, mixed under low shear in an orbital mixer, and coated to a thickness of 6mm onto mild steel substrates. The standard cure regime was twenty four hours at ambient temperature, followed by nine days at 55°C.

Although the full range of crystal types was tested at 750° - 800°C, since this regime provided the greatest amount of information about differences between crystal types, in the other two fire test regimes, some crystal types were not tested at a 30% level of incorporation. These were Dimelamine phosphate in a British Standard 476 Pt.8 time-temperature curve simulation test, since its performance might be expected to be similar or inferior to that of a sample containing thin reflective plates, and needles of $(C_3H_6N_6)_{1.0}.H_3PO_4$ at 850° - 900°C, as its performance would be expected to be similar to small needles of $(C_3H_6N_6)_{1.2}.H_3PO_4$, which intumesced to such an extent that no information of value could be obtained.

Gaps in the sequential numbering of the reported test results are due to tests aborted at an early stage.

In Tables A.4.5 to A.4.7 (tests at 850° - 900°C) early tests are identified in alpha-numeric sequence. The six series are as follows:

(a) : 30% melamine phosphate, tests for reproducibility

(b) : variable loading of melamine phosphate, to determine the optimum loading

(c) : variable cure regime for 12½% melamine phosphate

(d) : miscellaneous

(e) : determination of the effects of incorporating titanium dioxide

(f) : the first comparison of the performance of different crystal types, at a loading of 12½% melamine phosphate.

Abbreviations

amb. : ambient temperature

d : day (s)

h : hour (s)

mpM : moles sodium phosphate (as indicated) per mole melamine phosphate

vol. : voluminous intumescence (> 150 mm)

wk. : week (s)

C : cure regime

RM : incorporated by roll-milling at high shear

Key to Mixtures (Tables A.4.2, A.4.4, A.4.6)

Mixture I : Equal parts of Needles of $(C_3H_6N_6)_{1.0}.H_3PO_4$ and Thin Reflective Plates of $(C_3H_6N_6)_{1.3}.H_3PO_4$

Mixture IA : One part of Needles of $(C_3H_6N_6)_{1.0}.H_3PO_4$ to Three Parts Thin Reflective Plates of $(C_3H_6N_6)_{1.3}.H_3PO_4$

Mixture IB : One part of Needles of $(C_3H_6N_6)_{1.0}.H_3PO_4$ to Eight Parts Thin Reflective Plates of $(C_3H_6N_6)_{1.3}.H_3PO_4$

Mixture II : Equal parts of Large Block Plates of $(C_3H_6N_6)_{2.0}\cdot H_3PO_4$ and Small Needles of $(C_3H_6N_6)_{1.2}\cdot H_3PO_4$

Mixture III : Equal parts of Needles of $(C_3H_6N_6)_{1.0}\cdot H_3PO_4$ and Large Block Plates of $(C_3H_6N_6)_{2.0}\cdot H_3PO_4$

TABLE A.4.1 : Fire Test Results At 750° - 800°C (Range 190 mm) For Samples Incorporating 12½% Melamine Phosphate.

Crystal Type	Special Treatment (if any)	Test No.	Weight of Coating (g)	Time (min) To: 300°C	Time (min) To: 400°C	Duration (min)	Maximum Extent of Intumescence (mm)	Time to Maximum Extent (min)
Medium Needles		114	53.1	17	34½	34½	110	6¾
$(C_3H_6N_6)_{1.0}\cdot H_3PO_4$		115	50.1	20½	38	39	85	6
Very Large Needles		117	48.7	12	30	34	50	7¼
$(C_3H_6N_6)_{1.0}\cdot H_3PO_4$		123	48.9	12	33½	34½	70	7
Small Needles		32	~ 42	9	26	30	50	7
$(C_3H_6N_6)_{1.2}\cdot H_3PO_4$		36	41.2	11	28½	34	30	5½
	+30% NaCl	12	-	5½	15½	20	30	5
	+30% $NaH_2PO_4.2H_2O$	14	-	12	28	>40	40	9¾
	+30% Na_3PO_4	15	-	6	8	9	0	-
Small Block Plates		17	~ 44	4¼	18	20	50	5
$(C_3H_6N_6)_{1.2}\cdot H_3PO_4$		22	~ 44	12½	24	30	45	4½
	RM	92	58.5	14	34	34	70	8
	RM	94	50.8	8½	36½	40	30	7

Crystal Type	Special Treatment (if any)	Test No.	Weight of Coating (g)	Time (min) To: 300°C	Time (min) To: 400°C	Duration (min)	Maximum Extent of Intumescence (mm)	Time to Maximum Extent (min)
Small Block Plates	C ld, amb.	69	39.5	8½	22	24	10	9
$(C_3H_6N_6)_{1.2}\cdot H_3PO_4$	C 1wk., amb.	83	45.1	8	17	20	40	6
	C 4wk., amb.	90	39.3	8	17	19	35	7
	C 4wk., 55°C	87	43.8	5¼	17½	26½	30	9
Large Needles		16	~47	10	25½	28	70	3
$(C_3H_6N_6)_{1.2}\cdot H_3PO_4$		23	~47	17	37	38	70	4
Thin Reflective Plates		4	-	5½	17½	21	35	4¼
$(C_3H_6N_6)_{1.3}\cdot H_3PO_4$		7	-	5¾	18	20	30	3½
		29	-	8	21½	25½	15	5
		125	-	12	26½	27½	45	7¾
		127	-	6	20¼	21½	60	7½
	RM	110	55.6	4½	16	20½	40	5½
	RM	112	50.8	6	19	26	55	5½
	C ld., amb.	86	51.3	12	23	27	40	8
	C 9d., amb.	76	45.0	5	17½	20	20	4
	C 4wk., amb.	98	42.0	13	-	26½	25	10
	C 4wk., 55°C	96	41.9	7½	20	20	35	6

Crystal Type	Special Treatment (if any)	Test No.	Weight of Coating (g)	Time (min) To: 300°C	400°C	Duration (min)	Maximum Extent of Intumescence (mm)	Time to Maximum Extent (min)
Thin reflective plates (cont.)	RM, C 9d, amb.	80	64.2	8	18½	29	55	5
	RM	78	61.3	4½	17	21½	30	4½
Medium Block Plates		61	43.6	9½	24½	27	12	6½
$(C_3H_6N_6)_{2.0}\cdot H_3PO_4$		63	44.3	4½	15	21	12	5
Large Block Plates		2	-	6	20	24	40	7
$(C_3H_6N_6)_{2.0}\cdot H_3PO_4$		8	-	4	-	aborted	40	5

TABLE A.4.2 : Fire Test Results At 750° - 800°C (Range 190 mm) For Samples Incorporating 30% Melamine Phosphate

Crystal Type	Special Treatment (if any)	Test No.	Weight of Coating (g)	Time (min) to: 300°C	Time (min) to: 400°C	Duration (min)	Maximum Extent of Intumescence (mm)	Time to Maximum Extent (min)
Medium Needles		119	62.9	25	49	51	75	8
$(C_3H_6N_6)_{1.0}\cdot H_3PO_4$		121	63.9	25	55½	60	75	11
	Treated 210°C	142	64.3	9¾	24½	33½	100	8
Very Large Needles		120	64.2	27½	-	>68	125	7
$(C_3H_6N_6)_{1.0}\cdot H_3PO_4$		158	54.6	14	36½	43	100	8¾
	Treated 210°C	170	61.3	13½	30	36½	130	6½
Small Needles		35	54.9	15	34	42	140	9
$(C_3H_6N_6)_{1.2}\cdot H_3PO_4$		43	~62	22	38½	41½	75	6
	RM	144	63.2	10	20½	29	40	6
	RM	145	53.8	6½	19½	30	48	7½
	+1/6mpM NaH_2PO_4	146	56.3	10½	32	41½	82	8
	+1/3mpM NaH_2PO_4	147	60.8	13½	33	46½	100	10
	+2/3mpM NaH_2PO_4	148	70.2	27	67	67	35	11

Table A.4.2 (cont.)

Crystal Type	Special Treatment	Test No.	Weight of Coating (g)	Time (min) to: 300°C	400°C	Duration (min)	Maximum Extent of Intumescence (mm)	Time to Maximum Extent (min)
Small needles (cont)	+ 1/6mpM Na_2HPO_4	155	58.3	12½	26½	47	>150	7½
	+1/3mpM Na_2HPO_4	156	63.3	9	26½	32	85	10
	+2/3mpM Na_2HPO_4	157	~70	5¼	20	24	70	9½
Small Block Plates		45	-	17	30	39	80	8
$(C_3H_6N_6)_{1.2}\cdot H_3PO_4$		49	57.3	25	43	44	60	7
	Treated at 210°C	139	55.8	17½	35	36	>150	6½
	Treated at 210°C	141	53.6	21	-	>40	150	8
Large Needles		46	-	24	46	53½	45	7½
$(C_3H_6N_6)_{1.2}\cdot H_3PO_4$		51	54.7	18	32	38	95	7½
Thin Reflective Plates		34	52.9	9¼	18	34	20	9
$(C_3H_6N_6)_{1.3}\cdot H_3PO_4$		44	56.2	7¼	15½	20	45	6
		126	-	10	25	43	27	7¼
	Treated at 210°C	137	62.2	22	47	55	40	10
	Treated at 210°	143	60.8	14	36½	45	85	7¾

Table A.4.2 (cont)

Crystal Type	Special Treatment (if any)	Test No.	Weight of Coating (g)	Time (min) to: 300°c	400°C	Duration (min)	Maximum Extent of Intumescence (mm)	Time to Maximum Extent (min)
Thin reflective plates (cont)	Treated at 200°C (24h)	166	62.8	11½	34½	40	65	8
	+1/6mpM NaH_2PO_4	149	68.2	17	45	>64	75	11½
	+1/3mpM NaH_2PO_4	150	64.5	17	44	>64	40	9
	+2/3mpM NaH_2PO_4	151	-	7	27	45½	70	9½
	+1/6mpM Na_2HPO_4	152	65.7	5¾	15	25	200	7¼
	+1/3mpM Na_2HPO_4	153	68.7	8	28	35½	50	9¼
	+2/3mpM Na_2HPO_4	154	-	4	14½	40	17	11
Thin Plates		163	59.2	15	35	47	80	12¼
$(C_3H_6N_6)_{1.1}\cdot H_3PO_4$	Treated at 210°C	164	59.7	21½	48	48	100	6
Medium Block Plates		66	44.9	4½	12	28	10	6 ½
$(C_3H_6N_6)_{2.0}\cdot H_3PO_4$		67	52.6	5½	15¼	30	15	6
	Treated at 210°C	138	51.4	11	20	23½	120	5¼
	Treated at 210°C	140	56.5	10	26½	35½	120	4

Table A.4.2 (cont.)

Crystal Types	Special Treatment (if any)	Test No.	Weight of Coating (g)	Time (min) to: 300°C	400°C	Duration (min)	Maximum Extent of Intumescence (mm)	Time To Maximum Extent (min)
Large Block Plates		53	-	9	20	27	30	7¼
$(C_3H_6N_6)_{2.0}.H_3PO_4$		57	-	7½	17	25	40	6
Small Amorphous		103	53.2	8	19¾	25	30	9¼
Material		108	49.7	7½	19	25	40	8
$(C_3H_6N_6)_{2.0}.H_3PO_4$								
Encapsulated Small		101	47.6	6¾	13¼	25	7	9
Needles		105	51.7	5¾	12½	20	8	9
Mixture I		129	60.9	19½	-	>45	80	13
		132	62.3	22½	62½	66	85	10
Mixture IA		162	61.0	15	43	56	100	8
Mixture IB		161	59.9	10½	43	49	25	10
Mixture II		133	53.2	6	21	25	30	6
		136	56.9	5½	21	32	40	7
Mixture III		159	56.4	7½	28	36	80	7¼

TABLE A.4.3 : Fire Tests Results in British Standard 476 Pt. 8 Time-Temperature Curve Simulation Tests For Samples Incorporating 12½% Melamine Phosphate.

Crystal Type	Special Treatment	Test No.	Weight of Coating (g)	Time (min) to: 300°C and Face Temperature (°C) attained at these times (in brackets)	400°C	Maximum Extent of Intumescence (mm)
Medium Needles		113	~51	15 (745)	27¾ (855)	25
$(C_3H_6N_6)_{1.0}\cdot H_3PO_4$						
Very Large Needles		124	-	10½ (685)	-	25
$(C_3H_6N_6)_{1.0}\cdot H_3PO_4$						
Small Needles		31	43.2	12 (665)	23 (782)	30
$(C_3H_6N_6)_{1.2}\cdot H_3PO_4$		38	42.0	11 (685)	18¼ (760)	40
Small Block Plates		19	~44	15½ (735)	-	25
$(C_3H_6N_6)_{1.2}\cdot H_3PO_4$		26	~44	18 (753)	-	25
Large Needles		18	~46	17 (745)	-	20
$(C_3H_6N_6)_{1.2}\cdot H_3PO_4$		27	~46	16 (735)	27 (815)	20
Thin Reflective Plates		6	-	6½ (620)	17 (760)	40
$(C_3H_6N_6)_{1.3}\cdot H_3PO_4$		13	-	8 (645)	14½ (745)	10

Table A.4.3 (cont.)

Crystal Type	Special Treatment (if any)	Test No.	Weight of Coating (g)	Time (min) to: 300°C and Face Temperature (°C) attained at these times (in brackets)	400°C	Maximum Extent of Intumescence (mm)
Thin reflective plates (cont)						
	RM	109	52.0	11 (680)	17 (760)	10
Medium Block Plates		62	43.7	10 (675)	17½ (770)	10
$(C_3H_6N_6)_{2.0}\cdot H_3PO_4$						
Large Block Plates		5	-	8 (655)	17 (760)	10
$(C_3H_6N_6)_{2.0}\cdot H_3PO_4$		10	-	8½ (655)	16½ (755)	10

TABLE A.4.4 : Fire Test Results In British Standard 476 Pt. 8 Time-Temperature Curve Simulation Tests

For Samples Incorporating 30% Melamine Phosphate

Crystal Type	Test No.	Weight of Coating (g)	Time (min) to: 300°C and Face Temperatures (°C) attained at these times (in brackets)	400°C	Maximum Extent of Intumescence (mm)
Medium Needles $(C_3H_6N_6)_{1.0}\cdot H_3PO_4$	122	56.6	30 (865)	-	25
Small Needles $(C_3H_6N_6)_{1.2}\cdot H_3PO_4$	40	~65	27½ (860)	-	55
Small Block Plates $(C_3H_6N_6)_{1.2}\cdot H_3PO_4$	47	56.4	20½ (780)	31 (885)	32
Large Needles $(C_3H_6N_6)_{1.2}\cdot H_3PO_4$	50	54.2	20 (790)	29½ (850)	28
Thin Reflective Plates $(C_3H_6N_6)_{1.3}\cdot H_3PO_4$	41	57.9	17 (775)	23½ (820)	15
Large Block Plates $(C_3H_6N_6)_{2.0}\cdot H_3PO_4$	55	-	9½ (675)	18½ (775)	15

Table A.4.4 (cont.)

Crystal Type	Test No.	Weight of Coating (g)	Time (min) to: 300°C and Face Temperatures (°C) attained at these times (in brackets)	400°C	Maximum Extent of Intumescence (mm)
Small Amorphous Material $(C_3H_6N_6)_{2.0}.H_3PO_4$	106	48.5	11½ (710)	24½ (805)	25
Encapsulated Small Needles	104	50.4	9¼ (645)	16¾ (745)	10
Mixture I	130	59.0	27½ (845)	-	30
Mixture II	135	54.5	10 (675)	20 (750)	18

TABLE A.4.5 : Fire Test Results at 850° - 900°C (range 125 mm) For Samples Incorporating 12½% Melamine Phosphate.

Crystal Type	Special Treatment (if any)	Test No.	Weight of Coating (g)	Time (min) to: 300°C	Time (min) to: 400°C	Duration (min)	Maximum Extent of Intumescence (mm)
Medium Needles		116	51.0		7	7¼	80
$(C_3H_6N_6)_{1.0}\cdot H_3PO_4$							
Very Large Needles		118	46.3		~3	4½	vol.
$(C_3H_6N_6)_{1.0}\cdot H_3PO_4$							
Small Needles		33	42.9		7½	11	vol.
$(C_3H_6N_6)_{1.2}\cdot H_3PO_4$		37	~42		7¼	9½	vol.
	C 1wk., amb.	b(ii)	~80	6¼	19	~21	vol.
	C 2d., amb.	c(i)	~80	8½	15	18	vol.
	C 1wk., amb.	c(ii)	~80	8½	14	18	vol.
	C 2wk., amb.	c(iii)	~80	8½	13½	17	vol.
	C 1wk., amb. RM	f(ii)	~80	3	7	~8	vol.
Small Block Plates		24	~44		2¾	5½	vol.
$(C_3H_6N_6)_{1.2}\cdot H_3PO_4$		25	~44		6½	7	vol.

Table A.4.5 (cont.)

Crystal Type	Special Treatment (if any)	Test No.	Weight of Coating (g)	Time (min) to: 300°C	Time (min) to: 400°C	Duration (min)	Maximum Extent of Intumescence (mm)
Small block plates (cont.)	C ld., amb.	70	42.6		8¼	11	35
	C lwk., amb.	84	42.1		8¼	7½	65
	C 4wk., 55°C	88	44.6		9½	13	60
	C lwk., amb., RM	d(x)	~80	6	12	15¼	vol.
	C lwk., amb.,	f(iv)	~80	3½	6¾	8½	vol.
Large Needles		20	~46		7½	8¾	100
$(C_3H_6N_6)_{1.2}\cdot H_3PO_4$		28	~46		7¼	7¼	150
	C lwk., amb.,	d(i)	~80	8	17	20	vol.
	C lwk., amb.,	f(iii)	~80	4	6½	10	vol.
Thin Reflective Plates		3	-		6¼	8	100
$(C_3H_6N_6)_{1.3}\cdot H_3PO_4$		9	-		7¾	10½	100
		30	45.0		7¼	11	50
	c ld., amb.	85	47.3		6½	7½	vol.

Table A.4.5 (cont.)

Crystal Type	Special Treatment (if any)	Test No.	Weight of Coating (g)	Time (min) to: 300°C	Time (min) to: 400°C	Duration (min)	Maximum Extent of Intumescence (mm)
Thin reflective plates (cont)							
	C 9d., amb.	75	47.2		9½	12	65
	C 9d., amb.	82	43.3		9¼	12	50
	C 4wk., amb.	99	42.9		5½	8	150
	C 4wk., 55°C	97	41.1.		7	11	150
	C 9d., amb., RM	79	67.5		11¾	13½	80
	C 9d., 55°C, RM	77	65.3		10	19	100
	C 1wk., amb.	d(ii)	~80	5	12½	17	
	C 1wk., amb., RM	d(iii)	~80	6	13½	19	
Medium Block Plates		64	~43		7¾	11	130
$(C_3H_6N_6)_{2.0}\cdot H_3PO_4$							
Large Block Plates		11	-		3¾	5½	40
$(C_3H_6N_6)_{2.0}\cdot H_3PO_4$		d(ix)	~80	4½	16¼	21	
		f (i)	~80	5	9¼	13	

TABLE A.4.6 : Fire Test Results At 850° - 900°C (Range 125 mm) For Samples Incorporating 30% Melamine Phosphate

Crystal Type	Special Treatment (if any)	Test No.	Weight of Coating (g)	Time (min) to: 300°C	400°C	Duration (min)	Maximum Extent of Intumescence (mm)
Small Needles	C lwk., amb. RM	a(i)	~80	10½	13¾	18	vol.
$(C_3H_6N_6)_{1.2}\cdot H_3PO_4$	C lwk., amb. RM	a(iii)	~80	7½	9¼	10½	vol.
	C lwk., amb.	b(v)	~80	6	11½	18	vol.
Small Block Plates		48	56.2		6¼	7	vol.
$(C_3H_6N_6)_{1.2}\cdot H_3PO_4$							
Large Needles		52	55.1		7¼	7	vol.
$(C_3H_6N_6)_{1.2}\cdot H_3PO_4$							
Thin Reflective Plates		39	59.5		9¼	12½	vol.
$(C_3H_6N_6)_{1.3}\cdot H_3PO_4$	C lwk., amb.	d(vii)	~80	7	10¼	11	vol.
	C lwk., amb.,RM	d(viii)	~80	9	12¾	14	vol.
Medium Block Plates		65	49.3		9	10	100
$(C_3H_6N_6)_{2.0}\cdot H_3PO_4$							

Table A.4.6 (cont.)

Crystal Type	Special Treatment (if any)	Test No.	Weight of Coating (g)	Time (min) to: 300°C	Time (min) to: 400°C	Duration (min)	Maximum Extent of Intumescence (mm)
Large Block Plates		54	-		4½	5½	150
$(C_3H_6N_6)_{2.0}\cdot H_3PO_4$							
Encapsulated Small		102	48.0		6¾	8½	70
Needles							
Mixture I		131	58.9		7	7½	vol.
Mixture II		134	51.8		7¾	8½	vol.

TABLE A.4.7 : Fire TestResults In Early Tests At 850° - 900°C (Range 125mm) Investigating The Effects Of Percentage Melamine Phosphate Loading And The Incorporation Of Additional Materials. All Samples Were Produced With Small Needles $(C_3H_6N_6)_{1.2},H_3PO_4$ And Of Total Weight Approx. 80g, Cured For One Week At Ambient Temperature.

% Melamine Phosphate Loading	Additional Materials Incorporated	Test No.	Time (min) to: 300°C	400°C	Duration (min)
5%		b(i)	4	7	10
20%		b(iii)	5½	7¼	9
25%		b(iv)	7	12	14
20%	2% accelerator DY063	d(iv)	9	13	16
5%	10% TiO_2	e(i)	3½	4½	5½
12½%	2% TiO_2	e(ii)	7¼	10¾	15
28%	5% TiO_2	e(iii)	6	10½	11
30%	15% TiO_2	e(iv)	5	11	19
12½%	1% Bentone	d(xi)	8	15	17
12½%	3% TiO_2 + 1% Bentone	d(xii)	5¾	8¼	8¼
Pure Epoxy Resin		d(xiii)	2½	3	3¼

APPENDIX A5

COMPUTER PROGRAMS FOR THE QUANTITATIVE DETERMINATION OF THE RESISTANCE TO HEAT FLOW THROUGH CHARS

A.5.1 Calculation of the Film Coefficient of Heat Transfer to the Environment

The calculation of the value of the Film Coefficient h from the data for two tests, one with three values of the air temperature, T_a, and one with one value of T_a, is illustrated.

```
      MASTER COOL
      COMMON M,AM,TO,TEMPO,T(30),TEMP(30),I1
      REAL TEMPO(30),TEMPA(30,3)
      SLOPEC(M,N) = (TEMPO(N)-TEMPO(M))/(T(N)-T(M))
    2 READ (1,200) JA
      IF (JA.EQ.2) STOP
      IF (JA.EQ.1) READ (1,210)M,H,AM,(T(I),TEMPO(I),
     *TEMPA(I,1),I=1,M)
      IF (JA.EQ.3) READ (1,211)M,H,AM,(T(I),TEMPO(I),
     &(TEMPA(I,IA),IA=1,3),I=1,M)
      WRITE (2,220) M,H,AM
      IF (JA.EQ.1) WRITE(2,230) (T(I),TEMPO(I),TEMPA(I,1),
     7I=1,M)
      IF (JA.EQ.3) WRITE(2,231) (T(I),TEMPO(I),(TEMPA(I,IA),
     6IA=1,3),I=1,M)
      DO 3 IA =1,JA
      DO 30 I =1,M
      TEMP(I) =TEMPO(I) - TEMPA(I,IA)
   30 CONTINUE
      DO 31 I =1,M
      I1 = I+1
      I2 = I+2
      IF (SLOPEC(I1,I2).GE.SLOPEC(I,I1))GO TO 32
   31 CONTINUE
   32 TO = T(I1)
      TEMPO = TEMP(I1)
      WRITE (2,240) IA,TO,TEMPO
      F=H+1.
      IF (SUMSQ(F).GT.SUMSQ(H)) GO TO 9
      S = SUMSQ(F)
    6 F = F+1.
      IF (SUMSQ(F).GT.S) GO TO 10
      S = SUMSQ(F)
      WRITE (2,701) F ,S
      GO TO 6
    9 S = SUMSQ(H)
    8 H = H-1.
      IF (SUMSQ(H).GT.S) GO TO   11
      WRITE (2,702) H,S
      GO TO 9
C MINIMUM VALUE SO FAR IS S
   10 G=F-1.
      GO TO 7
   11 G=H+1.
    7 WRITE (2,703) G
      DO 12 I = 1,15
      H3 = G + 2.**(1.2 - FLOAT(I))
      H4 = G - 2.**(1.2 - FLOAT(I))
      WRITE (2,704) H3,H4 ,S
```

```
C LEAST OF G,H3,H4
      IF (S.GT. SUMSQ(H3)) CALL H34(G,S,H3)
      IF (S.GT. SUMSQ(H4)) CALL H34(G,S,H4)
   12 CONTINUE
      WRITE (2,300) G
      WRITE (2,301)
      DO 13 J=I1,M
      TC=EXP(ALOG(TEMPO)-(H*1.267E-4*(T(J)-TO)*60./(AM*460.)))
      TCG = TC +TEMPA(J,IA)
      WRITE (2,302) T(J),TC,TCG
   13 CONTINUE
      WRITE (2,303)
    3 CONTINUE
      GO TO 2
  200 FORMAT (I5)
  210 FORMAT (I5,F5.0,E10.0/(6F10.0))
  211 FORMAT (I5,F5.0,E10.0/(5F10.0))
  220 FORMAT (1X,'POINTS',6X,'H',4X,'MASS'/I5,5X,F5.0,2X,
     5E10.3//6X,'TIME',4X,'TEMPC',5X,'TEMPA--')
  230 FORMAT (3F10.2)
  231 FORMAT (5F10.2)
  240 FORMAT(/1X,'IA=',I3,3X,'TO=',F10.2,3X,'TEMPO=',F10.0/)
  300 FORMAT (/1X,'OPTIMUM H=',F15.5/)
  301 FORMAT (4X,'TIME',6X,'TEMP DIFF',6X,'TEMPG')
  302 FORMAT  (1X,3F10.3)
  303 FORMAT (1X,///)
  701 FORMAT (1X,'F=',F10.2,3X,'S=',F15.8)
  702 FORMAT (1X,'H=',F10.2,3X,'S=',F15.8)
  703 FORMAT (/1X,'G=',F10.2//8X,'H3',13X,'H4',15X,'S')
  704 FORMAT (1X,3F15.6)
      END

      SUBROUTINE H34(Q,S,H)
      Q = H
      S = SUMSQ(Q)
      RETURN
      END

      FUNCTION SUMSQ(H)
      COMMON M,AM,TO,TEMPO,T(30),TEMP(30),I1
         SUMSQ = 0.
      DO 5 J = I1,M
      TCALC = EXP(ALOG(TEMPO) - (H*1.267E-4*(T(J)-TO)*60./(AM*460.)))
      DIFF =(TCALC - TEMP(J))**2
      SUMSQ = SUMSQ + DIFF
    5 CONTINUE
      RETURN
      END
      FINISH
```

POINTS	H	MASS
19	5.	.001E-03

TIME	TEMPW	TEMPA--		
0.50	273.00	211.00	178.00	121.00
1.50	272.00	205.00	167.00	106.00
2.50	267.00	197.00	159.00	103.00
4.00	251.00	183.00	149.00	98.00
5.00	239.00	172.00	140.00	87.00
6.00	229.00	165.00	136.00	88.00
7.50	211.00	152.00	124.00	79.00
8.50	201.00	146.00	120.00	79.00
10.00	187.00	138.00	115.00	76.00
11.00	178.00	132.00	110.00	75.00
13.50	159.00	120.00	101.00	69.00
15.00	149.00	113.00	96.00	65.00
17.00	138.00	103.00	88.00	59.00
19.00	129.00	99.00	84.00	57.00
22.00	116.00	92.00	79.00	56.00
25.00	106.00	82.00	70.00	50.00
30.00	93.00	75.00	66.00	49.00
35.00	82.00	67.00	58.00	43.00
40.00	73.00	60.00	53.00	42.00

IA= 1 TC= 5.00 TEMPC= 67.

H= 4.00 S= 563.7877049 1

G= 4.00

H3	H4	S
5.148698	5.051302	53.319709
4.574349	5.425651	53.319709
4.287175	5.712825	53.319709
4.143587	5.856413	53.319709
3.928206	5.784619	49.378827
3.892310	5.820516	49.378827
3.910258	5.874361	49.129240
3.901284	5.883335	49.129240
3.887822	5.878846	49.112249
3.885579	5.881092	49.112249
3.886701	5.884457	49.111570
3.885018	5.886296	49.111498
3.885298	5.884738	49.111432
3.885158	5.884878	49.111432
3.884948	5.885088	49.111429

OPTIMUM H= 5.00495

TIME	TEMP DIFF	TEMPG
5.000	67.000	239.000
6.000	63.371	225.561
7.500	58.269	210.269
8.500	55.104	201.104
10.000	50.675	190.675
11.000	47.923	179.923
13.500	41.678	161.678
15.000	38.328	151.328
17.000	34.277	137.277
19.000	30.655	129.655
22.000	25.926	117.926
25.000	21.926	103.926
30.000	16.584	91.584
35.000	12.543	79.543
40.000	9.487	69.487

IA= 2 TO= 5.00 TEMPO= 99.

C= 4.00

H3	H4	S
5.148698	3.651302	148.951298
4.574349	3.425651	148.951298
4.287175	3.712825	148.951298
3.856413	4.569238	144.081002
3.928206	3.784619	131.773153
3.892310	3.820516	131.773153
3.874361	3.838464	131.773153
3.847438	3.865490	131.634788
3.842951	3.869977	131.634788
3.845195	3.867708	131.625892
3.844073	3.868830	131.625892
3.842391	3.870269	131.625388
3.842110	3.870549	131.625388
3.842250	3.870410	131.625344
3.842180	3.870480	131.625344

OPTIMUM H= 3.842211

TIME	TEMP DIFF	TEMPG
5.000	99.000	239.000
6.000	93.650	225.650
7.500	86.231	210.231
8.500	81.597	201.597
10.000	75.109	190.109
11.000	71.073	181.073
13.500	61.906	162.906
15.000	56.984	152.984
17.000	51.024	139.024
19.000	45.688	129.688
22.000	38.711	117.711
25.000	32.800	102.800
30.000	24.585	90.585
35.000	19.679	76.879
40.000	14.324	67.324

IA= 3 TO= 5.00 TEMPO= 152.

G= 4.00

H3	H4	S
5.148695	4.851302	473.883712
4.574349	5.425651	473.883712
4.287175	5.712825	473.883712
3.856413	3.569234	346.334232
3.784619	3.641032	346.334232
3.748722	3.676929	346.334232
3.730774	3.694877	346.334232
3.739748	3.721800	346.184488
3.726287	3.717313	346.114380
3.728530	3.724043	346.113311
3.725165	3.722921	346.104800
3.724604	3.723482	346.104800
3.724324	3.723763	346.104800
3.724183	3.723903	346.104800
3.724113	3.723973	346.104800

OPTIMUM H= 3.72411

TIME	TEMP DIFF	TEMP
5.000	152.000	239.000
6.000	144.076	232.076
7.500	132.958	211.958
8.500	126.027	205.027
10.000	116.302	192.302
11.000	110.239	185.239
13.500	96.429	165.429
15.000	88.908	153.908
17.000	79.951	138.951
19.000	71.833	128.833
22.000	61.174	117.174
25.000	52.097	102.097
30.000	39.062	82.062
35.000	30.500	73.500
40.000	23.337	65.337

POINTS	H	MASS
16	5.	.709E-03

TIME	TEMPw	TEMPA--
1.00	274.00	167.00
2.00	273.00	166.00
3.00	266.00	159.00
4.00	257.00	155.00
5.00	245.00	144.00
6.50	229.00	135.00
8.50	202.00	120.00
10.50	189.00	112.00
13.50	165.00	100.00
15.50	153.00	96.00
18.00	140.00	85.00
20.00	131.00	82.00
22.00	123.00	79.00
25.00	112.00	73.00
29.00	101.00	67.00
32.00	94.00	63.00

IA= 1 TO= 5.00 TEMPo= 101.

H= 4.00 S= 616.6058 0006

G= 4.00

H3	H4	S
5.148692	2.851302	50.917296
4.574349	3.425651	50.917296
4.287175	3.712825	50.917296
4.143587	3.856413	50.917296
4.071794	3.928206	50.917296
3.964103	3.892310	49.799344
3.982052	3.946155	49.544875
3.955129	3.973871	49.460496
3.959616	3.950642	49.454556
3.952885	3.948398	49.447702
3.951764	3.949520	49.447702
3.952325	3.951203	49.447015
3.952044	3.951483	49.447015
3.951904	3.951623	49.447015
3.951694	3.951553	49.447015

OPTIMUM H= 3.95169

TIME	TEMP DIFF	TEMP
5.000	101.000	245.000
6.500	83.001	229.001
8.500	85.332	205.332
10.500	77.496	189.496
13.500	67.170	167.170
15.500	60.911	156.911
18.000	54.002	139.002
20.000	49.143	131.043
22.000	44.539	123.539
25.000	38.547	111.547
29.000	31.793	98.793
32.000	27.515	90.515

A.5.2 Calculation of The Thermal Resistance of Chars for Two Fire Tests

A profile for the duration of the tests is given of the thermal resistance of the chars produced in two tests, viz.:

(a) Test 121 : 30% loading of medium needles of $(C_3H_6N_6)_{1.0}\cdot H_3PO_4$ tested at 750° - 800°C.

(b) Test 110 : 12½% loading of thin reflective plates of $(C_3H_6N_6)_{1.3}\cdot H_3PO_4$ tested at 750° - 800°C.

These are typical of the extremes of performance noted in fire tests. In both cases T_a, the air temperature, was supplied from three sources, by direct measurement and from two models.

A print-out of the results of the program which follows for the above fire tests may be found in the pocket at the end of the thesis.

```
      MASTER CHAR
      REAL TEMPP(80),TEMPQ(80),TEMPA(80),DTEMPQ(80),DTQ(80)
     1,TCHAR(80),TLOSS(3,80),COND(3,80)
      READ (1,9) K
      DO 100 KK =1,K
      IF(KK.EQ.1) WRITE (2,88)
      IF(KK.EQ.2) WRITE (2,89)
      READ (1,10) N,(TEMPP(I),TEMPQ(I),TEMPA(I),I=1,N)
      WRITE(2,11) N,(TEMPP(I),TEMPQ(I),TEMPA(I),I=1,N)
      WRITE (2,101)
      M = N-1
      DO 200 I = 2,M
C CALCULATE DTQ
      IPOS = I+1
      INEG = I-1
      DTEMPQ(I) = TEMPQ(IPOS) - TEMPQ(INEG)
      DTQ(I) = DTEMPQ(I)/120.
C CALCULATE TCHAR
      TCHAR(I) = TEMPP(I) - TEMPQ(I)
C CALCULATE TLOSS
      TLOSS(1,I) = 0.45*TEMPQ(I) - 20.
      TLOSS(2,I) = 0.34*TEMPQ(I) - 14.5
      TLOSS(3,I) = TEMPQ(I) - TEMPA(I)
C COND = K/X
      DO 300 J = 1,3
      COND(J,I) =(5447.*DTQ(I) + 3.90*TLOSS(J,I))/TCHAR(I)
  300 CONTINUE
      WRITE(2,102)I,TEMPP(I),TEMPQ(I),DTQ(I),(TLOSS(J,I),
     3J=1,3),(COND(J,I),J=1,3)
  200 CONTINUE
  100 CONTINUE
      STOP
    9 FORMAT (I5)
   10 FORMAT(I5/(12F5.0))
   11 FORMAT(1X,I5,'POINTS'/4X,'TQ',6X,'TP',6X,'TA',9X,'TQ'
     4,6X,'TP',6X,'TA',9X,'TQ',6X,'TP',6X,'TA'/3(3F5.0,3X))
   88 FORMAT('  TEST 121, MEDIUM NEEDLES 30%'/)
   89 FORMAT('  TEST 110, THIN REFLECTIVE PLATES 12.5%'/)
  101 FORMAT(/4X,'TIME',6X,'TP',6X,'TQ',2X,'DTQ',9X,
     5'TQ-TA(1)',4X,'TQ-TA(2)',4X,'TQ-TA(3)',4X,'K/X(1)',
     66X,'K/X(2)',6X,'K/X(3)')
  102 FORMAT (1X,I5,2F5.0,7F12.4/)
      END
      FINISH
```

APPENDIX A6

"A Review of Intumescent Materials, with Emphasis on Melamine Formulations"

reprinted from The Journal of Fire Retardant Chemistry, Vol. 6 (2), May 1979, p p. 69 - 91.

REFERENCES

Chapter 1

1. M. Kay, A.F. Price, I. Lavery : "A Review of Intumescent Materials, with Emphasis on Melamine Formulations", J. Fire Retard. Chem. 6 (May 1979) 69-91, reprinted in Appendix A.6.

2. Anon., "Fire Stopping in Ventilation Ducts", Heating and Ventilation Engineer, 44 (522) 1971, 361

3. R.E. Sempert, R.R. Harris : U.S. Patent 3,440,201 (Apr. 1969), assigned to Shenwin Williams Co.

4. A. Matsumura, Y. Sato : Japan Patent 77 103,431 (Aug. 1977), assigned to Nippon Synthetic Chemical Industry Co. Ltd.; Chem. Abs. 88 (1978) 52099a.

5. K. Hirota, S. Takahashi, S. Ozaki, G. Mizutani, H. Kikuchi : Japan Patent 77 38,062 (Sept. 1977), assigned to Mitsui Toatsu Chemicals Inc.; Chem. Abs. 88 (1978) 106914h

6. T. Kaide, Y. Koide, M. Takada, K. Ichikawa : Japan Patent 76 151,746 (Dec. 1976), assigned to Dainichi Nippon Cables Ltd.; Chem. Abs. 86 (1977) 141835p

7. W.J. Oberley : Belg. Patent 835,914 (March 1976); Chem. Abs. 86 (1977) 18644y

8. W. Scholles, H. Koddebusch, K.A. Rademacher : Brit. Patent 1,198,916 (July 1970), assigned to Desowag-Bayer Holzschutz G.m.b.H.

9. J.F. O'Rourke : "Use of Intumescent Coatings for Fire Protection of Structural Steels", Symposium : "Loss Prevention in the Process Industries", Philadelphia, Nov. 11-15, 1973; Am. Inst. Chem. Eng., New York, 1974, 69-72.

10. S. Hadvig : "The temperatures in steel profiles protected by intumescent coating systems and exposed to plastics fires", Proc. Internat. Symposium on Flammability & Flame Retardants, Lyngby, 1976; Tech. Univ. Denmark, p.13.

11. A. Dimitriev : "Swelling Fireproof Coatings for Steel Structures", Stroit. Mater. Silik. Prom-st., 1976, 17 (9) 13-15 (Bulg); Chem. Abs 86 (1977) 91852u.

12. G. Taschen, L. Denecke, M. Helm, K. Diedschies : Ger. (East) Patent 127,394 (Sept. 1977); Chem.Abs. 89 (1978) 26150q.

13. D.A. Yeadon, E.T. Rayner, G.B. Verburg, L.L. Hooper, F.G. Dollear, H.P. Dupuy : U.S. Patent 3,396,129 (Aug. 1968), assigned to U.S. Secretary of State for Agriculture.

14. R.G. Fessler, B.C. Tredinnick : Brit. Patent 1,270,624 (Feb. 1970), assigned to American Cyanamid Co.

15. J.B. Lloyd-Lucas, C. Lloyd-Lucas : Ger. Patent 2,710,463 (Sept. 1977), assigned to Advanced Fireproofing Systems Ltd.; Chem. Abs. 87 (1977) 153551b

16. W. Unsworth, G.A. Clegg : Brit. Patent 1,476,238 (June 1977), assigned to Magnesium Elektron Ltd.

17. J.D. Leman, A.J. Robertson, : Canadian Patent 998,325 (Oct. 1976), assigned to American Cyanamid Co.; Chem.Abs. 86 (1977) 57083j.

18. S. Hirao, M. Ishida, Y. Oka : Japan Patent 77 20,699 (Feb. 1977), assigned to Matsushita Electric Works Ltd.; Chem. Abs. 86 (1977) 194060p.

19. W.J. Oberley : Canadian Patent 1,033,908 (July 1978) assigned to Koppers Co. Inc.; Chem. Abs. 89 (1978) 112956k

20. T. Yoshinaga : Japan Patent 78 121,905 (Oct. 1978), assigned to Eidai Co. Ltd.; Chem.Abs. 89 (1978) 56651p.

21. K. Takaya, K. Matsumoto, Y. Katayama : Japan Patent 78 49,054 (May 1978), assigned to Asahi Chemical Industry Co. Ltd.; Chem. Abs. 89 (1978) 111478u.

22. Y. Koide, T. Kaide, M. Takada, K. Ichikawa : Ger. Patent 2,621,115 (Nov. 1976); Chem. Abs. 86 (1977) 31125z.

23. C. Savides, J.F. Cannelongo : U.S. Patent 4,003,861 (Jan. 1977) assigned to American Cyanamid Co.; Chem. Abs. 86 (1977) 91113d.

24. C. Robu, I.I. Balint, C. Nichitus, N. Insuratelu : Romanian Patent 59,118 (Sept. 1975), assigned to Intreprinderea de Lacuri si Vopsela "Policolor"; Chem.Abs. 89 (1978) 112709g.

25. A.W. McRowe, W.J. Kroenke : U.S. Patent 4,053,453 (Oct. 1977), assigned to Goodrich, B.F. Co.; Chem. Abs. 88 (1978) 38576x.

26. M. Ohhora, T. Nagasawa, H. Fugii : Japan Patent 77 27,457 (Mar. 1977), assigned to Unitika Ltd.; Chem.Abs. 86 (1977) 172473y.

27. M.W. Lindvay : U.S. Patent 4,028,333 (June 1977), assigned to Velsicol Chemical Corporation; Chem.Abs. 87 (1977) 85831r.

28. J.H. Warren, A.A. Corona : "This Method Tests Fire Protective Coatings", Hydrocarbon Process., 54 (1) 1975, 121-37; RAPRA Abs. 12 (11) 1975, 31803L.

29. C. Anderson, et al. : "Railroad Tank Car Fire Test : Test No. 6. Final Report". U.S. Dept. of Transportation, Federal Railroad Administration, Office of Research, Development and Demonstrations; Report FRA - OR & D 75-36, Washington, Aug. 1973.

30. C. Anderson, et al. : "Railroad Tank Car Fire Test : Test No. 7. Final Report", ibid; Report FRA - OR & D 75-37, Washington, Dec. 1973.

31. C. Anderson, E.B. Norris : "Fragmentation and Metallurgical Analysis of Tank Car RAX 201. Final Report", ibid; Report FRA - OR & D 75-30, Washington, Apr. 1974.

32. C. Anderson, et al. : "The Effects of a Fire Environment on a Rail Tank Car Filled with LPG. Final Report", ibid; Report FRA - OR & D 75-31, Washington, Sept. 1974.

33. W. Townsend, et al. : "Comparison of Thermally Coated and Uninsulated Rail Tank Cars Filled with LPG Subjected to a Fire Environment. Final Report", ibid., Report FRA - OR & D 75-32, Washington, Dec. 1974.

34. A.J. Taylor, D.J. Hards : "Engulfment Fire Tests on Road Tanker Sections, Technical Report", Ministry of Defence - Royal Armaments Research & Development Establishment; July 1975.

35. Anon.,"New Methods of Fire Protection for External Steelwork", The Architects J., 160 (28 Aug.), 1974, 494-516.

36. H.L. Malhotra : "The Meaning of Fire Resistance Tests", Conference of the Institution of Structural Engineers : "Structural Design for Fire Resistance", Aston University, Sept. 9-11, 1975, 92-114.

37. H.L. Malhotra : "The Philosophy & Design of Fire Tests", Symposium : "Fire Safety of Combustible Materials", Edinburgh, Oct. 15-17, 1975, 149-55.

38. W. Becker : "Systematics of Fires and Fire Test Methods", ibid, p.p. 162-68.

39. G.R. Nice : "Fire Tests and the Assessment of Fire Hazard", 25th Annual Conference of Fidor, Ltd., 7-10 June 1978; London. Fidor 1978.

40. A.E. Eagles, K.A. Scott : "The International Position of Tests for Fire Safety", Symposium : "Fire Safety of Combustible Materials", Edinburgh, Oct. 15-17, 1975, 131-40.

41.. I.A. Benjamin : "Problems in Correlation of Small and Large Scale Tests", ibid., 141-8.

42. D.P. Crowley, M.P. Brash, B.W. Burrell, F.L. Tempesta, F. Niehaus : "Test Method for the Analysis of Toxic Products from Burning Materials - Phenolic Foam", Fire Technology, 8 (3) Aug. 1972, 228-36.

43. A. Hall : "Flammability Report : Standards - Are there too many? Retardants - Are there enough? and Solutions - Are they in sight?", Mod.Plast.Internat., 2 (11) 1972, 50-3.

CHAPTER 2

44. S. Kler, B.Sc. project, Dept. of Chemical Engineering, Aston University, 1979/80.

45. K. Bann, S.A. Miller : "Melamine and Derivatives of Melamine", Chem.Rev., 58 (1), Feb. 1958, 131-71.

46. F.F. Purdon, V.W. Slater : "Aqueous Solution and The Phase Diagram", Chapter 7, publ. Arnold, London 1946..

47. ibid, Chapter 10.

CHAPTER 3

48. H.W. Bost, E.A. Zuerch, U.S. Patent 4,140,856 (Feb. 1979), assigned to Phillips Petroleum Co.; Chem.Abs. 90 (1979) 169548d.

49. W.J. Smothers, Yao Ching : "Handbook of Differential Thermal Analysis", Chapter 3, publ. Chemical Publishing Co. Inc., New York, 1966.

50. S.H. Roth, J. Green : "use of Thermal Analysis to Screen Binders for Intumescent Coatings", J. Paint Technology, 46 (590) 1974, 58-62.

CHAPTER 4

51. J. Chedaille, Y. Braud : "Industrial Flames, Vol. I : Measurements in Flames", Chapter 2 : "Gas Temperatures", International Flame Research Foundation, publ. Arnold, 1972.

52. J.H. MacGuire, H. Wraight : "Radiometer for Field Use", J. Scientific Instruments, 37 (Apr. 1960), 128-130.

53. NAG Computer Library Routine G02CAF, for Linear Regression Analysis in Fortran programming.

CHAPTER 5

54. G.M. Phillips, U.K. Patent, 1,373,908 (Nov. 1974), assigned to National Research Development Corporation.

55. Ciba-Geigy (UK) Ltd., Technical Data.

56. Cray Valley Products Ltd.,Technical Data.

57. NL Industries Inc., "A Practical Guide to Rheological Additives"

58. E.T. Severs, J.M. Austin : "Flow Properties of a Vinyl Chloride Resin Plastisol", Ind.Eng.Chem., 46 (1954) 2369-75.

59. A.H.P. Skelland : "Non-Newtonian Flow & Heat Transfer", Chapter 2, Wiley, New York, 1967.

CHAPTER 6

60. J.P. Fletcher, A.P.H. Jordan, Chemical Engineering Department, Aston University; Private communication.

61. R.M. Tennant (ed) : "Science Data Book", publ. Oliver & Boyd, Edinburgh, 1971.

CHAPTER 7

62. J.H. Morris, P.G. Perkins, A.E.A. Rose, W.E. Smith : "The Chemistry and Binding Properties of Aluminium Phosphates", Chem.Soc. Rev., 6 (2), 1977, 173-94.

APPENDIX A.1

63. A.I. Finkel'shtein, E.N. Boitsov, V.A. Petukhov : "Electronic Spectra of Derivatives of s-triazine", Zhur.Fiz.Khim., 29 (1955), 1937; and Fiz.Probl.Spektroskopii, 1 (1960), 257-60; Chem. Abs. 59 (1963), 10896a.

64. J.A. Barnard, R. Chayen : "Modern Methods of Chemical Analysis", 91-2, publ. McGraw-Hill, 1965.

65. A.L. Robinson : "The Solubility of Potassium Bromide in Acetone as related to the Inter-ionic Attraction Theory", J.Phys.Chem., 32 (1928), 1089-93.

66. H.K. Zimmerman, Jr.: "The Experimental Determination of Solubilities", Chem.Rev., 51 (1952), 25-65.

```
 *****   ****   ****   *****  *****  *****   ***
** *      *      *  *      *  *   *  *   *  *   *
** *      *      *  *      *  *   *  *   *  *   *
  ****    *      ****     *   *   *  *   *  *****
** *      *      *       *    *   *  *   *  *   *
** *      *      *       *    *   *  *   *  *   *
 *****   ****   *       *     *****  *****   ***
```

:ECP7008.CONDUCT

#LISTING OF :ECP7008.MKCOND(1/) PRODUCED ON AUG80 AT 12.33.35

#GF.63EC AT ASTON IN :ECP7008.CONDUCT' ON AUG80 AT 12.44.37 USING U15

DOCUMENT MKCOND

TEST 121, MEDIUM NEEDLES 30%

50POINTS

TQ	TP	TA	TQ	TP	TA	TQ	TP	TA
645.	85.	90.	685.	142.	115.	720.	190.	131.
750.	221.	139.	775.	233.	144.	810.	249.	145.
845.	256.	144.	865.	260.	142.	882.	263.	141.
900.	265.	140.	935.	267.	141.	930.	270.	142.
925.	270.	145.	920.	268.	147.	915.	268.	149.
910.	270.	152.	908.	273.	154.	906.	276.	155.
904.	280.	156.	902.	285.	156.	900.	288.	160.
895.	291.	162.	888.	295.	164.	882.	298.	165.
876.	301.	167.	870.	304.	169.	867.	306.	171.
864.	309.	172.	861.	314.	174.	856.	317.	176.
851.	320.	178.	845.	320.	180.	840.	321.	182.
835.	322.	184.	830.	325.	186.	826.	324.	188.
822.	326.	190.	820.	328.	192.	817.	331.	194.
814.	334.	196.	811.	335.	199.	808.	343.	201.
805.	350.	204.	802.	358.	206.	800.	370.	208.
799.	381.	210.	798.	391.	213.	797.	396.	216.
796.	402.	219.	795.	405.	222.			

TIME	TP	TQ	DTQ	TQ-TA(1)	TQ-TA(2)	TQ-TA(3)	K/X(1)	K/X(2)	K/X(3)
2	685.	142.	0.8750	49.5200	33.7600	27.0000	9.1335	9.0200	8.9713
3	720.	190.	0.6583	73.1000	50.1000	59.0000	7.3036	7.1346	7.2261
4	750.	221.	0.4000	88.2900	60.6400	82.0000	4.7696	4.5658	4.7223
5	775.	233.	0.2333	96.6200	66.4200	94.0000	3.0685	2.8492	3.0495
6	810.	249.	0.1500	102.0100	70.1600	104.0000	2.1656	1.9442	2.1794
7	845.	256.	0.0917	105.4400	72.5400	112.0000	1.5459	1.3260	1.5593
8	865.	260.	0.0583	107.4000	73.9000	118.0000	1.2175	1.0016	1.2659
9	882.	263.	0.0417	108.8700	74.9200	122.0000	1.0526	0.8387	1.1153
10	900.	265.	0.0333	109.8500	75.6000	125.0000	0.9606	0.7502	1.0536
11	935.	267.	0.0417	110.8300	76.2800	126.0000	0.9866	0.7651	1.0754
12	930.	270.	0.0250	112.3000	77.3000	128.0000	0.8699	0.6631	0.9627
13	925.	270.	-0.0167	112.3000	77.3000	125.0000	0.5301	0.3217	0.6057
14	920.	268.	-0.0167	111.3200	76.6200	121.0000	0.5266	0.3191	0.5845
15	915.	268.	0.0167	111.3200	76.6200	119.0000	0.8113	0.6022	0.8576
16	910.	270.	0.0417	112.3000	77.3000	118.0000	1.0390	0.8257	1.0737
17	908.	273.	0.0500	113.7700	78.3200	119.0000	1.1276	0.9099	1.1599
18	906.	276.	0.0583	115.2400	79.3400	121.0000	1.2177	0.9955	1.2534
19	904.	280.	0.0750	117.2000	80.7000	124.0000	1.3872	1.1591	1.4297
20	902.	285.	0.0667	119.6500	82.4000	127.0000	1.3448	1.1094	1.3713
21	900.	288.	0.0500	121.1200	83.4200	128.0000	1.2169	0.9766	1.2607
22	895.	291.	0.0583	122.5900	84.4400	129.0000	1.3176	1.0715	1.3590
23	888.	295.	0.0583	124.5500	85.8000	131.0000	1.3550	1.1001	1.3974
24	882.	298.	0.0500	126.0200	86.8200	133.0000	1.3079	1.0461	1.3545
25	876.	301.	0.0500	127.4900	87.8400	134.0000	1.3384	1.0694	1.3825
26	870.	304.	0.0417	128.9600	88.8600	135.0000	1.2896	1.0133	1.3312
27	867.	306.	0.0417	129.9400	89.5400	135.0000	1.3079	1.0270	1.3431
28	864.	309.	0.0667	131.4100	90.5600	137.0000	1.5777	1.2907	1.6170
29	861.	314.	0.0667	133.8600	92.2600	140.0000	1.6183	1.3217	1.6620
30	856.	317.	0.0500	135.3300	93.2800	141.0000	1.4845	1.1802	1.5255
31	851.	320.	0.0250	136.8000	94.3000	142.0000	1.2612	0.9490	1.2994
32	845.	320.	0.0083	136.8000	94.3000	140.0000	1.1027	0.7870	1.1265
33	840.	321.	0.0167	137.2900	94.6400	139.0000	1.2066	0.8861	1.2194
34	835.	322.	0.0167	137.7600	94.9800	138.0000	1.2244	0.8993	1.2261
35	830.	323.	0.0167	138.2700	95.3200	137.0000	1.2427	0.9123	1.2329
36	826.	324.	0.0250	138.7600	95.6600	136.0000	1.3493	1.0144	1.3278
37	822.	326.	0.0333	139.7400	96.3400	136.0000	1.4648	1.1236	1.4354
38	820.	328.	0.0417	140.7200	97.0200	136.0000	1.5768	1.2304	1.5495
39	817.	331.	0.0500	142.1900	98.0400	137.0000	1.7014	1.3471	1.6594
40	814.	334.	0.0583	143.6600	99.0600	138.0000	1.8292	1.4669	1.7532
41	811.	338.	0.0750	145.6200	100.4200	139.0000	2.0644	1.6917	2.0098
42	808.	343.	0.1000	148.0700	102.1200	142.0000	2.4133	2.0279	2.3624
43	805.	350.	0.1250	151.5000	104.5000	146.0000	2.7950	2.3921	2.7479
44	802.	358.	0.1667	155.4200	107.2200	152.0000	3.4098	2.9865	3.3793
45	800.	370.	0.1917	161.3000	111.3000	162.0000	3.6909	3.4374	3.8972
46	799.	381.	0.1750	166.6900	115.0400	171.0000	3.8357	3.3534	3.6759
47	798.	391.	0.1417	171.5900	118.4400	178.0000	3.5402	3.0309	3.6016
48	797.	396.	0.0917	175.0200	120.8200	182.0000	2.9621	2.4323	3.0303
49	796.	402.	0.0583	176.9800	122.1800	183.0000	2.5583	2.0158	2.6179

TEST 110, THIN REFLECTIVE PLATES 12.5%

20POINTS

TQ	TP	TA	TQ	TP	TA	TQ	TP	TA
670.	115.	200.	710.	200.	246.	755.	255.	260.
800.	295.	263.	825.	321.	253.	865.	324.	238.
860.	333.	231.	850.	341.	240.	842.	347.	262.
835.	353.	290.	832.	361.	312.	828.	366.	317.
823.	373.	323.	819.	381.	330.	815.	390.	340.
812.	398.	351.	810.	409.	363.	807.	420.	371.
804.	432.	384.	800.	445.	398.			

TIME	TP	TQ	DTQ	TQ-TA(1)	TQ-TA(2)	TQ-TA(3)	K/X(1)	K/X(2)	K/X(3)
2	710.	200.	1.1667	78.0000	53.5000	-46.0000	13.0569	12.2696	12.1087
3	755.	255.	0.7917	104.9500	72.2000	-25.0000	9.4430	9.1876	8.4294
4	800.	295.	0.5500	124.5500	85.8000	15.0000	6.8942	6.5950	6.0482
5	825.	321.	0.2417	137.2900	94.6400	68.0000	3.6742	3.3442	3.1380
6	865.	324.	0.1000	138.7600	95.6600	86.0000	2.0071	1.6964	1.6388
7	860.	333.	0.1417	143.1700	98.7200	102.0000	2.5238	2.1948	2.2191
8	850.	341.	0.1167	147.0900	101.4400	101.0000	2.3755	2.0257	2.0224
9	842.	347.	0.1000	150.0100	103.4800	85.0000	2.2825	1.9157	1.7701
10	835.	353.	0.1167	152.9700	105.5200	63.0000	2.5562	2.1722	1.8282
11	832.	361.	0.1083	156.8900	108.2400	49.0000	2.5519	2.1491	1.6586
12	828.	366.	0.1000	159.3400	109.9400	49.0000	2.5241	2.1071	1.5926
13	823.	373.	0.1250	162.7700	112.3200	50.0000	2.9237	2.4665	1.9484
14	819.	381.	0.1417	166.6900	115.0400	51.0000	3.2460	2.7861	2.2159
15	815.	390.	0.1417	171.1000	118.1000	50.0000	3.3858	2.8994	2.2745
16	812.	398.	0.1583	175.0200	120.8200	47.0000	3.7319	3.2214	2.5259
17	810.	409.	0.1833	180.4100	124.5600	46.0000	4.2449	3.7017	2.9377
18	807.	420.	0.1917	185.8000	128.3000	49.0000	4.5701	3.9906	3.1415
19	804.	432.	0.2083	191.6600	132.3800	48.0000	5.0601	4.4364	3.5537